UMSCORE

University of Michigan

Self Contained Orbital Research Experiment

A Student Design Project
Department of Aerospace Engineering
The University of Michigan
Winter Term 1979

ensn

UMR0950

FOREWORD

In late 1977 the Department of Aerospace Engineering at the University of Michigan made a reservation for a small self-contained payload to be flown on a future Shuttle flight. This action was formalized by the payment of earnest money to NASA and the attendance at a workshop at NASA Headquarters in Washington, D. C. on November 11, 1977.

It is the intention of the Department that this payload design be primarily an undergraduate student effort and that all aspects of the enterprise from initial experiment definition through post-flight analysis, be handled by students enrolled in a specified senior design course. Since the total activity related to this project may span a few years and certainly will extend over several semesters, some students at the sophomore level are encouraged to take part in order to provide the necessary continuity. Also it is hoped that students from other disciplines may be attracted to bring their expertise to the overall design effort.

During the present semester (Winter 1979) nine aerospace engineering students (7 Seniors, one Junior and one Sophomore) did the initial spade work on Project UM/ SCORE : University of Michigan Self-Contained Orbital Research Experiment. The report at hand is the first progress report and represents the work completed during this first term.

Although no single experiment was decided upon, several attractive areas were researched in depth and reported on in Chapter 4. Parallel

to this activity much work was accomplished investigating the many peripheral areas necessary for any meaningful experimentation. Results of this research into such fields as electrical power, data recording, event timing, etc., are contained in Chapter 3.

Under the guidance of student manager Greg Ruselowski, the total class effort, in addition to the technical engineering aspects, ranged from team organization to the final preparation of this report.

Professor Harm Buning
Professor Leslie M. Jones

SCORE Team--Winter 1979
left to right: Moy, Buning, Thomas, Bush,
Stebbins, Moore, Pitera, Weir, Ruselowski, Denson

TABLE OF CONTENTS

1. PROJECT PERSONNEL

1.1 Project SCORE Organizational Chart

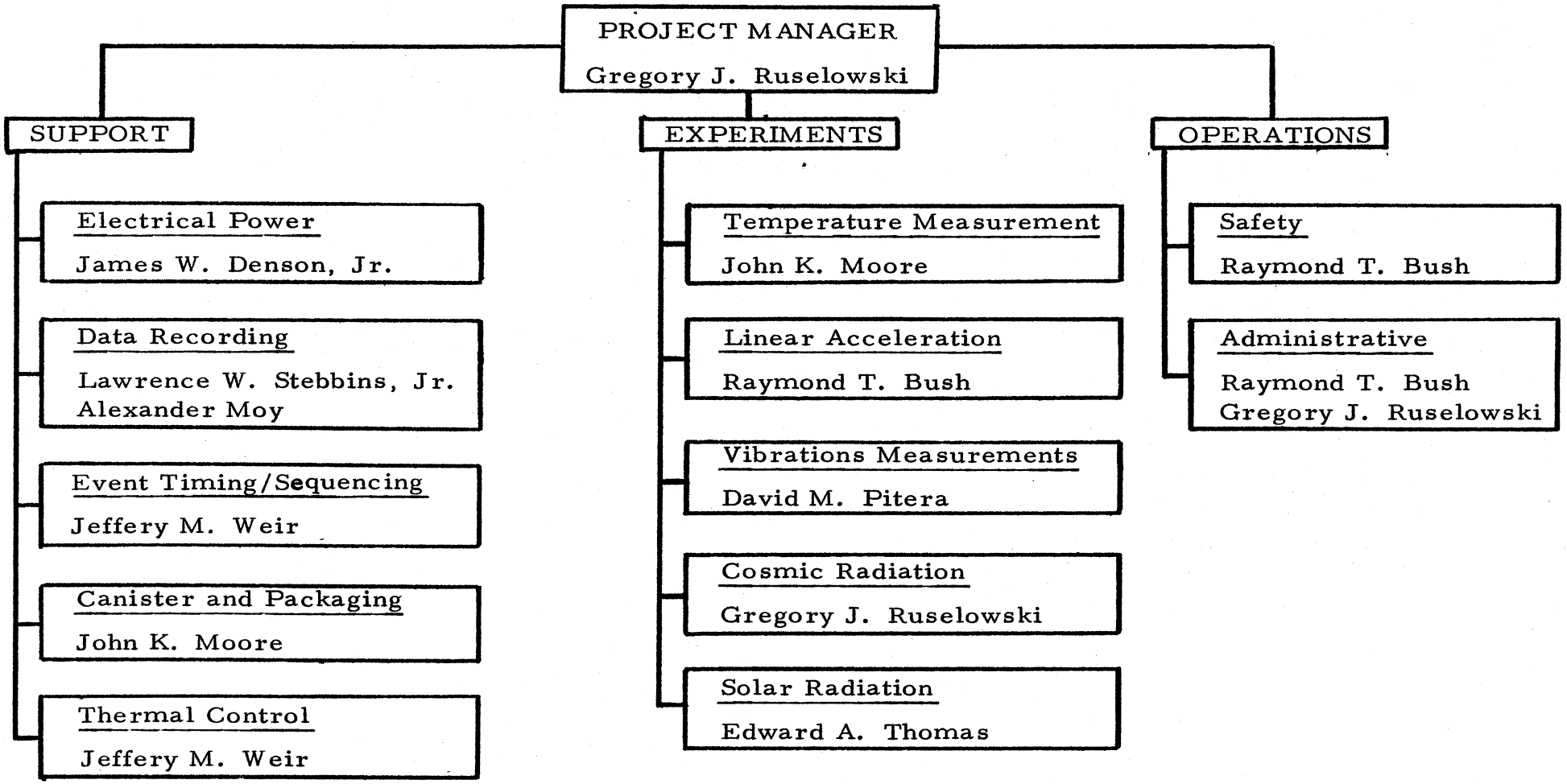

1.2 Acknowledgements

The SCORE team wishes to express thanks to all of the people who have given their time and energy to make this project a success:

Professor Harm Buning Aerospace Engineering	Faculty Advisor, Coordinator Space Shuttle Operations
Professor Leslie M. Jones Atmospheric and Oceanic Science	Aeronomy Instrumentation Sounding Rockets
Mr. Jack Caldwell Space Physics Research Laboratory	Data Recording Temperature Measurement Power Conditioning
Mr. David R. Taeusch Space Physics Research Laboratory	Vibrations Mass Spectrometer
Mr. J. Horvath Space Physics Research Laboratory	Vibrations
Professor William W. Willmarth Aerospace Engineering	Data Recording
Professor Frederick Bartman Atmospheric and Oceanic Science	Orbital Mechanics
Mr. Jim Monroe Bendix Corporation	Vibrations
Mr. Derek Perkins Bendix Corporation	Space Shuttle programs at Bendix
Ernest Ott NASA/ Goddard	Get Away Special Coordinator
John Hudgins NASA/ Goddard	Data Recording
Mr. Jack R. McDowell Battelle Memorial Institute at Columbus	Briefing on Get Away Special

John M. Hayes NASA/ Goddard	Data Recording
Gene McCoy NASA/ KSC	Safety
Dean Zimmerman NASA/ KSC	Launch Site Processing
Chester M. Lee NASA Headquarters	Safety
Mrs. Maurita P. Holland, Head Engineering Transportation Library -- U of M	Using the Library System
Ann L. Gee Aerospace Engineering	Report Typist

Special thanks goes to Professor Buning and Professor Jones for their hard work in coordinating and organizing the project.

1.3 Lecturers

Project SCORE personnel express warm gratitude to the following speakers whose lectures to the class were most helpful and timely towards getting SCORE off the ground.

Speaker	Topic(s)
Professor Harm Buning Aerospace Engineering	Space Shuttle Operations
Professor Leslie M. Jones Atmospheric and Oceanic Science	Aeronomy, Instrumentation, Sounding Rockets
Mr. David R. Taeusch Space Physic Research Laboratory	Vibrations, Tour of Space Physics Research Laboratory
Professor Frederick L. Bartman Atmospheric and Oceanic Science	Orbital Mechanics
Professor William W. Willmarth Aerospace Engineering	Data Recording
Mr. Jim Monroe Bendix Corporation	Vibrations Tour of Bendix
Mr. Derek Perkins Bendix Corporation	Current Bendix Space Progra
Mrs. Maurita P. Holland, Head Engineering Transportation Library	Using the Library System
Mr. Jack R. McDowell Battelle Memorial Institute at Columbus	Briefing on Get Away Special

2. INTRODUCTION AND SUMMARY

2.1 NASA, The Space Shuttle, and GAS -- Gregory J. Ruselowski

A new era of space transportation will begin as NASA's Space Shuttle becomes operational in the early 1980's. Man in space will become almost commonplace and payloads such as Spacelab will be launched routinely. Human knowledge will be greatly expanded as the Shuttle unlocks new doors in astronomy, physics, materials, zero-g technology and countless other areas of science and engineering.

NASA has realized that most of its primary payloads which are flown in the shuttle will not always occupy the total cargo bay area of the orbiter. Therefore, NASA has initiated the Get-Away Special (GAS) program to take advantage of this extra space as it is made available. Basically, the GAS consists of a small canister of not more than 5 ft.^{3} in volume and 200 lbs in weight to be placed in the orbiter bay. The canister will be completely self-contained or autonomous. That is, the canister will not be serviced by the crew and it must supply its own power, data recording equipment, etc.

The GAS program provides an excellent opportunity for small scale investigators such as Universities, organizations, private companies, and even individuals to experiment in outer space without realizing the prohibitive cost of launching an entire space mission by themselves. Thus,

the Get-Away Special enables the shuttle to be more cost effective by utilizing extra space and it also fills an experimental void created by the lack of small scale researchers in outer space.

2.2 The University of Michigan, SCORE, and GAS

The Department of Aerospace Engineering at the University of Michigan realized the value of the Get-Away Special and, in 1977 SCORE began when the University reserved a canister for a future Shuttle flight. Presently, the Department plans to use a canister with a volume of 1.5 $ft.^3$ and a weight not exceeding 60 lbs. The space was reserved with the intention that several (3 or 4) Aerospace Engineering Senior Design classes would decide upon, develop, and launch an experimental package for SCORE. This report presents the work completed on SCORE by the first design group. Thus far, the SCORE team has laid the groundwork for subsequent design groups by defining the payload and completing preliminary design.

2.3 SCORE Package

After several weeks of soliciting for ideas, careful thought, and deliberation, it was decided that the project would concentrate on measuring the environment of the Shuttle during launch, orbit, and reentry. This would include the measurement of parameters such as temperature, acceleration, vibration, cosmic radiation, and solar radiation. Measurement of the environment was chosen because it was felt that a package of this sort would be of suitable scope for the design team to insure project success. Also, the Space Physics Research Laboratory (SPRL) at the University can provide a wealth of information about measurement and measuring devices. The scientists and engineers at SPRL are more than willing to help.

Preliminary design for the aforementioned experiments (temperature, acceleration, vibration, cosmic radiation, and solar radiation) has been completed. Preliminary design for the subsystems to support these experiments has also been done. These subsystems include electrical power, data recording, event timing and sequencing, thermal control, vibrations environment, and packaging and the canister. Each section of this report describes their experiment or subsystem, discusses the option or options available, and makes recommendations. Ideally, subsequent design groups will fully utilize this report to complete the design work, construct the package and eventually launch the student configured payload into orbit.

3. SUPPORT

3.1 Electrical Power Supply System -- James W. Denson, Jr.

3.1.1. Introduction

The electrical power supply system of the shuttle orbiter "Get-away Special" package is a vitally important support system for all of the active functions in the package. This power supply or supplies, as the case may be, must be capable of functioning without the aid of a human hand, quite possibly in the most hostile conditions, e.g., vacuum, exposure to direct sunlight or shadow, radiation and magnetic fields, etc., existing in a low Earth orbit. To the individual sections in the package requiring them, the power supply must deliver specific voltages at adequate levels of current (some of which may need to be regulated to within fractions of a percent of desired values in order to preserve the performance of the powered item). This power may have to be delivered in a long duty cycle mode, or in short, pulsed segments, or possibly on demand at irregular intervals and should electrical shorts or overloads arise in the experiment package, the power system must have both a redundance and an overload protection capability to preserve the package instrumentation.

Since the package is autonomous, all power is carried internally. This means that chemical batteries must be utilized. These batteries must contain enough energy to meet the mission requirements with regard to time of use and power needed plus all inefficiency losses, as there is

no possibility for recharging these batteries in flight. In order to interface the batteries with the package system, use is made of combinations of d. c. to a. c. inverters, d. c. to d. c. converters, voltage and current regulators and rectifiers. In this report, the emphasis is placed on making recommendations on the best available hardware and alternative methods for performing various functions in power conditioning, rather than on specific, finalized power distribution circuit designs.

3.1.2. Chemical Battery Selection

In considering the problems involved with the selection of the specific battery type or types (one may possibly wish to use separate power systems for individual devices in the package -- and different types of batteries, as well) one wishes to use, several things must be considered.

Due to the extremely limited volume we have available to us (1.5 - 2 cubic feet), the batteries must be as small as possible and even more important, they must have as great an energy content per unit battery volume as is obtainable. The maximization of this quantity aids the designer by packing as much energy into a certain amount of space as possible, allowing the reduction of battery size. Also, we are limited in the amount of weight we are allowed to fly (60-100 pounds) in the package and the specific energy (energy per unit mass) of the batteries should also be chosen to be as large as possible. This would allow a low-mass battery pack. Batteries chosen according to both of these parameters would be a small, lightweight and high energy system.

Another problem encountered when choosing batteries is that they only work within a certain temperature range (which is different for each battery system), their performance depending on the temperature in that range. Finally, the battery should be chosen so as to generate as little gas at the anode as possible -- minimizing the danger of explosion due to built-up gas pressure in the battery (only hermetically sealed batteries should be used as they can operate in vacuum) which could severely damage the entire payload package.

There are three types of Lithium battery systems that information could be obtained about. One of these is the Lithium/ Vanadium Pentoxide (L_i / V_2O_5) type [1] . It has an energy density of 11 watt-hours per cubic inch and 120 watt-hours per pound. This is a relatively low discharge rate system as well as a low pressure one. This system is a very safe one, making it ideally suited to the delicate, low power aspects of the package.

The next system is the Lithuim/ Sulfur Dioxide (Li SO_2) type [1] . This sytem has an energy density of 7 watt-hours per cubic inch and 120 watt-hours per pound. This is a relatively high pressure system which requires gas pressure relief. This system is made in low, medium and high discharge rate configuration, which would make it suitable for any aspect of the package electronics.

The third Lithuim system is the Lithuim/ Thionyl Chloride ($Li / SOCl_2$) type [1] . This is a system capable of low, medium and high discharge rates, but it is a new system and the extent to which gas

pressure venting is needed is not yet known. The energy density for this system is 18 watt-hours per cubic inch and 300 watt-hours per pound. From these figures this battery system boasts, it is potentially better than the previous two, but it is still an unproven system as far as safety is concerned. When these problems have been corrected, the system could easily fill every need of our package.

Another high energy density battery system of the Silver Zinc (Ag-Zn) type was found [2]. This type of battery system is manufactured in a wide range of discharge rates, from very low to very high. The specific energy of this system is in the range of 40 to 50 watt-hours per pound and 2.5 to 3.2 watt-hours per cubic inch. This system has an additional advantage in that these batteries have a recharge capability. A disadvantage of this system is that gas is generated which requires that venting be provided in order to prevent explosion of the batteries. Another disadvantage of this type of cell is that it should not be operated in an inverted position when under the influence of gravity. This is due to the fact that the shuttle may undergo roll, pitch and yaw variations during orbit injection and deorbit manuevers. This type of battery has been proven to be a reliable and well performing system on actual spacecraft missions and its use should be seriously considered.

A second battery system containing silver is the Silver Cadmium (Ag-Cd) battery type [2]. The specific energy range of values for this system is the lowest of all of the systems discussed, being only 22 to

34 watt-hours per pound and 1.5 to 2.7 watt-hours per cubic inch. These are manufactured in a wide range of discharge capabilities making them suitable for use with any of the package instrumentation. This system shares the advantage of recharging capability with the Silver-Zinc system as well as the advantage of having been proven spaceworthy on actual spaceflights. It also shares the disadvantages of requiring a gas pressure vent and a non-inverted operating orientation when under the influence of gravity due to the aqueous electrolyte used in the system.

The five different battery systems just described are the ones which are, in my opinion, the best available battery technology for the needs of our package. Information is available for other battery systems from the manufacturers of these systems, but were not considered adequate for our needs, due to the technical limitations on our payload. Subsequent design classes inheriting the task of further designing the payload should request current information concerning battery systems, because significant improvements may occur in these products in the interval between the payload design and the actual flight.

3.1.3. Power Conditioning Devices

Once the job of selecting the individual types of batteries desired for the package functions is completed, it may be necessary to convert the power required by the load to a voltage different from that supplied

by the battery. In addition, the current delivered to the load may need to be controlled for the protection and proper operating of the load device (for some of package functions, the voltage may also have to be regulated within fractions of a percent of a certain value). In some cases, an altenating current supply may be needed for a piece of equipment and must be converted from a direct current source. Finally, overload safeguards must be provided in this power conditioning equipment should excess power levels occur in the package stemming from damaged components. A capability for redundant operation must be built into the system to reduce the chances of a catastrophic failure and the resultant loss of all data-gathering ability by the payload.

When one wishes to convert one d. c. voltage level into an a. c. voltage, use is made of a circuit designed to perform this service. It is called a Power Inverter, and it provides, basically, an oscillating signal (which is powered by a d. c. source) applied across the primary of a transformer, the secondary of which carries an a. c. power output. By adjusting the number of turns of wire in the coils on the transformer, one may select desired output voltage and current levels. For a method by which the voltage and current requirements for transformers may be calculated, see Appendix 1, p. 1 .

If the utilization of the power must be on a d. c. to d. c. basis, use is made of a circuit called a D. C. to D. C. Converter . Now, quite

simply put, a d. c. to d. c. converter is nothing more than an Inverter (discussed previously) mated at the secondary winding of the output transformer to a rectifying-filtering network plus any appropriate regulation devices desired by the user of the power. So, given any Inverter, one can change it into a d. c. to d. c. Converter by adding to the output a rectifying-filtering circuit. (For several examples of Inverters and D. C. to D. C. Converters, see Appendix 1, pgs. 6-9. [3] .)

For those portions of the package needing highly stable voltage and current inputs, there are electronic regulating devices and circuits one can use to obtain such stability. The better the required regulation is, the more likely is the user to want to purchase from a manufacturer the device capable of such performance. Some of these regulators even have built-in overload protection circuits. For a simple but effective regulator, a Zener diode of the desired voltage in parallel with the load will work very well (see Fig. 1).

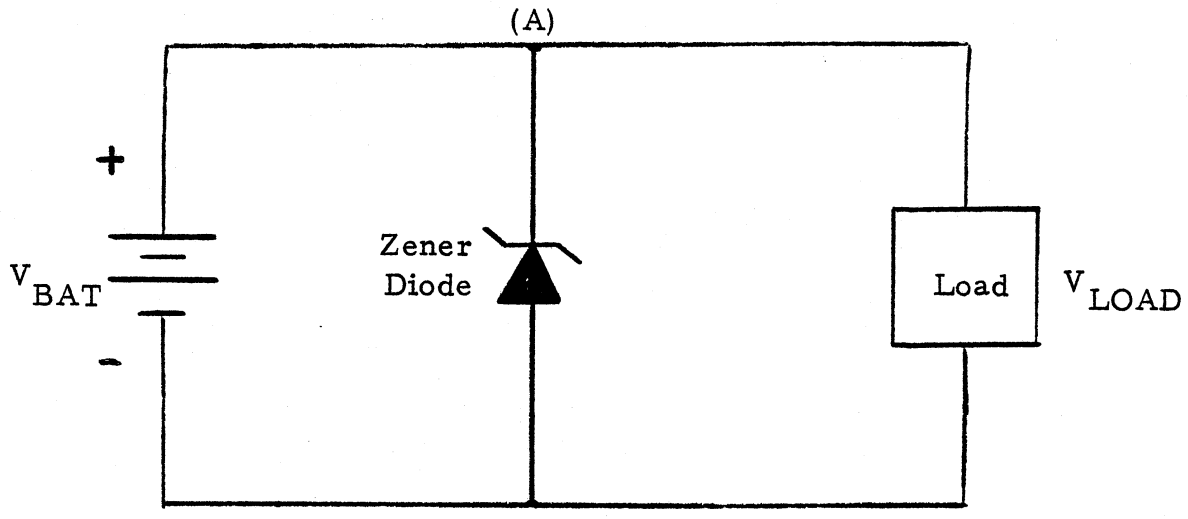

Figure 3.1.1. Basic Zener-Diode Regulation Circuit. The Zener diode in this circuit is chosen to conduct when the V_{BAT} attempts to rise above the desired V_{LOAD}, in effect shorting the V_{BAT} and dropping point (A) back down to V_{LOAD}.

Many other regulators are shown on pages 2-5 in the Appendix of this report and it should be noted that a switching-regulator type was suggested because it wastes less power than other types. Also, overload protection in the regulator would be desired.

Next, the problem of providing the package with a battery redundancy capability arises. This may be provided at two levels, the first level being simply giving each subsystem in the experiment package its own power supply and the second level being that of giving more than one battery cell to each subsystem power supply. The multiplicity of batteries would be connected in parallel, each individual cell having a small electronic device capable of electrically isolating that cell from the system should its voltage fall below a predetermined safety level. Two possible systems are shown in Figures 3.1.2 and 3.1.3.

Much more research should be done in the area of battery redundancy systems, as very little information could be found on it and the two examples given have not, to my knowledge, been used.

Another problem encountered when using batteries in space is the problem of battery temperature control. The battery systems discussed earlier in this report do not work below certain temperatures or above certain temperatures. In between the high and low operating temperatures lies a range (which depends on the particular batteries in question) in which the battery will function with its highest efficiency range. Note that the efficiency of the battery varies with temperature within the operating range. Now, if the battery must function in an

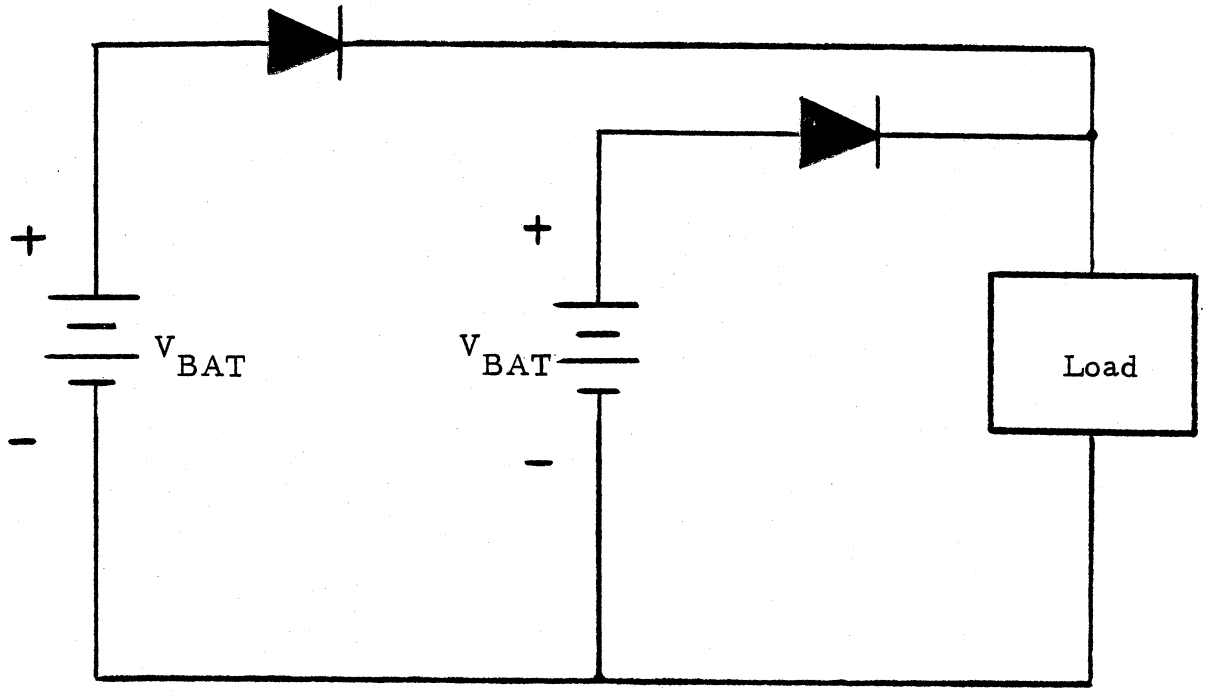

Figure 3.1.2. Possible Battery Redundancy System.

This is one possible redundance circuit for the battery system. Here the cells would discharge alternately most likely, and should either cell short internally, the diode prevents the surviving cell from discharging through it. Caution should be used here though, because it is possible that the cells will discharge alternately at high rate of speed, giving a pulsed output--which must not occur.

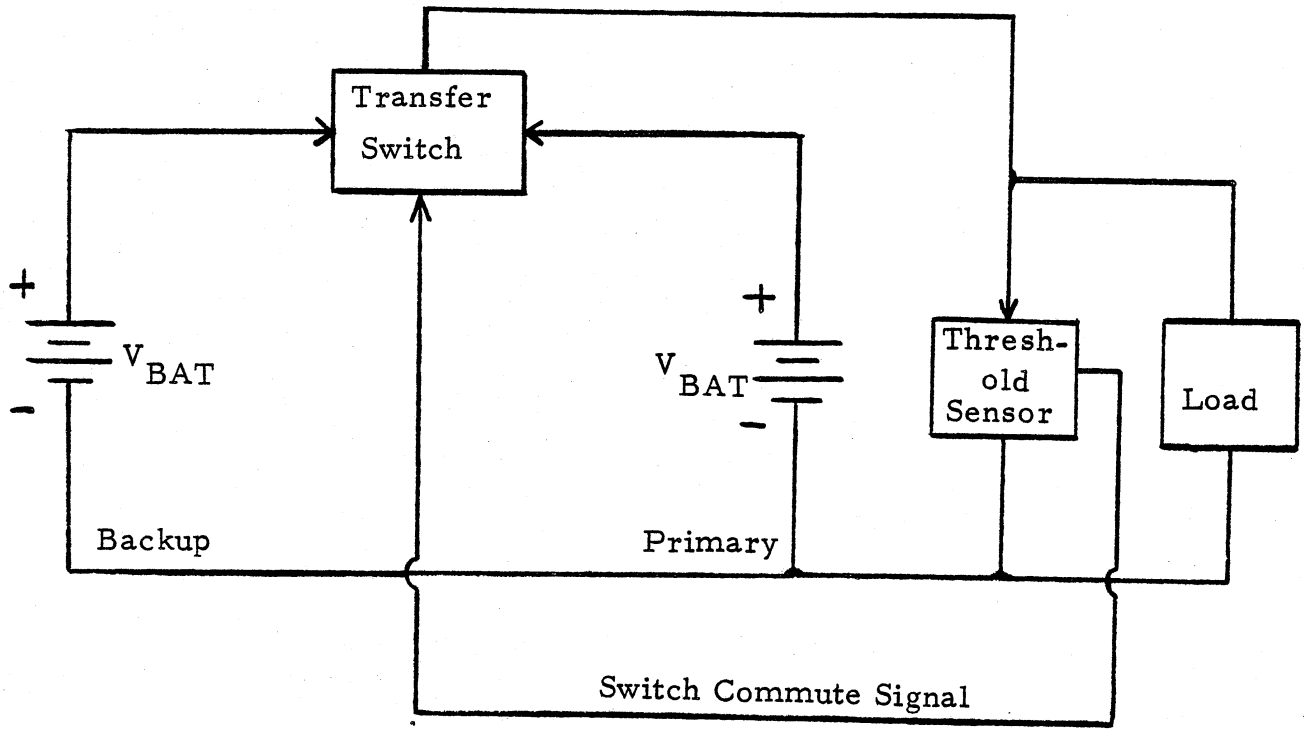

Figure 3.1.3. Possible Battery Redundancy System .

In this circuit, when the primary voltage is sensed to be too low, a signal is sent to a relay and power drain is switched from the primary to the backup cell.

extremely cold environment, e.g., in a shadow, then it will be necessary to insulate and/or actively heat the battery. If active heating must be used, then additional battery power for ohmic heating devices must be provided, along with a method of temperature sensing coupled with a heater current control device. This system would automatically heat the battery when necessary and shut itself down when the desired temperature is reached. The block diagram is shown in Figure 3.1.4.

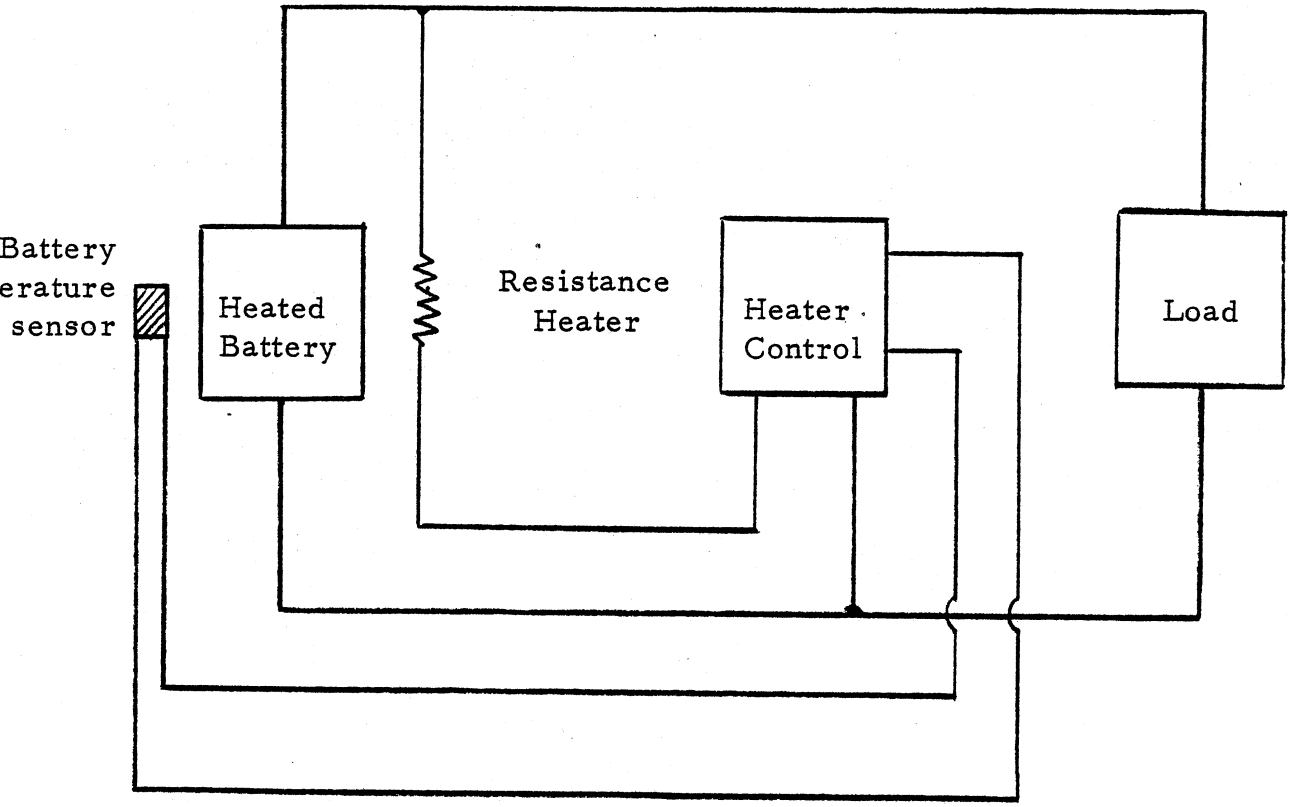

Figure 3.1.4. Battery Temperature Control System.

In this battery heater system, the temperature is sensed at the battery body and the resulting signal is used to control the heater through an electronic switch. The heater power may have to be drawn from the heated battery.

On the other hand, if the batteries become too hot (this could happen due to ohmic power dissipation building up in the canister from every electrically operated device in the canister) they must be cooled. Since carrying an active cooling system in the package is out of the question, the problem of canister overheating must be investigated jointly with the team in charge of thermal control.

The final problem concerning the battery concerns pressure. If the canister is pressurized, then almost any battery could be used--as long as it is leakproof and adequately vented for relief of internally produced pressure. If the batteries are exposed to the vacuum of space, then they must themselves be hermetically sealed as well as vented. Now since the battery gas is thrown away, one must be cautious as to where it goes. If there are optical windows in the experiment package, they may be fogged, and the performances of other devices may be degraded by the roaming gas clouds. Consultation with the other designers of the package is necessary to determine how to dispose of these gases.

3.1.4. Experiment Power Requirements

Now that the job of finding out ways of getting and controlling the electrical power is done, the next step is to determine how much power is required by each device in the total package and to relate it to the battery specifications available.

When the battery information is provided by the manufacturere, included in this information is the AMPERE-HOUR rating. This number tells you the product of the current drain in amperes and the length of time available at a level of current drain, in hours. This product is a constant value and is a measure of the total amount of charge stored in the battery. In other words, at a chosen current level, a battery will operate for a certain amount of time. If the current is reduced, it can be delivered for a longer period. If current is increased, it can only be delivered for a shorter period. The manufacturer should also supply any limitations on maximum and minimum current levels and drain times.

Now that the basis for comparison of the battery power and device power is established, some rough estimates on power requirements may be made. As of this report, there are seven device systems requiring electrical report and they are: (1) Data Recording, (2) Event Timing, (3) Transducer-to-Data Recorder interfacing electronics, (4) Accelerometer, (5) Temperature measurements, (6) Infrared sensing, and (7) Vibrometer.

In order to make the needed calculations, two simple equations will be used:

$$P = V I \qquad (3.1.1)$$

where P equals power measured in watts, V equals voltage required, and I equals current.

$$\# \text{ Amp - Hrs.} = I\,T \qquad (3.1.2)$$

where I equals the current drain and T equals the time of operation of the device.

For the Data Recording electronics, the estimated values of 15 volts at .125 amps are used in the calculations. Since this recorder can only record 3.5 hours of data, this is as great an amount of time any other device in the package need function.

$$P = (15\ \underline{v})\ (.125\ \underline{a}) \qquad P = 1.875 \text{ watts}$$

$$\# \text{ Amp. Hrs.} = (125\ \underline{a})\ (3.5 \text{ hrs.}) \qquad \# \text{ Amp. Hrs.} = .4375 \text{ amp. hrs.}$$

From the calculated figures, the Data Recorder will need .125 amps at 15 volts, resulting in a power requirement of 1.875 watts. This power may be supplied by a battery with a total capacity of .4375 amp-hours. To insure stability in the recorder operation, a 100% reserve capacity is added, bring the capacity of the battery to: .4375 + (100%) .4375 = .875 amp-hours.

For the Event Timing electronics, the estimated value of 2 watts and the assumed value of 15 volts are used in the calculations.

$$2 \text{ watts} = (15\ \underline{v})\ (I) \qquad I = .133 \text{ amps}$$

$$\# \text{ Amp Hrs.} = (.133\ \underline{a})\ (3.5 \text{ hrs}) \qquad \# \text{ Amp. Hrs.} = .4655 \text{ amp-hrs.}$$

Adding a 100% safety margin to this value gives:

$$.4655 + (100\%)\ .4655 = .931 \text{ amp-hours}\ .$$

Thus, the Event Timing electronics need a battery with a capacity of .931 amp-hours for delivering 15 volts at .133 amps for a power consumption of 2 watts.

For the Transducer-to-Data Recorder interfacing electronics the estimated value of 1 watt and the assumed value of 15 volts are used in the calculations.

$$1 \text{ watt} = (15 \underline{v})\, I \qquad I = .067 \text{ amps}$$

$$\#\text{ Amp. Hrs.} = (.067 \underline{a})(3.5 \text{ hrs.}) \qquad \#\text{ Amps Hrs.} = .2345 \text{ amp-hrs.}$$

Adding a 100 % safety margin to this value gives:

$$.2345 + (100\,\%)\, .2345 = .469 \text{ amp-hrs.}$$

Thus, the Transducer-to-Data Recorder interfacing electronics need a battery with a capacity of .469 amp-hours for delivering 15 volts at .067 amps for a power consumption of 1 watt.

For the Accelerometer, the known values of 6 volts at 3 amps for -5 hours are used in the calculations.

$$P = (6 \underline{v})(3 \underline{a}) \qquad P = 18 \text{ watts}$$

$$\#\text{ Amp. Hrs.} = (3 \underline{a})(.5 \text{ hrs}) \qquad \#\text{ Amp. Hrs.} = 1.5 \text{ amp-hours.}$$

Adding a 100% safety margin to this values, gives,

$$1.5 + (100\%)\, 1.5 = 3 \text{ amp-hours} .$$

Thus, for the Accelerometer, a battery with a capacity of 3 amp-hours is needed for delivering 6 volts at 3 amps for a power consumption of 18 watts. This experiment operates in a pulsed mode, however, and should have its own power supply.

For the temperature measurement electronics (Thermistors) the values of 5 volts and .001 watts are used in the calculations.

.001 watts = (5 v) I I = .0002 amps

Amp. Hrs. = (.0002 a) (3.5 hrs) # Amp. Hrs. = .0007 amp. hrs.

Adding a 100% safety factor to this value, gives:

.0007 + (100%) .0007 = .0014 amp. hrs.

Thus, for the thermistor, a battery with a capacity of .0014 amp-hrs. is required for delivering 5 volts at .0002 amps for a power consumption of .001 watts. This power must be of a very stable nature and should be well regulated.

For the Infrared sensing electronics, the assumed values of 5 volts and 1 ampere are used in the calculations.

P = (5 v) (1 a) P = 5 watts

Amp-Hrs. = (1 amp)(3.5 hrs.) # Amp-Hrs. = 3.5 amp-hours

Adding a 100% safety margin to this value gives

3.5 + (100%) 3.5 = 7 amp-hrs.

Thus, for the Infrared sensing electronics, a battery with a capacity of 7 amp-hours is required for delivering 5 volts at 1 ampere for a power consumption of 5 watts.

For the Vibrometer, the assumed values of 5 volts and 1 ampere are used in the calculations.

P = (5 v) (1 a) P = 5 watts

Amp-Hrs. = (1 a) (.5 hrs.) # Amp.-Hrs. = .5 amp-hours .

Adding a 100 % safety margin to this value, gives,

.5 + (100%) .5 = 1 amp-hour .

Thus, for the Vibrometer, a battery with a capacity of 1 amp-hour is required for delivering 5 volts at 1 ampere for a power consumption of 5 watts.

For the ohmic heater power if needed, no guess can be made at this time, because little information on the thermal characteristics of the canister is known.

The total capacity of the payload's power system is just the sum of the individual parts and is calculated here:

$$\#\ \text{Amp. Hrs. (total)} = .875 + .931 + .469 + 3.0 + .0014 + 7.0 + 1.0$$

$$\#\ \text{Amp. Hrs. (total)} = 13.2764\ \text{amp-hours}$$

For a two-level redundant system, this figure becomes,

$$\#\ \text{Amp. Hrs. (total)} = 26.5528\ \text{amp-hours} \quad .$$

Now, if the efficiency of the package is assumed to be around 75%, then 25 % of the power consumed is thrown away as heat, In order to regain the 25% of power thrown away, the amp-hour capacity of each battery must be increased by 25%. Doing so increases the total package battery (redundancy equipped) capacity by 25% and this figure is calculated to be:

$$\#\ \text{Amp. Hrs. (total, with redundancy)} = 26.5528 + (.25)\ 26.5528 \quad .$$

So, our Getaway Special Rackage would contain in total:

Amp. Hrs. (total, with redundancy) = 33.191 ampere-hours .

This means that a single battery of this capacity would contain all of the payload's energy (again, excluding battery heating).

Now that the total battery capacity required has been calculated, it is necessary to know both the weight and the volume occupied by this equivalent battery. Before we are able to calculate these quantities, we must calculate the total number of watt-hours contained in this equivalent battery. In order to do this, we must calculate the individual watt-hour capacities of each subsystem in the package and sum the results. For calculating the watt-hour quantities, the formula below must be used.

$$\text{\# Watt-Hours} = PT \qquad (3.1.3)$$

where P is the power consumption in watts and T is the time of operation of the device.

For the Data Recorder, T = 3.5 hours and P = 1.875 watts. The # Watt-Hours quantity works out to:

Watt-Hours = (1.875 w)(3.5 hrs.) # Watt-Hours = 6.563 watt-hrs.

For the Event Timing electronics, T = 3.5 hours and P = 3 watts. The # Watt-Hours quantity works out to:

Watt-Hours = (2w)(3.5 hrs.) # Watt-Hours = 7 watt-hrs.

For the Transducer-to-Data Recorder interfacing electronics, T = 3.5 hours and P = 1 watt. The # Watt-Hours quantity works out to:

Watt-Hours = (1 w)(3.5 hrs.) # Watt-Hours = 3.5 watt-hours.

For the Accelerometer, T = .5 hours and P = 18 watts. The # Watt-Hours quantity works out to:

Watt-Hours = (18 w)(.5 hrs.) # Watt-Hours = 9 watt-hours.

For the temperature measurement electronics, T = 3.5 hours and P = .001 watts. The # Watt-Hours quantity works out to:

Watt-Hours = (.001 w)(3.5 hrs.) # Watt-Hours = .0035 watt-hours..

For the Infrared sensing electronics, T = 3.5 hours and P = 5 watts. The # Watt-Hours quantity works out to:

Watt-Hours = (3.5 hrs.)(5 w) # Watt-Hours = 17.5 watt-hours.

For the Vibrometer, T = .5 hours and P = 5 watts. The # Watt-Hours quantity works out to:

Watt-Hours = (.5 hrs.)(5 w) # Watt-Hours = 2.5 watt-hours.

From these values, the Watt-Hour content of the equivalent battery can be found and its value is:

Watt Hours (total, with no redundancy) = 6.563 + 7 + 3.5 + 9 + .0035 + 17.5 + 2.5

= 46.0665 watt-hours.

Adding 100% for a safety margin, this value becomes:

46.0665 + (100%) 46.0665 = 92.133 watt-hours.

Doubling this value for a two-level redundancy yields:

(2) (92.133) = 184.266 watt-hours .

Assuming a package efficiency of 75% and adding 25% to the value above to recover the lost power yields:

184.266 + (.25) 184.266 = 230.3325 watt-hours .

Now that the total Watt-Hour capacity of the equivalent battery has been calculated, the volumes and weights of the five battery systems discussed previously may be determined. Volume and weight calculations follow:

For the Lithium/ Vanadium Pentoxide system, the volume of the equivalent battery is:

$$\frac{230.3325 \text{ W-H}}{11 \text{ W-H/ in}^3} \qquad \text{Volume} = 20.94 \text{ in}^3 \quad .$$

The weight of the equivalent battery is:

$$\frac{230.3325 \text{ W-H}}{120 \text{ W-H/ lb.}} \qquad \text{Weight} = 1.92 \text{ lbs.}$$

For the Lithium /Sulfur Dioxide system, the volume of the equivalent battery is:

$$\frac{230.3325 \text{ W-H}}{7 \text{ W-H/ in}^3} \qquad \text{Volume} = 32.90 \text{ in}^3 \quad .$$

The weight of the equivalent battery is:

$$\frac{230.3325 \text{ W-H}}{120 \text{ W-H/ lb.}} \qquad \text{Weight} = 1.92 \text{ lbs.}$$

For the Lithium/ Thionyl Chloride system, the volume of the equivalent battery is:

$$\frac{230.3325 \text{ W-H}}{18 \text{ W-H/in}^3} \qquad \text{Volume} = 12.80 \text{ in}^3 .$$

The weight of the equivalent battery is:

$$\frac{230.3325 \text{ W-H}}{300 \text{ W-H/lb}} \qquad \text{Weight} = .768 \text{ lbs.}$$

For the Silver Zinc system, the volume of the equivalent battery is:

$$\frac{230.3325 \text{ W-H}}{2.5 \text{ W-H/in}^3} \qquad \text{Volume} \left(\begin{matrix} \text{Largest} \\ \text{Case} \end{matrix} \right) = 92.133 \text{ in}^3 .$$

The weight of the equivalent battery is:

$$\frac{230.3325 \text{ W-H}}{40 \text{ W-H/lb.}} \qquad \text{Weight} \left(\begin{matrix} \text{Largest} \\ \text{Case} \end{matrix} \right) = 5.76 \text{ lbs.}$$

For the Silver Cadmium system, the volume of the equivalent battery is:

$$\frac{230.3325 \text{ W-H}}{1.5 \text{ W-H/in}^3} \qquad \text{Volume} \left(\begin{matrix} \text{Largest} \\ \text{Case} \end{matrix} \right) = 153.56 \text{ in}^3$$

The weight of the equivalent battery is:

$$\frac{230.3325 \text{ W-H}}{22 \text{ W-H/lb.}} \qquad \text{Weight} \left(\begin{matrix} \text{Largest} \\ \text{Case} \end{matrix} \right) = 10.47 \text{ lbs.}$$

These figures do not include heater power requirements.

References

[1] Honeywell Power Sources Division, Tithium Battery brochure, (1976).

[2] Yardney Electric Corporation, Silvecel and Silvercade Battery brochure.

[3] Discrete Transistor Circuit Sourcemaster, Kendall Webster Sessions (1978). John Wiley and Sons .

[4] Mallory Battery Company, Battery System brochures, (1974) and (1978).

3.2. Data Handling -- Lawrence W. Stebbins, Jr. and Alexander Moy

3.2.1. Introduction

3.2.1.1. The Need to Record Data on SCORE. As with almost any experiment, SCORE is going to produce data that will need to be collected for further analysis. Each of the measuring devices that make up SCORE will be taking many data readings that have to be collected and brought back to Earth so that useful information can be derived from the raw data. Since this project is an autonomous Get-Away Special (GAS) package, the data cannot be telemetered back to Earth while in the Space Shuttle Orbiter. It is necessary that a data handling package be included in SCORE.

3.2.1.2. Requirements of the Data Handling Equipment. Due to the hostile environment of space and certain mission constraints, the data handling equipment must meet special requirements. The data handling package must be able to survive the maximum vibrations during a Space Shuttle launch and the maximum temperature reached by the Orbiter during reentry and post landing. The equipment must be able to function in the space environment of vacuum and zero-g.

Some of the other considerations of the data handling package that must be looked at are:

A. How many channels of information need to be recorded?

B. What is the maximum frequency content?

C. What is the allowable accuracy (signal/ noise)?

D. Whether to record each channel directly or to sample "n" channels?

E. What type of recording?

1. Digital
2. Analog
   a. Direct
   b. FM

3.2.1.3. Task of the Data Handling Group. A preliminary analysis of the data handling package for the project was needed so that the requirements could be established. Determining suitable data handling equipment for SCORE had to be done so that the search for the equipment could begin.

The Data Handling Group was charged with the task of determining the requirements and make any recommendations as to the type of equipment most suited for SCORE. This information was to be passed on to the next design teams that will be working on this project.

3.2.2. Summary of Conclusions and Recommendations

The choice as to the best recorder to use in SCORE has been found to be very dependent upon the experiments that comprise the project. The number and type of measuring devices that will make up SCORE will determine, for instance, the data rate and capacity needed of the recorder. The recorder will not be able to run continuously

throughout the flight since a typical Space Shuttle mission may last up to seven (7) days. The data handling capacity will limit it to run for only several hours.

A digital recorder will be the best suited for SCORE's purpose. Digital recorders are the most reliable, and have better data compression. With the use of a digital recorder, an Analog-to-Digital (A-D) converter will be needed to turn the analog voltage levels put out by the measuring devices into digital form to enable the recorder to record the data. The use of a Buffer device is recommended in the package to extend the recorder's useful duration by compressing the data.

3.2.3. Discussion of Data Handling

3.2.3.1. Data Storage Methods. Storing data by using magnetic tape is the method recommended for use in SCORE. Magnetic tape is very reliable, plus it has the highest storage density. Many magnetic tapes have multiple tracks, thus allowing simultaneous recording from several different inputs (measuring devices).

The solid state method, the type of memory used by computers, uses many microscopic capacitors to store information. Solid state was found to be unsuitable for use in SCORE. As soon as power is cut off, as will occur several times throughout the mission, the capacitors lose their charge, and hence lose all of the stored data. The solid state data recorder has a capacity in the kilobyte range, rather than in the megabyte

range that is needed. It was thought to be too large and too expensive for use in this project.

The disk storage method is unnecessary. The disk storage of data, of which a record album is a good example, has the distinct advantage of having Random Access Memory (RAM) capability. RAM is the ability to move to different locations on the disk to store, or to reproduce data quickly. The added advantage of RAM, which is also an added expense, is unnecessary in SCORE, since its data will be purely sequencial (data recorded in sequence).

3.2.3.2. Magnetic Tape Recording: Reel Tape vs. Cassette. While investigating the equipment available from manufacturers, it was found that most of the specialized recording machines, those built for use in space enviornments, were of the reel type. The reel tape recorders were found to have greater duration, higher density, better frequency response, and better signal-to-noise ratio (signal/ noise) than cassette tape recorders.

Cassette tape machines are more limited since the ordinary cassette is not designed for the space travel environment. Ordinary cassette machines would have to be readapted by building a special pressurized container to house the machine. This would prevent small pockets of air that lie in between the layers of tape from expanding, and destroying the tape. The ordinary cassette machine would need to be

modified to prevent the recording head from separating from the tape during the higher vibrations and steady state g's to be experienced during a Space Shuttle mission.

Cassette tape would only have one usable track since there is no way that the cassette could be flipped over. A possible solution that deserves further investigation is to modify a machine so that it has dual recording heads. This would allow recording on two tracks of the cassette tape.

Additional disadvantages come from the tape being housed in a cassette. The cassette housing limits the length, and thus the duration, of the tape. The cassette housing also adds unnecessary weight.

3.2.3.3. Digital vs. Analog Recording. Raw data from the various measuring devices will most likely be of the form of smoothly varying voltages. This form of data is called Analog electrical signals. These signals can be recorded one of two methods: (A) Digital , or (B) Analog [Ref. 2] .

Digital recording is the least prone to errors, for example, tape skew and reading errors, than the other methods. Whereas, analog records variations, digital records 1's and 0's in the form of on and off signals. Calibration of the varying signals of analog is more difficult because of these potential errors. Digital recorders, though, will need an Analog-to-Digital converter to change the analog signals from the instruments into digital form so that it can be recorded. (See Section 3.2.3.5 for more on A-D converters.)

The Direct method of Analog recording, which measures amplitude variations has the highest frequency response, but has no D. C. capability. The Frequency Modulation (FM) method of Analog recording does have D. C. capability. FM replays faster and at different speeds, but it's upper frequency is limited by its playback capabilities.

3. 2. 3. 4. Digital Recording . Digital recorders can only store data in the form of one's and zero's. To change the varying analog signals of the measuring devices into digital form for the recorder, an Analog-to-Digital Converter is also needed in the Data handling package (see Section 3. 2. 3. 5). There are two methods that digital recording systems can encode the data. Data can either be encoded by Non-Return to Zero (NRZ) or can be Phase encoded.

The standard for small scientific recorders is Non Return to Zero (NRZ). NRZ measures a voltage-no voltage signal and converts it into one's and zero's. When a voltage is being read, a one is recorded. If there is a no-voltage reading, a zero is recorded. (See Fig. 3. 2. 1). Most of the recorders investigated, as of this report, use NRZ.

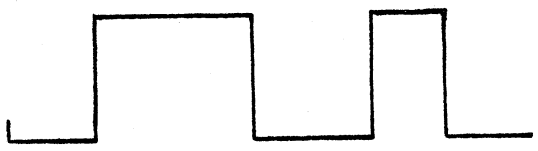

0 1 1 1 0 0 1

Figure 3. 2. 1. Non Return to Zero [2] ,

The other method in which data might be encoded is called "Phase encoded." Phase encoding measures flux changes instead of flux density. If the signal is increasing, a one is read. If the signal is decreasing, a zero is read into the system. The encoded data is

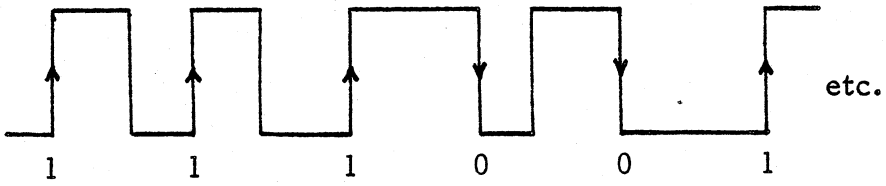

Fig. 3.2.2. Phase Encoded . [2]

stored on tape in blocks of data. The data blocks are separated by short gaps. The gaps indicate position and content of the data block (e. g., which measuring device this particular data is from).

3.2.3.5. Analog-to-Digital Converters. An Analog-to-Digital (A/ D) converter is simply a circuit that takes an analog signal and converts it into a digital signal. The incoming voltage variations are read and assigned a specific digital code of one's and zero's. One A/ D converter will handle only one channel, so multiple circuits may be necessary if multi-channel recording is used. There are converters available with multi-channel capacity. These would be the best type to use in SCORE. No further research was conducted in this area due to the dependence on the final system configuration.

3.2.3.6. A Buffer in the Data Handling Package. The buffer is the middleman of the data handling equipment. It's main duty is to match the data rates of the two devices attached to it. In the case of SCORE, the buffer will receive digitized data from the A/D converter and hold on to it until enough has been accumulated to efficiently turn on the recorder and dump the data from the buffer into the recorder.

The buffer is essentially a "waiting room." A simple analogy is a bucket under a leaking roof. Rather than empty every drop, you empty the bucket when it is full.

The type of buffer we would use is a temporary solid state memory board. In this way, hours of intermittent data can be stored and then recorded onto a few minutes of tape. The whole key to increasing the data capacity is data sampling, instead of continuous data recording, data points are taken at specific time intervals. This necessitates an accurate sequencer but economizes on the amount of tape that is used.

The entire buffer can consist of one circuit board; simple and durable. Typically, it would need power inputs, data in/ data out, and data recorder control contacts (to activate/ deactivate). Ideally, the memory chips inside should be of the static type so they do not lose their data in case of a power interrupt, although not as much data would be lost as in a wholly solid state data storage system.

The use of a buffer vastly increases the mission duration of the data recorder by compressing the data, without greatly increasing cost. Using both the solid state buffer and a magnetic tape recorder yields

a hybrid system of data storage better than each alone. No hardware research was conducted because the buffer is also totally dependent on the final package configuration and needs.

3.2.3.7. Capacity and Duration of the Data Handling Equipment.

Most of the recorders used in space missions are made for telemetry use, rather than complete data storage. They are, therefore, of short duration. Telemetry recorders have a cycle of:

A. Record data

B. Rewind

C. Play and transmit the stored data

D. Rewind and erase the old data

E. Ready to record new data.

As of this report, no recorder suitable for SCORE has been found that has the capacity to run continuously for a full Space Shuttle mission, or even for over three (3) hours. Therefore, the recorder will only be able to operate at certain times during the mission. The use of a Buffer device is recommended to extend the recorder's duration. By storing data at times when the recorder isn't operating, the Buffer is helping to optimize the recorders capacity (see Section 3.2.3.6).

In order to have greater data capacity, a magnetic tape with four (4) tracks is recommended. Three of the tracks would be for data recording, while the fourth track would be for a time signal. The

3.2.3.8. Types of Recording Machines Available. Space Recorders, recorders designed specifically for use in a space flight environment, seem to be the type of equipment most suited for SCORE. They are already packaged and sealed in a pressurized housing container to prevent the tape from exploding. They are designed to withstand the temperature ranges and vibrations of a space mission. Most of them have sufficient storage, meet NASA specifications, and have guaranteed reliability of up to 97%.

Audio Recorders, such as cassette recorders, are analog type recording devices. They are either reel-to-reel, which are too large for SCORE, or cassette tape. The disadvantages of the cassette tape recorders have already been discussed (see Section 3.2.3.2). Audio recorders cannot be relied upon in the space flight environment since they are not built for that use. They might be adaptable to that environment, though, but this could be unpractical for this project.

Microcomputer tape decks have also been looked into, but are not yet designed to be flown in a space environment, and are, therefore, unproven. They are expected, though, to be used in future space missions. They usually use cassette tape. They may be adapted by using either autoreverse or fullwidth heads. This would require additional work to implement these modifications.

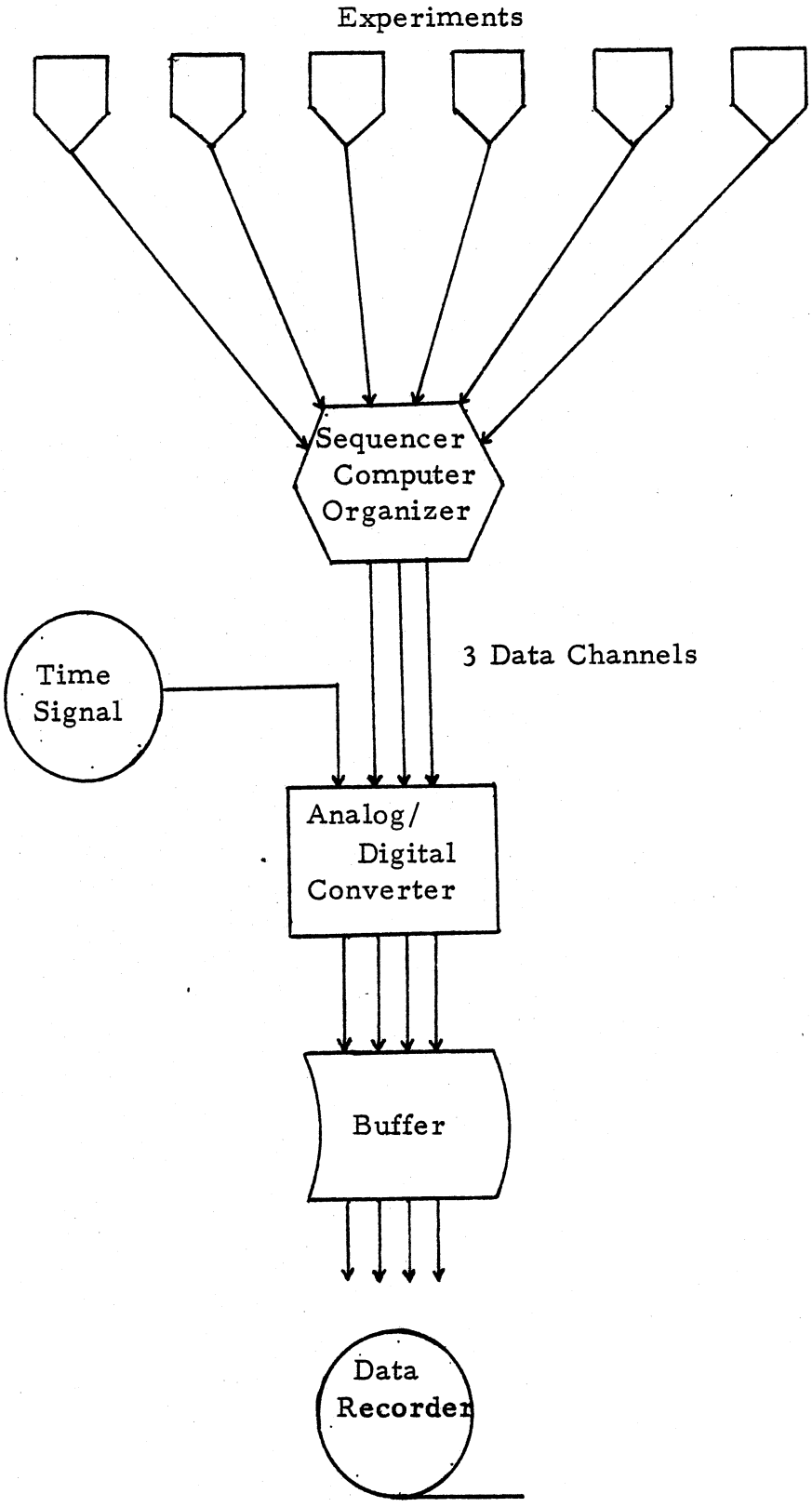

Figure 3.2.3. Data Control/ Storage System .

time track would receive a time signal from a clock and would indicate on the tape at what times the recorder was receiving data.

To help eliminate the waste of tape, the recording should be optimized so that all of the tracks are being used for recording simultaneoulsly. A switching system is needed to insure that all three data tracks are used simultaneously, for the optimization of track usage. This would mean that a particular measuring device might have data stored on any and all of the data tracks. Therefore, an identification signal for each measuring device would be required to indicate which experiment's data is on what track at which time.

When using a digital recorder, the useful duration of the tape can be increased by using longer data blocks to minimize lead tape (gap) waste. The longer the data blocks, the fewer number of gaps there will be, and the more usable tape there will be. A buffer would help compress the data into longer data blocks (see Section 3.2.3.6) by storing more data before it dumps it all into the recorder.

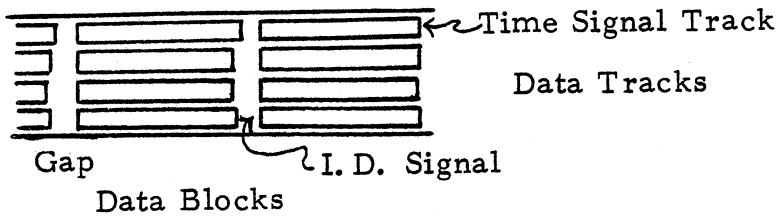

Figure 3.2.4. Four Track Tape .

3.2.3.9. Post-Flight Analysis. Equipment will be needed on the ground for post-flight reproduction, translation, and analysis of the data that was recorded. Its basic job would be to translate digital into uncompressed analog signals. These would then be reconstructed into numbers. The selection of this equipment will be very dependent upon the type of data handling equipment used.

3.2.4. Contacts with Manufacturers.

Appendix B list the addresses of some equipment manufacturers that were suggested by NASA-Goddard Space Flight Center for possible GAS use. It should be noted that this is not a comprehensive list of all of the manufacturers that should be contact about equipment. A comparison of some of the recording equipment, based on information that this Data Handling Group has received is also given in Appendix B.

3.2.5. Conclusions and Recommendations

The selection of Data Handling Equipment will be totally dependent upon the type, amount, and rate of the data to be collected. It is recommended that the Data Handling package consist of a digital recorder using four-track reel tape. This means that an A/D converter is also needed. The use of a Buffer device is recommended so that the duration of the recorder's use can be extended. The purchase of equipment

designed and certified for use in a space flight environment is recommended. The possibility of adapting or constructing equipment suitable for space use could be looked into more closely. Equipment will be needed on the ground for post-flight reproduction, translation, and analysis of the recorded data.

What this Data Handling Group has done is acquire a knowledge of data handling techniques, do a preliminary analysis, and get an idea of some of the equipment available, and make some preliminary recommendations. The next Data Handling Group should determine more specifically the requirements of data collecting and storage in SCORE. Then the hardware that best meets these requirements can be bought or constructed.

References

[1] Caldwell, John R., Sr. Research Associate Engineer, Space Physics Research Laboratory, The University of Michigan, personal contact, April 1979.

[2] Willmarth, William W., Professor of Aerospace Engineering, The University of Michigan, lecture notes, 1978-79.

[3] Athey, Skipwith W., Ph. D., Magnetic Tape Recording Technology Survey, NASA SP-5038, Technology Utilization Division, NASA, Jan. 1966.

[4] Gruenberg, Elliot L., Editor-in-Chief, Handbook of Telemetry and Remote Control, McGraw-Hill, 1967.

[5] Stiltz, Harry L., Editor, Aerospace Telemetry: Volume I, Prentice-Hall, Inc., 1961.

3.3 Event Timing -- Jeffery M. Weir

3.3.1 Introduction

Due to the limited amount of power available in the SCORE canister, experiments and any other power dissapating elements must be turned on and off according to a predetermined schedule. Since the SCORE payload is only allowed three signals supplied by the astronauts, an alternate means of coordinating the sequence of events must be found. This leads to the concept of event timing. The purpose of this section is to explore the basic devices needed to sequence the events at precise times into the mission. Once these have been explored, a possible schedule of requirements for each experiment is examined, and suggestions for the future are given.

3.3.2 Summary

Two devices are needed to keep track of the acquisition of data and the regulating of power to the elements of the SCORE payload. The first considered is a clock or timer. It must be able to supply a decipherable time signal to the tape recorder, one that will enable a determination of the specific point in the mission profile when data was recorded. It must also be used to activiate power to the elements contained inside. There are two types which have been discussed. The first is a simple timer that keeps track of elapsed time into the mission. It can be started at launch,

and remain on throughout the mission. The second one is a clock that keeps track of the year, month, day, hour, minute, second, millisecond, etc. By synchronizing this with the master clock used by NASA, the specific times into the mission can be directly determined by comparison with NASA's timetable.

The second device needed is a sequencer. A sequencer is a device that regulates the turning on and off of experiments, heaters, etc. It may be activated with a time signal, or it may simply use an increase in the acceleration of gravity to accomplish the task. Three types of sequencers were considered, G-switches, mechanical sequencers, and electronic sequencers. G-switches close relays for changes in the acceleration of gravity. They may be used at specific stages in the mission where there is a noticable increase in acceleration, such as launch and deorbit. Mechanical sequencers can be activated by a time signal, a signal supplied by the astronauts, or even G-switches. They are a series of cams driven by small electric motors. By varying the size and rotation speed of the cams, relays may be opened or closed to sequence events. Electronic sequencers work on the principal of matching predetermined time signals from the clock with preprogrammed signals inside the sequencer itself. When the signals match, a relay is correspondingly opened or closed. They are usually of solid state construction, and are quite readily available on the market today.

To regulate the events, a definite schedule of when the elements of the SCORE payload are to be on or off is needed. This schedule is dependent on available power, data recording capacity, and the required power of each element. Once this is determined, the timing of events may be carried out by the use of a well chosen system made up of combinations of the devices discussed above.

3.3.3 Discussion

Due to the isolated nature of the SCORE payload from the orbiter all of the experimental data must be recorded independently within the canister. This implies that some method to keep track of the turning on and off of the experiments must be found, leading to the concept of event timing. Each experiment will have optimum times to collect data during specific stages in the mission profile. All other times, the experiments must be turned off due to the limited amount of power contained in the batteries within the canister. In the following discussion, methods to handle this problem will be discussed. First, the concept of some sort of time signal will be examined. Next sequencers, which are devices capable of switching the experiments on or off will be discussed. Finally, typical requirements of each experiment will be examined.

3.3.3.1 Timer/Clock. Some sort of device is needed to keep track of the elapsed time into the mission. This elapsed time can be

analogous to the starting of a stopwatch at launch. Since launch is a well defined time in the mission, the elapsed time at any point in the mission may be correlated to specific stages in the mission, such as solid rocket or external tank jettison, orbital insertion, etc. By knowing the time of these events from NASA, the exact moment in the mission can be determined from the elapsed time signal. The timer would start at time zero (launch) and would continue to run throughout the mission.

Another type of timer to be considered is one in which the year, month, day, hour, minute, second, millisecond, etc. is available. This type of timer is actually a precise clock. It has the advantage of being directly related to the time used by NASA, providing it is synchronized with NASA's prior to lift-off. The use of such a device would enable the specific stages in the mission profile to be directly evaluated from NASA's timetable.

The type of clock/ timer to be used is contingent upon specific considerations. It must be accurate in operation, and draw a small amount of power. Many such devices are on the market today, generally being of solid state electronic nature. It must also be capable of supplying some sort of time signal to the data recorder, to be recorded along with the experimental data.

3. 3. 3. 2 Sequencers. A sequencer is a device that is generally clock/ timer driven, and activates switches according to desired times in the mission profile. There are three types consiered in the following discussion. These are G-switches, mechanical, and electrical sequencers.

G-switches or gravity switches close or open a relay with the onset of an increase in the acceleration of gravity. G-switches having the characteristics of activating with the onset of an acceleration of gravity one and one-half that of normal would be practical for our use. They can be used in key stages of the mission, such as lift-off and the firing of the engines at the beginning of deorbit, since these stages produce the required one and one-half g's or more of acceleration. They have the advantage of being completely independent of the time signal.

Mechanical sequencers are based on the use of cams driven by motors. By varying the size of the cams and the speed of rotation, intricate event sequences can be programmed. Each cam will have at least one notch, possibly more, cut out of the circumference. A pin would ride along the circumference of the cam as it rotates until it falls into the notch. At this point, the pin could either connect or disconnect a switch hooked up to the electrical system, completing or breaking the circuit. In this way, experiments, heaters, etc., could be turned on and off. At the end of the sequence, the cam would come back to the initial position, ready to initiate the sequence all over again. For a simple example, see Figure 3. 3. 1. This type of sequencer could be activated by one of the three

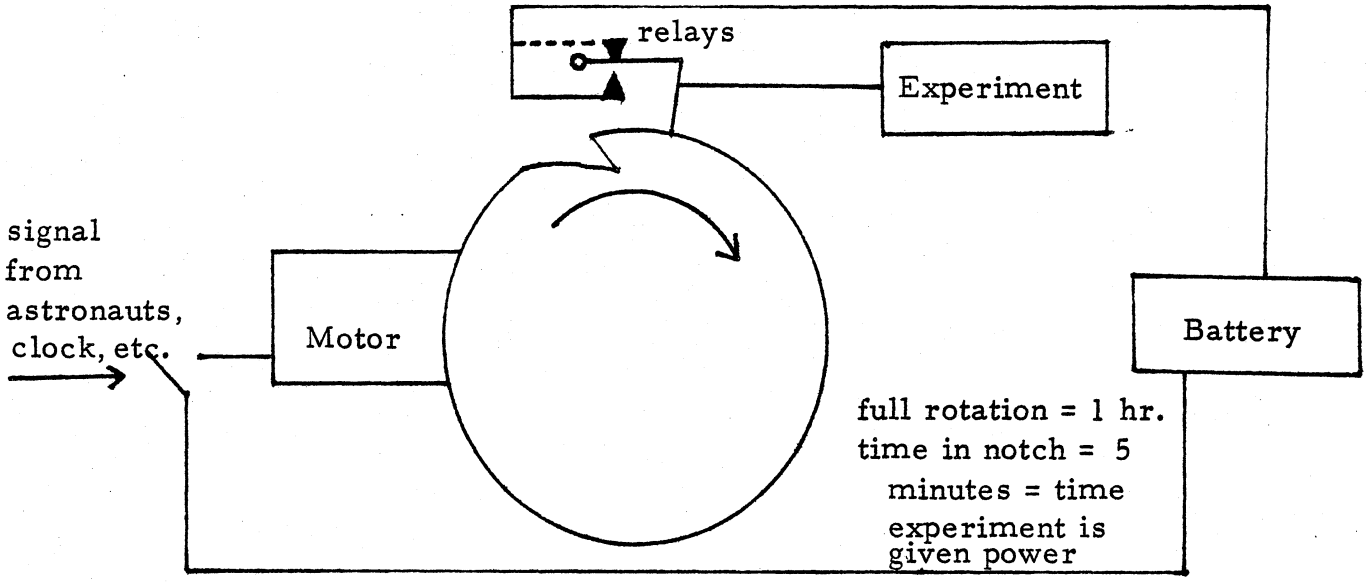

Fig. 3.3.1. Example of a Mechanical Sequencer .

provided signals from the astronauts. By having the astronauts complete the circuit to a motor running the main cam at a certain prescribed time, the sequence could be initiated. Small power drawing motors and the determination of the size and rotation speeds of the cams are required.

The final type of sequencer available is the electronic solid state type. This type is programmed to match certain time signals from the clock, and correspondingly close or open relays. These switches are readily available on the market today, and should be considered for possible use. A list of possible sources for timers and sequencers has been included in Appendix C .

3. 3. 3 Schedule of Requirements for Each Experiment. Due to the lack of available power, experiments must be turned on and off at predetermined times into the mission. A tentative schedule is listed in Table 3. 3. 1. The sequencer must be designed to meet the requirements of the schedule effectively. Table 3. 3. 2 examines the possible choices that could be used to sequence the events.

When the accelerometer is on, the sequencer must be able to turn it on and off in predetermined intervals to conserve power. A tentative data acquisition sequence is one in which the accelometer is on 5 seconds, off for 10 seconds, on for 5 seconds, etc. throughout the launch and deorbit phases. The data recorder must also be activated every time that an experiment is working in order to collect the data. Therefore, it should be interconnected to all of the experiments in such a way so that it can be turned on whenever a particular experiment is activated.

3. 3. 3. 4 Suggestions for Future Consideration. For successful utilization of the proposed experiments, precise event timing is important. The type of devices used should depend on their associated reliability and accuracy. A combination of the discussed sequencers is recommended to accomplish the task in the most economical and reliable way. In order to time the events, a much more detailed schedule of events is needed than that presented in Table 3. 3. 1. From there, the problem is supplied with the given information, and the unknowns are then to be determined.

TABLE 3.3.1.

Tentative Schedule for Experiments

Experiment	On	Off	On	Off	On	Off
Vibrometer	lift-off	orbit insertion ~ 10 minutes	random sample to be determined while in orbit	after 1 min of random sample	beginning of deorbit	touchdown ~80-90 min after deorbit
Accelerometer	lift-off	orbit insertion ~ 10 min	beginning of deorbit	touchdown ~ 80-90 min after deorbit		
Thermistor	lift-off data-every 1/2 minute	orbit insertion ~ 10 min	predetermined time in orbit data according to recorder capacity		beginning of deorbit- data every 5 minutes	touchdown ~ 80-90 min after deorbit
Bolometer	predetermined time while in orbit	related to specific capacity of recorder while in orbit				

TABLE 3.3.2.

Choices to Sequence Events

Experiment	On-signal	Off-signal	On-signal	Off-signal	On-signal	Off-signal
Vibrometer	G-switch or sequencer	Sequencer	Sequencer	Sequencer	G-switch or sequencer	Sequencer
Accelerometer	G-switch or sequencer	Sequencer	G-switch or sequencer	Sequencer		
Thermistor	G-switch or sequencer	Sequencer	Sequencer or Astronaut signal		G-switch or sequencer	Sequencer
Bolometer	Astronaut signal or sequencer	Sequencer				

3.4 Thermal Control - Jeffery M. Weir

3.4.1 Introduction

In order for the SCORE payload to function as an effective research experiment, the canister in which it is contained must be able to maintain a compatible environment for the proper function of the equipment enclosed. To sustain this enviornment, heat transfer equations must be used to calculate heat flow; therefore, determining specific design parameters. The purpose of this report is to discuss the different parameters that will be instrumental in determining the expected heat flow; therefore, influencing the final canister design. Also, temperature extremes are examined, along with three different types of possible temperature control systems. It is hoped that this brief overview will give the future teams a solid starting point from which the canister's thermal design can be integrated toward a functional end.

3.4.2 Summary

In the environment that the orbiter encounters, conductive and radiative heat transfer needs to be considered. These phenomenon are dependent on characteristic parameters of the specific material through which the heat transfer takes place. In order to determine the heat transfer, conductive and radiative transfer equations have been developed and generalized when applicable to a cylindrical canister. From these

equations, heat flow may be calculated knowing characteristic dimensions, material properties, and absolute boundary temperatures. By knowing the heat flow, specific parameters may be altered by the use of appropriate materials to compensate for the adverse temperature extremes expected.

In order to protect the payload efficiently from the adverse temperatures, an understanding of the different orbital attitudes and how they relate to the expected temperature extremes is needed. There are five typical orientations that the orbiter may use, each one a characteristic of a certain mission profile. These orientations range from hot, in which the orbiter and the cargo bay is exposed to the sun all of the time during orbit, to cold, in which the orbiter is exposed to the sun all of the time, but the cargo bay is exposed to deep space. These orientations are instrumental in determining the temperatures expected during orbit, and must be considered when selecting a thermal design for the canister.

Temperature control systems need to be considered for efficiency and practicality. There are three types; namely, passive, semi-passive, and active. The active control system has been disregarded on the basis of complexity, and needed versus allowable volume. The specific determination of the type of temperature control system used is related to the orientation of the orbit, and is dependent on the most efficient means by which the payload can be protected. It is recommended that the passive system be used if possible due to its relative simplicity and powerless operation.

Design of the specific type of system for temperature control is dependent on the most extreme temperatures that the SCORE payload can withstand and still operate accurately and effectively. By determining this range, the thermal protection system for the canister may be designed, and the orbit orientation may be chosen to compliment this design. Once determined, the SCORE payload will be able to function properly, oblivious of the extreme environment in which it is placed.

3.4.3 Discussion

Due to the lack of any measurable atmosphere, the orbiter and its cargo will experience wide temperature extremes. These extremes will in turn affect the components of the SCORE payload, and must be explored and compensated for. To do this, types of heat transfer will be discussed, along with their calculations and specific parameters affecting each. Next, temperature extremes for various mission profiles will be examined. Finally, specific temperature control systems will be examined, and suggestions for future considerations will be given.

3.4.3.1 Heat Transfer. There are three types of heat transfer which may be considered. These are convection, conduction, and radiation. Convection is a form of heat transfer that depends on mechanical mass transport for its operation, which requires some form of fluid flow. Since fluid flow requires gravity for operation, convective heat

transfer cannot be considered for our application due to the near zero gravity environment that the orbiter will encounter. Conduction may be considered as the dominant type of heat transfer at low temperatures, while radiation becomes the dominant mode of heat transfer at high temperatures.

A. Conduction-Low Temperatures.

Conduction is a series type of energy transfer between adjacent molecules. For simplicity's sake, one-dimensional conduction of heat will be considered. The general relation for one-dimensional heat conduction is:

$$\dot{Q} = -kA \frac{dT}{dx} \qquad (3.4.1)$$

where $\dot{Q}$ = heat flow (BTU/HR), k = thermal conductivity of a material (BTU/HR-FT$^{\circ}$F), A = area normal to heat flow (FT^2), $\frac{dT}{dx}$ = rate of change of temperature with repect to the thickness of the material. The negative sign in Eq. (3.4.1) indicates that there is a positive heat flow in the direction of decreasing temperature. In general, the thermal conductivity (k) is temperature dependent for homogeneous materials, but for moderate temperature differences it may be considered constant. Eq. (3.4.1) can be generalized to determine the heat flux through any type of insulating material as follows:

$$\frac{Q}{A} = \frac{k}{\Delta x} (T_{hot} - T_{cold}) \qquad (3.4.2)$$

where $\frac{Q}{A}$ = heat flux through insultaion (BTU/ HR-FT^2), k = thermal conductivity of insulation (BTU/ HR-FT^oF), Δx = insulation thickness (FT), T = temperature (^oF). The most important parameters affecting conductive heat transfer are the thermal conductivity of the material or insulation, along with the representative dimensions. Values of thermal conductivity for various insulating materials of different thicknesses as measured in a vacuum of $5x10^{-4}$ Torr are presented in Table 3.4.1.

TABLE 3.4.1.

The Effective Thermal Conductivity of Various Materials
Over the Temperature Range of 70 to 750° F
As Measured in a Vacuum of $5x10^{-4}$ Torr

Material	Thickness (in.)	Thermal Conductivity k (BTU/HR-FT^oF)	Boundary Temperatures $T_H(^oF)$	$T_C(^oF)$
Aluminized Mylar	1	3.7×10^{-3}	328	67
Aluminized Mylar	0.5	0.73×10^{-3}	237	67
Aluminized Mylar	0.25	1.04×10^{-3}	339	65
Aluminum Foil	0.5	1.86×10^{-3}	349	61
Aluminum Foil	0.5	2.9×10^{-3}	627	65
Quilted Aluminum	0.75	0.88×10^{-3}	402	65
Quilted Aluminum	0.75	1.13×10^{-3}	530	65
Quilted Aluminum	0.75	1.66×10^{-3}	825	65

The basic heat transfer equation can be rewritten to include conduction through cylindrical walls. This can therefore model the conductive heat transfer occuring in the SCORE container, since it may be considered a cylinder. Details of the transformation may be viewed in Appendix D . Briefly, the heat transfer due to conduction through homogeneous cylindrical walls may be written as:

$$\dot{Q} = \frac{2\pi Lk(T_1 - T_2)}{\ln(r_1/r_2)} \qquad (3.4.3)$$

where $\dot{Q}$ = heat flow (BTU/ HR), L = length of cylinder (FT), k = thermal conductivity of material (BTU/ HR-FT^{o}F), r = radius at specific point (FT), and T = temperature of specific wall (^{o}F).

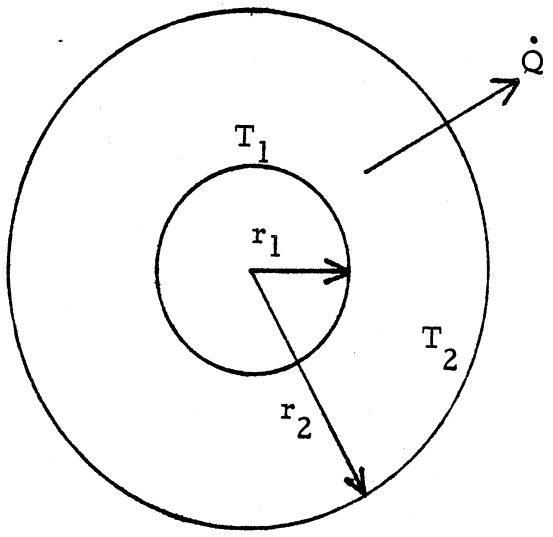

Fig. 3.4.1. Conduction Through Homogeneous Cylindrical Walls .

This in turn may be expanded to facilitate heat flow calculations through composite cylindrical walls, such as an insulated SCORE container as shown in Fig. 3.4.2.

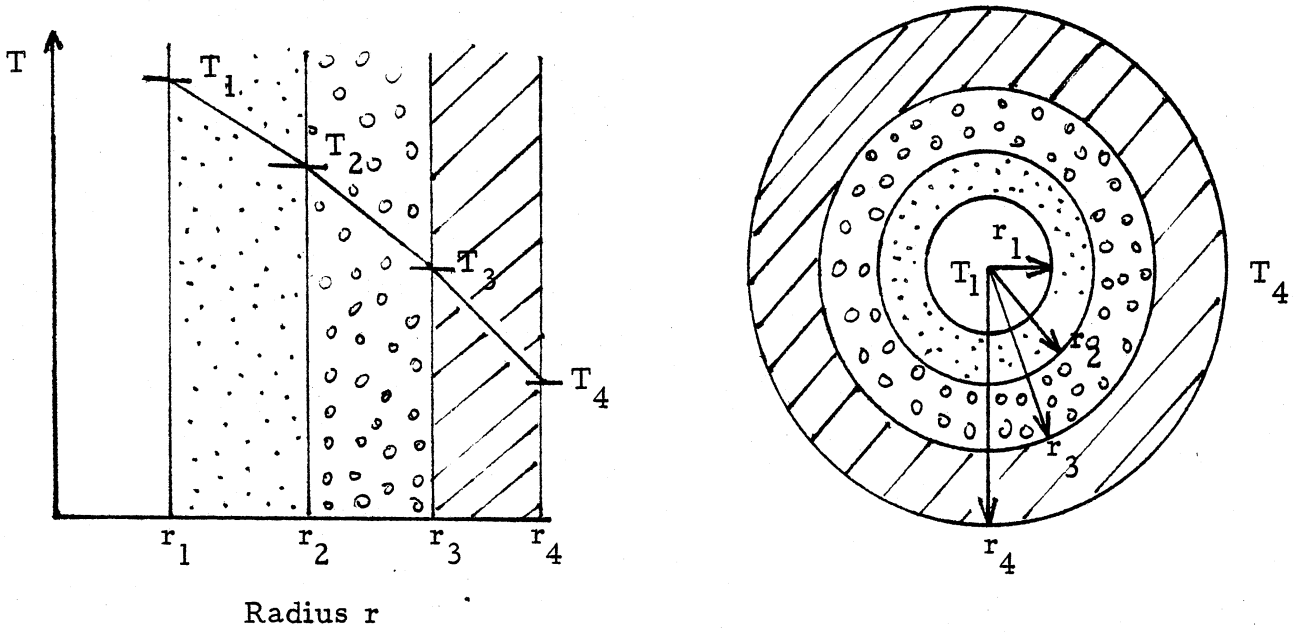

Fig. 3.4.2. Temperature Distribution in a Composite Cylindrical Wall of Three Different Materials

From the general relation, the heat flow through a cylindrical wall of three different materials can be written as:

$$\dot{Q} = \frac{2\pi L(T_1 - T_2)}{\left[\frac{\ln(\Delta r_1)}{k_1} + \frac{\ln(\Delta r_2)}{k_2} + \frac{\ln(\Delta r_3)}{k_3}\right]} \qquad (3.4.4)$$

where

$$\Delta r_1 = \frac{r_2}{r_1}$$

$$\Delta r_2 = \frac{r_3}{r_2}$$

$$\Delta r_3 = \frac{r_4}{r_3}$$

Eq. (3.4.4) is only a general relation, and can be expanded to include more than three different materials.

To determine the conductive heat flow through an object, certain parameters must be known. The thermal conductivity of each object must be known, along with its characteristic dimensions. The final parameter needed is the temperatures at the boundaries. If all of these can be determined, the heat flow due to conduction may be easily calculated.

B. Radiation-High Temperatures

Radiant heat transfer is an electromagnetic pheomenon similar to the transmission of light, radio waves, and x-rays. It is transmitted at the speed of light and is the result of body's temperature. Unlike conduction, radiant heat transfer can pass through a medium, such as air, without heating it appreciably. All substances emit radiant energy, and radiant heat is best transferred through a vacuum, such as outer space.

In order to intelligently discuss the laws of radiant heat transfer, the term black body must be defined. A black body is a theoretical substance that will absorb without reflection all of the radiant energy incident upon it at all wavelengths. It is also a perfect emitter of radiant energy. Though black bodies exist only in theory, it is possible to obtain black surfaces that will absorb up to 99% of the radiation incident upon them. This concept of a black body has been used to establish, both theoretically and experimentally, the Stefan-Boltzman law of radiation

which states:

The rate of radiant energy per unit area emitted by a black body is equal to a constant times the fourth power of the absolute temperature of the body. In equation form:

$$\dot{Q} = A\sigma T^4 \tag{3.4.5}$$

where $\dot{Q}$ = heat flow (BTU/ HR), A = area (FT^2), σ = Stefan-Boltzman constant, = 0.174×10^{-8} BTU/ HR $FT^2{}^oR^4$ and T = absolute temperature of the body (^oR).

Though no true black body exists, this concept has been used to measure the radiating effectiveness of actual radiating surfaces. This radiating effectiveness, termed emmissivity, is the ratio of the energy emitted from a body at a given temperature to the energy that would be emitted from a black body at the same temperature. In equation form,

$$\text{emissivity} = \epsilon = \frac{E \text{ (real body)}}{E \text{ (black body)}} \tag{3.4.6}$$

where

E = energy (BTU/ HR FT^2).

By using this notion of emissivity (ϵ), the Stefan-Boltzman law, Eq. (3.4.5) can be modified to account for the radiation actually emitted from a real or natural body as follows:

$$\dot{Q} = A\epsilon\sigma T^4 \tag{3.4.7}$$

where $\dot{Q}$ = heat flow (BTU/ HR), A = area (FT^2), σ = Stefan-Boltzman constant = 0.174×10^{-8} BTU/ HR $FT^2{}^oR^4$, ϵ = emissivity of the body, and T = absolute temperature of the body (^oR).

Eq. (3.4.7) applies to bodies found in nature which do not exhibit the black body characteristics of absorption and emission of all the radiant energy upon them. From this point on, these non-ideal black bodies will be referrred to as grey bodies.

When radiant energy strikes a material surface, part of the radiation is reflected, part is absorbed, and part is transmitted.

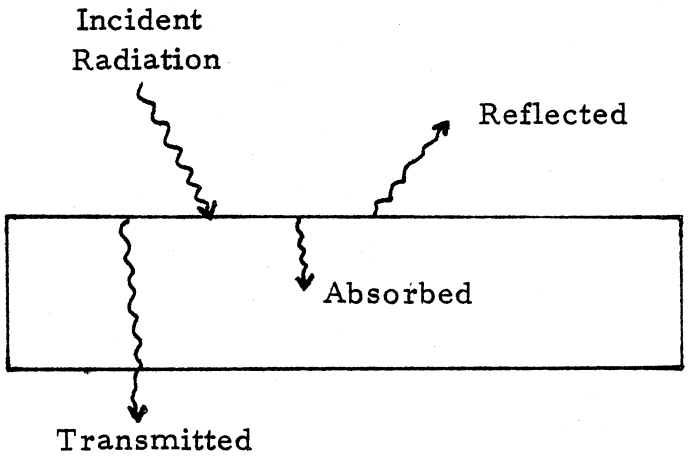

Fig. 3.4.3. Properties of Incident Radiation on a Material.

Now, defining the parameters,

ρ = reflectivity (% reflected)

α = absorptivity (% absorbed)

τ = transmissivity (% transmitted) .

The equality holds

$$\rho + \alpha + \tau = 1 \qquad (3.4.8)$$

Since most solid bodies generally do not transmit thermal radiation ($\tau = 0$), Eq. (3.4.8) may be written as,

$$\rho + \alpha = 1 \qquad (3.4.9)$$

Eq. (3.4.9) states that the amount of radiant energy that is refelcted plus the amount that is absorbed is equal to the amount of incident radiation upon the surface in question. Though simple, this relation is fundamental to an understanding of the concepts of radiant heat transfer.

The Stefan-Boltzman law, Eq. (3.4.5) applies to the energy emitted by a body. The net heat transfer which takes place between two radiating bodies depends upon the ability of each body to emit and absorb radiation, and upon the quantity of radiation emitted from each body that reaches the other body. Since radiation travels in straight lines and emanates equally in all unobstructed directions from all points on a radiating surface, the geometric factor involved in the net heat transfer between any two objects is extremely important. The net radiation heat transfer between two grey bodies can be written as follows, taking into account the aforementioned geometric factor:

$$Q = F_{\epsilon} F_G \sigma A (T_1^4 - T_2^4) \qquad (3.4.10)$$

where Q = heat flow (BTU/HR), F_{ϵ} = emissivity function, F_G = geometric view factor function, T = absolute temperature of body (^{o}R), σ = Stefan-Boltzman constant = 0.174×10^{-8} BTU/HR $FT^2\,^{o}R$, and A = area (FT^2). Eq. (3.4.10) brings in the concept of the shape factor, which is discussed in detail in Appendix E .

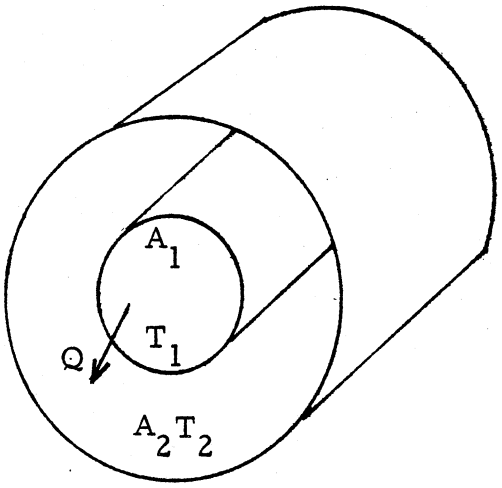

Fig. 3.4.4. Long Concentric Cylinders .

3.4.3.2 Temperature Extremes for Various Mission Profiles.

Temperatures are expected to vary according to the orientation of the orbiter. If the cargo bay is oriented towards the sun, the temperature can be expected to be quite high. On the other hand, if the cargo bay is oriented towards deep space, the associated temperature will be quite low. It is therefore extremely important that the specific mission profile is known in order to determine the expected temperatures. In the following discussion, orbiter bay temperature extremes will be displayed for certain points of interest in a typical mission profile. Next, various orientations of the shuttle orbit will be examined, along with corresponding predicted empty canister equilibrium temperatures.

(A) Orbiter Bay Temperature Extremes

The orbiter bay is expected to experience distinct temperature ranges during four key stages in the mission profile. These stages are prelaunch, on-orbit, and entry and post landing. In order to design the experiment to successfully function, it must be able to withstand these different temperature ranges in the mission profile. The temperatures listed below in Table 3.4.2 represent the extremes that can occur in the orbiter bay walls, considering all of the possible stages of flight.

TABLE 3.4.2.

Orbit Bay Temperatures - The Extremes

Temperature ^{o}F

Condition	Minimum	Maximum	Average Payload
Prelaunch	20	120	70
Launch	40	150	85
On-Orbit	-250	200	30-120
Entry and Post Landing	-50	200	50-130

The SCORE container should not experience more extreme temperatures than those listed in the Table, providing that excessive internal heat is not produced. The average values shown in Table 3.4.2, column 4, are estimates of the temperatures that the average payload can expect, by using specific temperature control devices integrated into the design.

(B) Orientation of the Shuttle Orbit

There are five basic attitudes that the orbiter may be oriented in during orbit. These are defined as hot, moderately hot, Earth viewing, moderately cold, and cold. To examine these different attitudes, several parameters must be defined. First, β is the angle between the orbit plane and the ecliptic plane. Next, the +z axis is directed vertically upward out of the cargo bay. Finally, Solar Inertial refers to a given parameter always pointing at the sun, while Local Vertical refers to a given parameter always pointing at the Earth.

The hot orbit is one in which $\beta = 90^{\circ}$ and the +z axis is Solar Inertial. During this type of orbit, the orbiter sees the sun 100% of the time. The moderately hot orbit is one in which $\beta = 45^{\circ}$ and the nose of the orbiter is oriented 55° from Solar Inertial. During this orbit, the orbiter is exposed to the sun 63% of the time, and is in the Earth's shadow 37% of the time. The Earth viewing orbit refers to an orbit in which $\beta = 0^{\circ}$ and the +z axis is Local Vertical. During this orbit, the orbiter is exposed to the sun 59% of the time, and enveloped in the Earth's shadow 41% of the time. The next type of orbit is the moderately cold one, in which $\beta = 45^{\circ}$, as in the case of the moderately hot orbit. In this case though, the -z axis is Solar Inertial, and the orbiter again sees the sun 63% of the time, and is in the Earth's shadow 37% of the time. Finally, the cold orbit is one in which $\beta = 90^{\circ}$ and the -z axis is Local Vertical.

This orbit, like the hot one, allows the orbiter to experience the sun 100% of the time, but the cargo bay is never directly exposed to the sun. To develop a better understanding of these different orbits, a visual comparison is made in Figure 3.4.5.

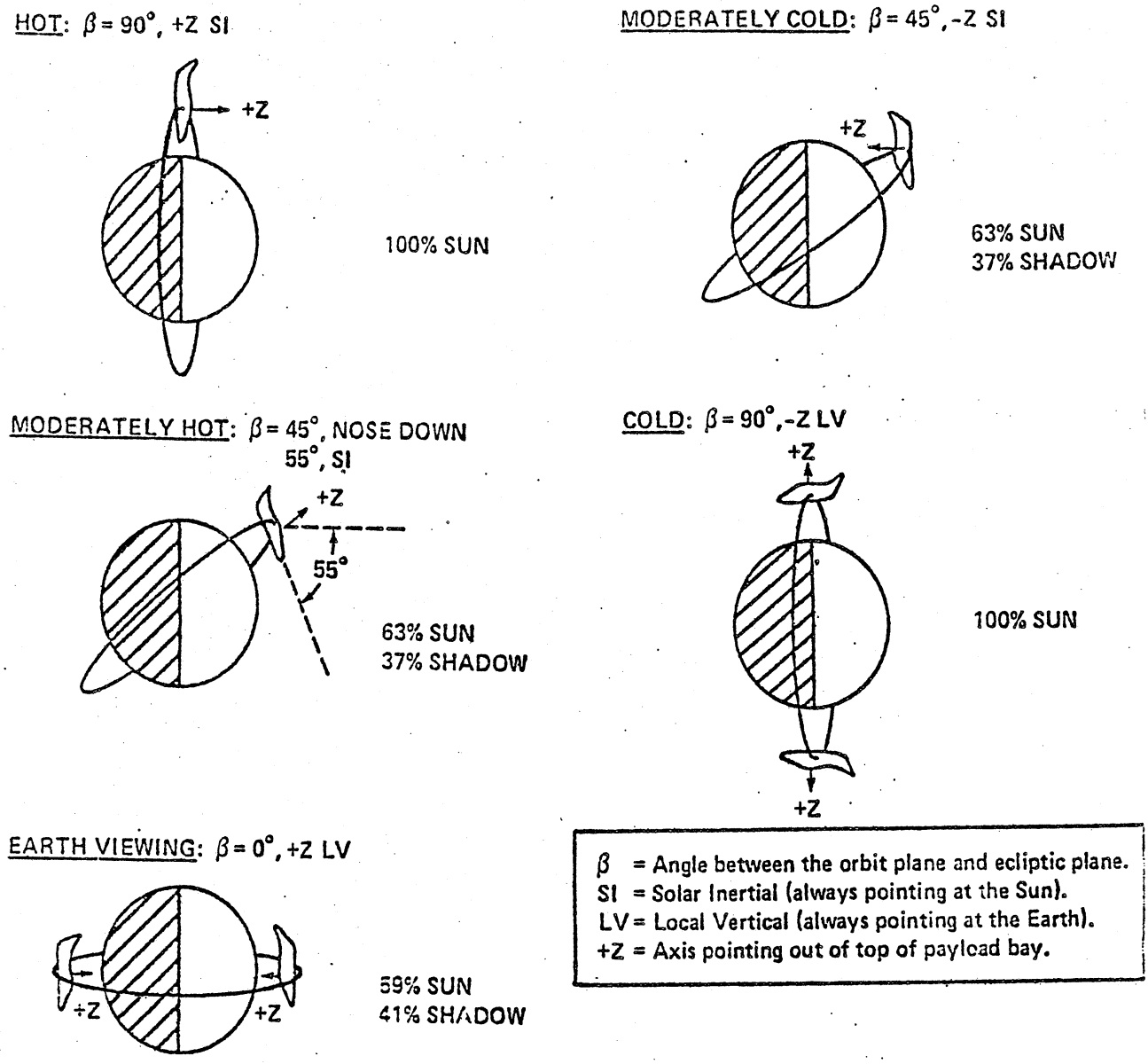

Fig. 3.4.5. Attitude Orientations of the Orbiter [3].

(C) Predicted Empty Canister Equilibrium Temperatures for Various Orbiter Attitudes

For the preceding description of different attitudes, preliminary theoretical results of empty SCORE canister predicted equilibrium temperatures have been compiled and appear in Table 3.4.3. These temperatures vary according to whether the canister is insulated or not. Values of heater power needed to maintain a minimum temperature of 32°F are also included for insulated and non-insulated canisters. Though these values are not intended to represent absolute values used in the ultimate design, they will help to orient the reader to the magnitude of the temperature variations, and the possible alteration of these temperatures.

TABLE 3.4.3.

Predicted Empty Canister Equilibrium Temperatures
For Different Orbital Attitudes

Orbital Attitude	Heater Power (Watts) Needed to Maintain a Minimum Temperature of 32° F		Insulated No Heater
	No Insulation	Insulated	Temperature °F
Hot	------	-------	110
Moderately Hot	------	-------	35
Earth Viewing	118	2.2	5
Moderately Cold	293	5.4	-50
Cold	553	10.3	-296

3.4.3.3. Types of Temperature Control Systems. There are three types of temperature control systems that could be incorporated in the SCORE canister. They fall under the dategories of passive, semi-passive, and active.

Passive temperature control systems incorporate coatings of suitable emissivity and absorptivity, or the use of insulation. Certain well chosen coatings can be used to protect the SCORE canister from the sun's radiation. The use of insulation of a specified thickness and thermal conductivity can be used to retard the heat transfer by conductive means.

Semi-passive temperature control systems may be needed to control the canister temperature more efficiently. These incorporate coatings and insulation in conjunction with internal heaters, shutters, heat pipes, and change of phase material. Though generally more complex, they allow better temperature control of the canister.

Active temperature control systems involve the use of pumps or radiaters to dissipate any internally generated heat. These systems are more than likely too complicated for our needs, and are not suggested for consideration. Besides their complexity, they require an appreciable volume of the SCORE canister, something that is already quite limited.

3.4.3.4. Suggestions for Future Consideration. In order to efficiently design the canister for thermal protection, there are many considerations. The most important is to determine the temperature limits that the payload can withstand and continue to function. These limits are then designed for by careful selection of the temperature control system best suited to maintain the stated limits. In the selection of this particular system, parameters such as internally generated heat due to batteries and equipment, along with exposure time to the sun or deep space must be considered. Judicious selection of coatings, insulation, an internal heater, etc., along with a desired compatible orbit orientation will enable the payload to function effectively as an autonomous research experiment completely independent of the orbiter.

In the subsequent design, the determination of these thermal parameters is extremely important. Without an effective thermal protection scheme, the SCORE payload will not be able to withstand the harsh environment encountered during orbit, and the malfunction or destruction of the equipment enclosed is inevitable.

REFERENCES

[1] Durham, Franklin P., Thermodynamics, 2nd Edition, New Jersey, Prentice-Hall, 1959.

[2] Holman, J. P., Heat Transfer, 4th Edition, New York, McGraw-Hill, 1976.

[3] NASA, Space Transportation System-Small Self-Contained Payload Program, Washington, D.C., Government Printing Office 1977.

[4] NASA, Experimenter Handbook, Washington D.C., Government Printing Office, 1978.

[5] *Simms-Bendix, "Temperature Control System Devices,"

[6] * "V-Thermal Considerations."

[7] * "Thermal Analyses."

* 482 Library

3.5. The Canister and Packaging -- John K. Moore

3.5.1. Introduction

On each Space Shuttle flight, there will be one or more large experiments on board, called "primary payloads." These payloads will not always occupy all the available space in the payload bay of the orbiter which is the reason why NASA can provide canisters to hold smaller experiments which would take advantage of this extra space. These smaller experiments or Get-Away Special (GAS) Payloads as they are called are to be self-contained; that is, they will not be allowed to draw upon any Shuttle services beyond three on-off controls to be operated by the crew. Power, heating and data handling facilities must be provided within each GAS canister.

Each GAS payload must have:

1. Mounting lugs or surfaces to attach to the experiment mounting plate furnished by NASA.

2. A configuration which will fit into the NASA provided cylindrical canister.

3. A weight not exceeding 200 lbs.

4. A volume not more than 5 ft^3.

3.5.2. Discussion

There will be two available canister sizes, 5 ft^3 and either a 2.5 or 1.5 ft^3 size. The 1.5 ft^3 canister has a minimum (no options) cost of $3,000. The other volumes, 2.5 ft^3 and 5.0 ft^3 are available at prices of $5,000 and $10,000, respectively. All prices are based on 1975 dollars.

The internal dimensions of all canisters will accomodate a payload of 19.75 inches in diameter. The length of the canister will vary depending on its' volume. Figure 3.5.1. indicates these dimensions as a function of payload volume.

Payload Wt. (Lbs.)	Payload Volume (Cu. Ft.)	Payload Size (Dia. × Height, inches)
200	5	19.75 × 28.25
100	2½	19.75 × 14.13
60	1½	19.75 × 8.46

Figure 3.5.1. Canister dimensions as a function of payload volume.

Each experiment must be mounted on a shipping mounting plate which is provided by NASA. The shipping mounting plate will have a bolt hole pattern identical to the flight experiment mounting plate. The experiment will be transferred to this plate at a NASA facility and then attached to a canister. The bolt pattern of the experiment mounting

plate is given in Fig. 3.5.2. [3] . This mounting plate will become the top of the canister. The canister top will be insulated except when heat dissipation is required or when a window or port, if available (at an extra cost), is required. The sides and bottom of the canister will also be insulated; thus making it easier to control the temperature within the canister itself. The empty canister temperature range for the extremes of orbital altitudes will be between $0^{\circ}C$ ($32^{\circ}F$)(as maintained by heaters provided by the experimentor) and $43.3^{\circ}C$ ($110^{\circ}F$). For the most extreme temperatures anticipated, the 5 ft^3 canister with a 200 lb. payload will have a temperature range of $-60^{\circ}F$ to $80^{\circ}F$.

3.5.3. Orientation

The canisters will be mounted with the experiment mounting plate always directed towards the outside of the payload bay. There are, however, two different GAS canister ground handling orientations. During the insertion of the mounting plate and attached experiment, and during checkout and transportation, the canister's major axis will be vertical. After the canister is installed in the payload bay, the orientation of the major axis will be perpendicular to that of the Shuttle. Current Shuttle preparation schedules indicate that the canister's major axis will be vertical at least 80% of the time between insertion of the experiment into the canister and launch. This information must be specifically considered if wet cell batteries, for example, are to be used. The ground orientation is shown pictorially in Fig. 3.5.3.

GET AWAY SPECIAL
SMALL SELF-CONTAINED PAYLOADS

STANDARD EXPERIMENT MOUNTING PLATE

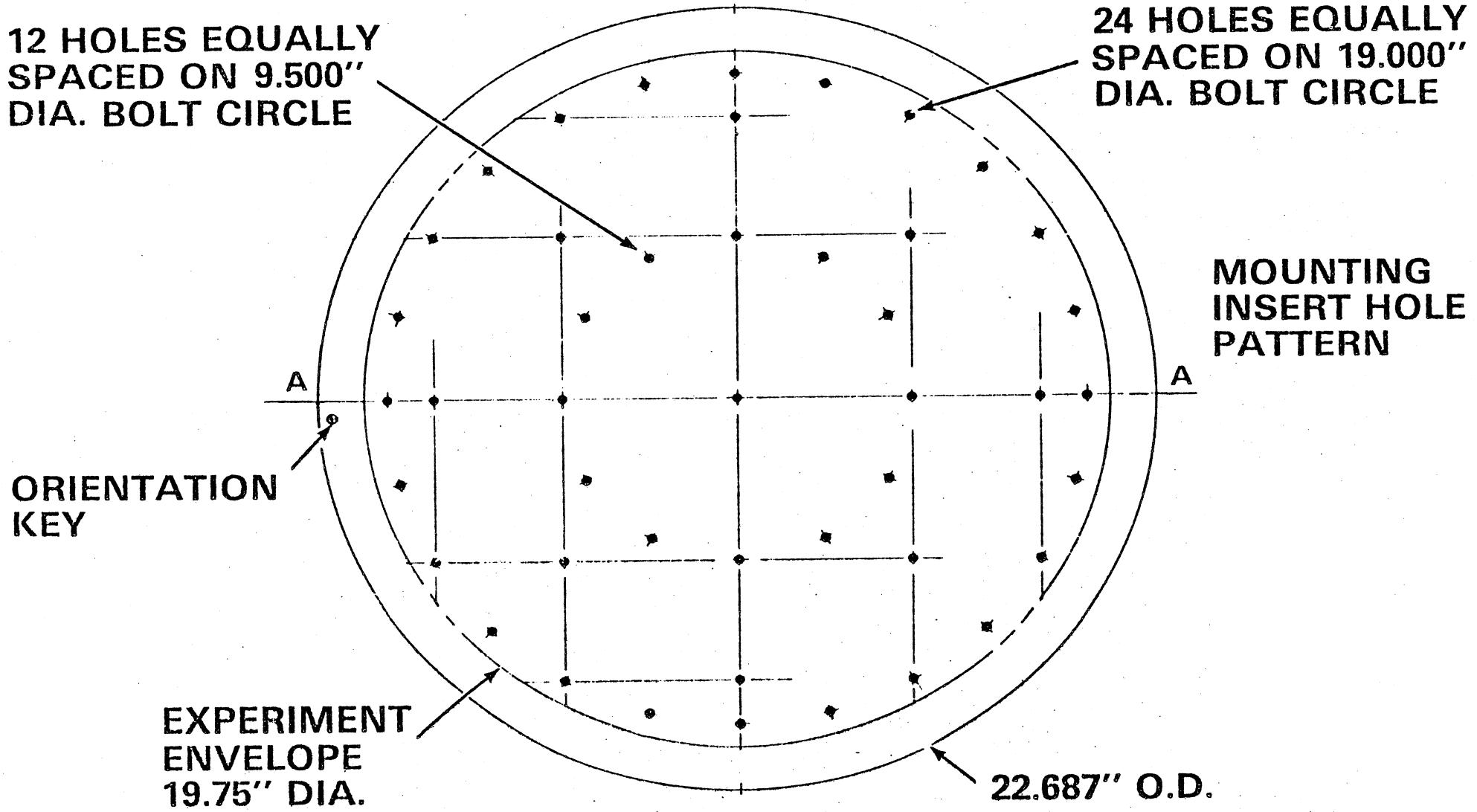

Figure 3.5.2

GET AWAY SPECIAL
SMALL SELF-CONTAINED PAYLOADS

CONTAINER GROUND ORIENTATION

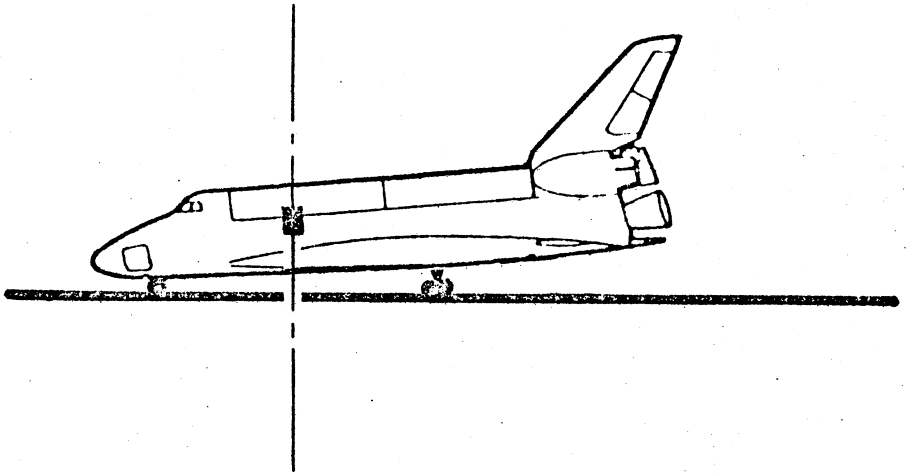

CONTAINER MAJOR AXIS NEARLY
VERTICAL AT INSTALLATION
AND AFTER LANDING

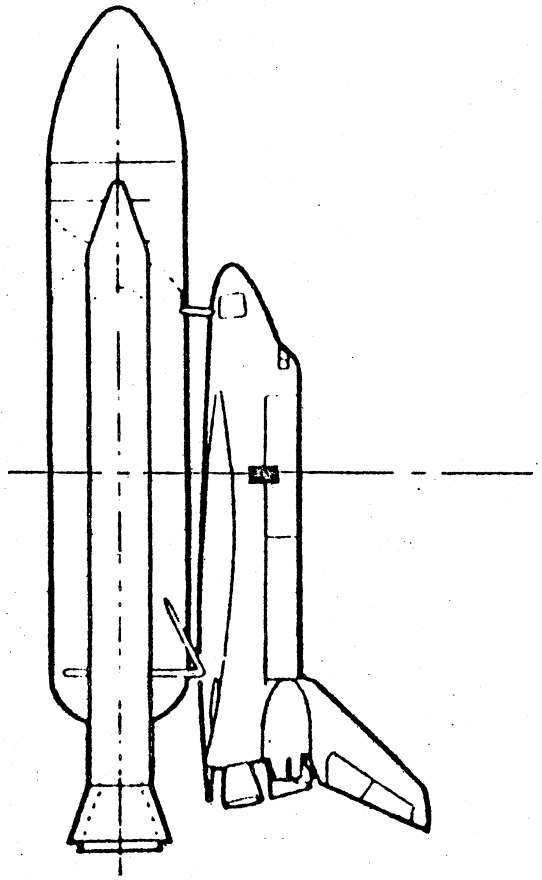

CONTAINER MAJOR AXIS
HORIZONTAL ON LAUNCH PAD

Fig. 3.5.3. [3].

3.5.4. Pressurization

It is possible to pressurize the canister to approximately one atmosphere. Venting of the canister is possible also, which will allow it to be in equilibrium with the vaccum in space. The payload vent sequence is shown in Fig. 3.5.4.

Prelaunch	Closed (vent no. 6 in purge position)
Lift-off (T = 0)	Closed
T + 10 seconds	All open
Orbit insertion	All open
On orbit	All open
Preentry preparation	All closed
Entry (high heat zone)	All closed
Atmospheric (75 000 ±5000 feet (23 ± 1.5 kilometers)) to landing	All open
Postlanding purge	Closed (vent no. 6 in purge position)

Fig. 3.5.4. Payload Vent Sequence

3.5.5. Window/ Lid

If available, an optional window may be installed in the top of the canister which could be as large as eight (8) inches in diameter. A lid in the canister top could also be available which would be opened and closed according to commands given from the crew.

3.5.6. Internal Structure

The bottom three (3) inches of every canister will contain NASA interface equipment such as the control signal relays and vents. This bottom area is shown in relation to the remaining dimensions of the canister in Fig. 3.5.5.

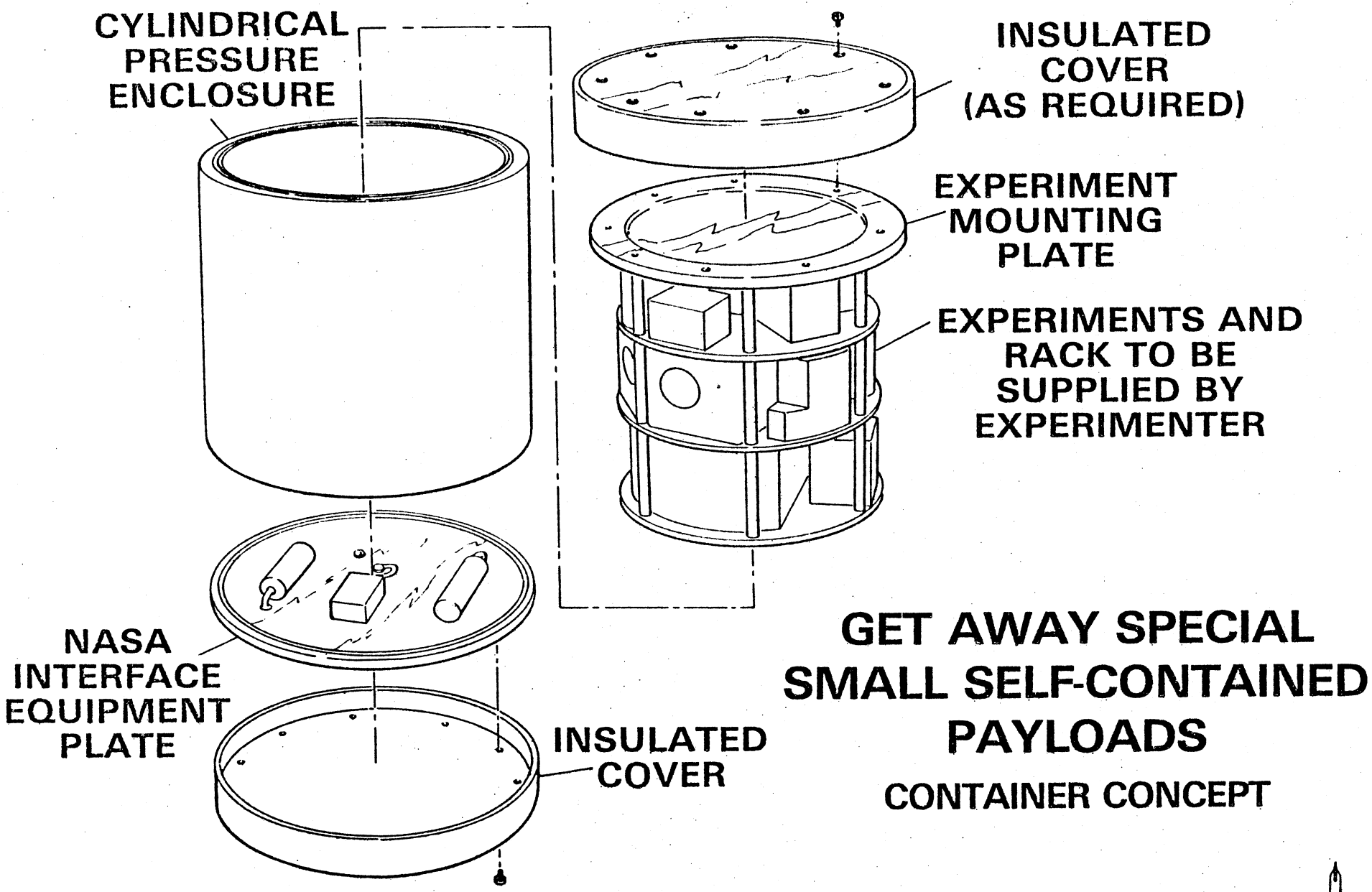

Fig. 3.5.5. Canister Dimensions . [3] .

The interior of the canister may be subdivided if the need arises. There are three basic structures which can be installed, at the experimentor's expense, to solve any subdivision problem.

1. Shelves may be constructed which are supported by bars or channels. An example of this is shown below. This type of structure would provide good thermal isolation for the end plate, but easy access

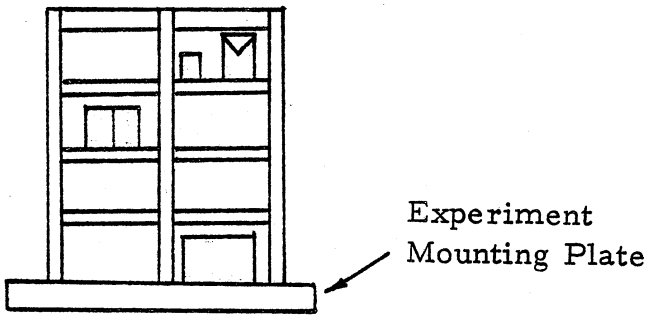

to experimental components is restricted to the outside of the shelves.

2. A central tube can be used to support the shelves, which would provide easy access to the shelves. Any wires that are needed may be run throughout the inside of the tube and accessed accordingly.

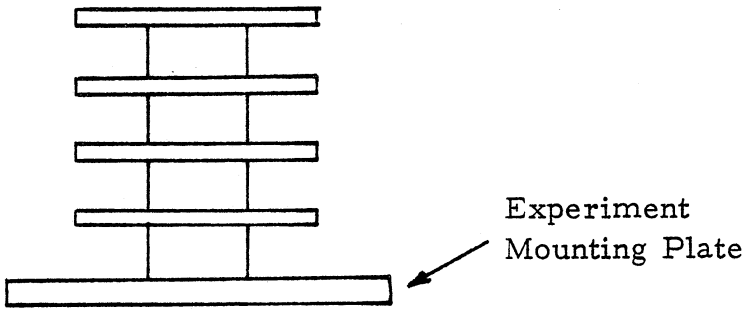

GET AWAY SPECIAL SMALL SELF-CONTAINED PAYLOADS

5.0 CU. FT. (NET) CONTAINER

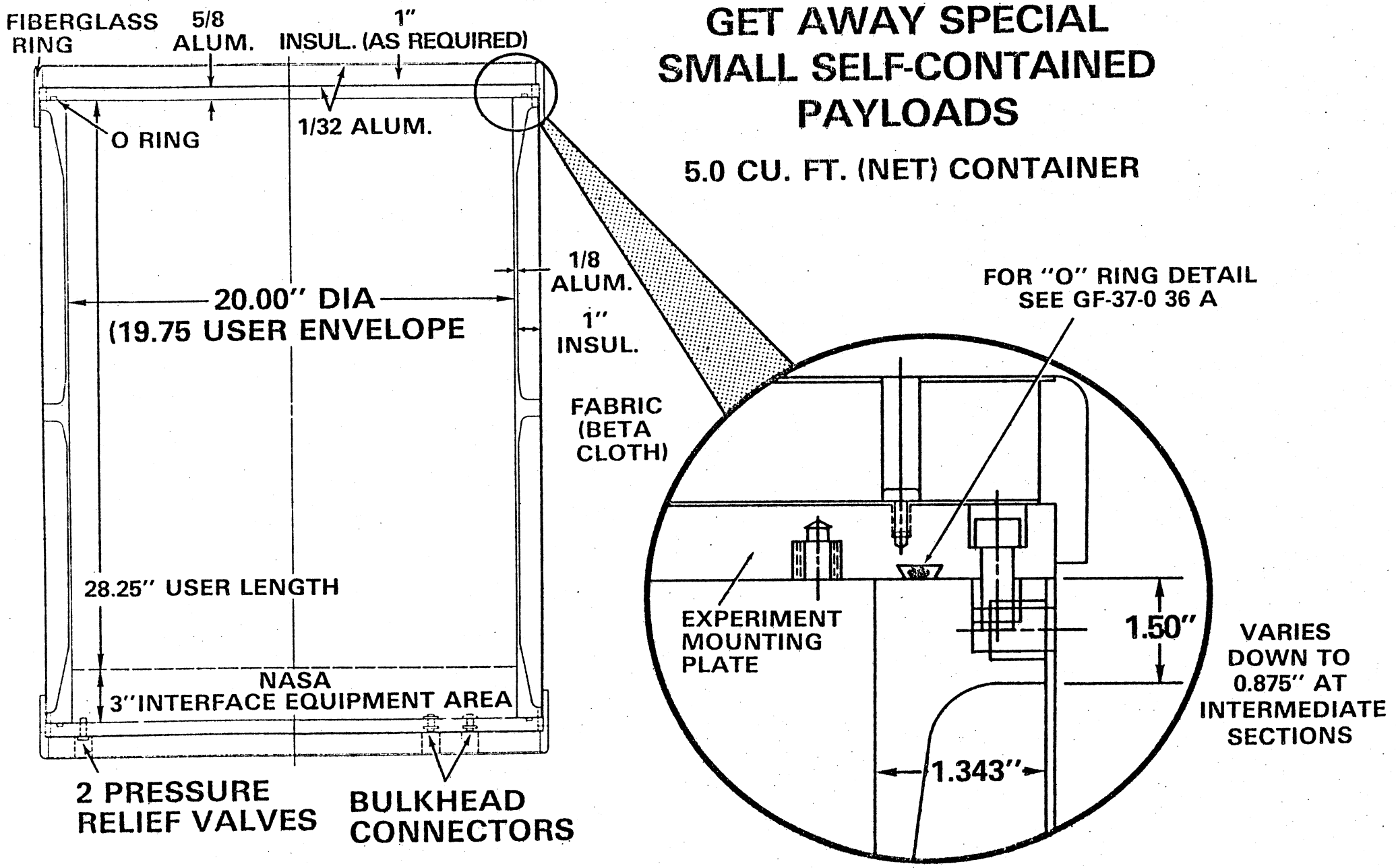

3. Radial webs may be used to separate the experiments while still providing good access to the mounting plate.

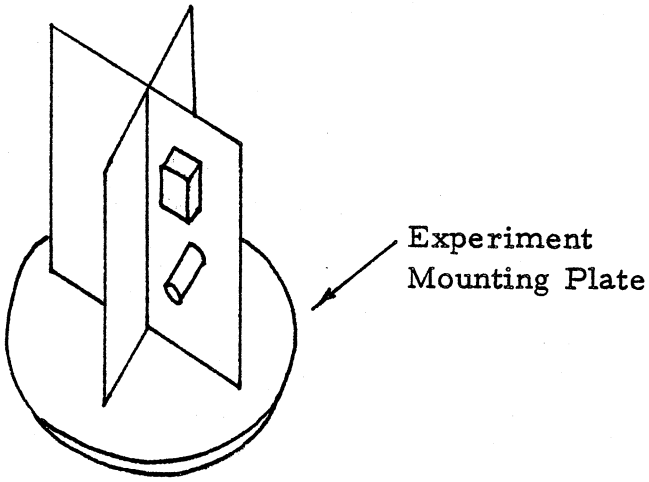

References

[1] NASA Publication, "Space Transportation System -- Small Self-Contained Payload Program," August 1978.

[2] NASA Publication, "Space Transportation System -- Users Handbook," July 1977.

[3] NASA Publication, "Getaway Special (GAS) Small Self-Contained Payloads," Experimenter Handbook, Dec. 1978.

4. EXPERIMENTS

4.1. Temperature Measurements -- John K. Moore

4.1.1. Introduction. The measurement of temperature is usually accomplished by the use of a thermocouple or a thermistor. The main difference between the two is that a thermocouple circuit needs an amplifier, whereas a thermistor does not. The addition of an amplifier would greatly increase the cost, complexity and volume needed to measure temperature. A thermocouple and a thermistor are roughly equal in size and sensitivity. On the basis of the above considerations, the use of thermistors is recommended for SCORE.

4.1.2. Discussion. The standard size of a thermistor is shown in Figure 4.1.1. Inside the bulb of the thermistor is a small plate to

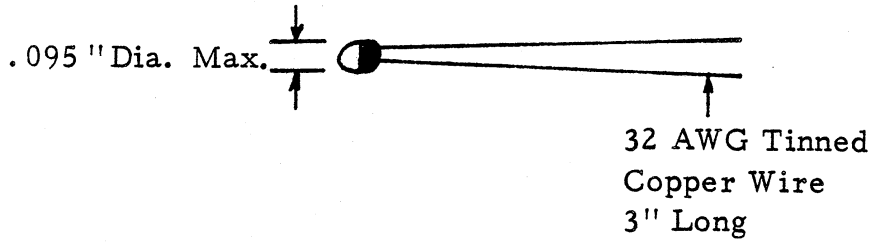

Figure 4.1.1. Standard Size Thermistor .

which the two lead wires are connected, one to each side. Since the resistance of the thermistor varies greatly with temperature, the temperature of the thermistor is found by measuring the resistance across the plate. A resistance versus temperature chart for a Y. S. I. (Yellow Springs Instrument) 44008 thermistor is given in Figure 4. 1. 2. [4]. Most of the information that has been collected dials with this particular thermistor. The 44008 thermistor has been used on previous temperature measurement missions into space and is recommended for use in the SCORE payload.

RESISTANCE VERSUS TEMPERATURE —40° to +150°C

TEMP°C	RES	TEMP°C	RES	TEMP°C	RES	TEMP°C	RES	TEMP°C	RES	TEMP°C	RES	TEMP°C	RES
−40	884.6K	−10	158.0K	+20	37.30K	+50	10.97K	+80	3843	+110	1550	+140	701.2
39	830.9K	9	150.0K	21	35.70K	51	10.57K	81	3720	111	1507	141	684.1
38	780.8K	8	142.4K	22	34.17K	52	10.18K	82	3602	112	1465	142	667.5
37	733.9K	7	135.2K	23	32.71K	53	9807	83	3489	113	1425	143	651.3
36	690.2K	6	128.5K	24	31.32K	54	9450	84	3379	114	1386	144	635.6
35	649.3K	5	122.1K	25	30.00K	55	9109	85	3273	115	1348	145	620.3
34	611.0K	4	116.0K	26	28.74K	56	8781	86	3172	116	1311	146	605.5
33	575.2K	3	110.3K	27	27.54K	57	8467	87	3073	117	1276	147	591.1
32	541.7K	2	104.9K	28	26.40K	58	8166	88	2979	118	1241	148	577.1
31	510.4K	− 1	99.80K	29	25.31K	59	7876	89	2887	119	1208	149	563.5
−30	481.0K	0	94.98K	+30	24.27K	+60	7599	+90	2799	+120	1176	+150	550.2
29	453.5K	+ 1	90.41K	31	23.28K	61	7332	91	2714	121	1145		
28	427.7K	2	86.09K	32	22.33K	62	7076	92	2632	122	1114		
27	403.5K	3	81.99K	33	21.43K	63	6830	93	2552	123	1085		
26	380.9K	4	78.11K	34	20.57K	64	6594	94	2476	124	1057		
25	359.6K	5	74.44K	35	19.74K	65	6367	95	2402	125	1029		
24	339.6K	6	70.96K	36	18.96K	66	6149	96	2331	126	1002		
23	320.9K	7	67.66K	37	18.21K	67	5940	97	2262	127	976.3		
22	303.3K	8	64.53K	38	17.49K	68	5738	98	2195	128	951.1		
21	286.7K	9	61.56K	39	16.80K	69	5545	99	2131	129	926.7		
−20	271.2K	+10	58.75K	+40	16.15K	+70	5359	+100	2069	+130	903.0		
19	256.5K	11	56.07K	41	15.52K	71	5180	101	2009	131	880.0		
18	242.8K	12	53.54K	42	14.92K	72	5007	102	1950	132	857.7		
17	229.8K	13	51.13K	43	14.35K	73	4842	103	1894	133	836.1		
16	217.6K	14	48.84K	44	13.80K	74	4682	104	1840	134	815.0		
15	206.2K	15	46.67K	45	13.28K	75	4529	105	1788	135	794.6		
14	195.4K	16	44.60K	46	12.77K	76	4381	106	1737	136	774.8		
13	185.2K	17	42.64K	47	12.29K	77	4239	107	1688	137	755.6		
12	175.6K	18	40.77K	48	11.83K	78	4102	108	1640	138	736.9		
11	166.6K	19	38.99K	49	11.39K	79	3970	109	1594	139	718.8		

Figure 4. 1. 2. Resistance Versus Temperature [4].

It can be seen from this chart that as the temperature increases, the resistance decreases.

4.1.3. Circuitry. A typical thermistor circuit is shown in Figure 4.1.3. where:

1. The power supply (A. C. or D. C.) has to be regulated in order to avoid errors in the voltage output (V_o). The standard value for the power needed is based on data recording specifications and ranges from zero to five volts. The value usually used is five volts and will be done so in future examples.

2. R represents an arbitrary resistance whose value needs to be determined according to the temperature range the circuit will be measuring. The determination of this R value will be discussed later.

3. R_{TH} represents the resistance value of the thermistor used. For example, the U. S. I. 44008 thermistor has a R_{TH} equal to 30K ohms. Different types of thermistors will have different R_{TH} values.

4. V_o is the output voltage.

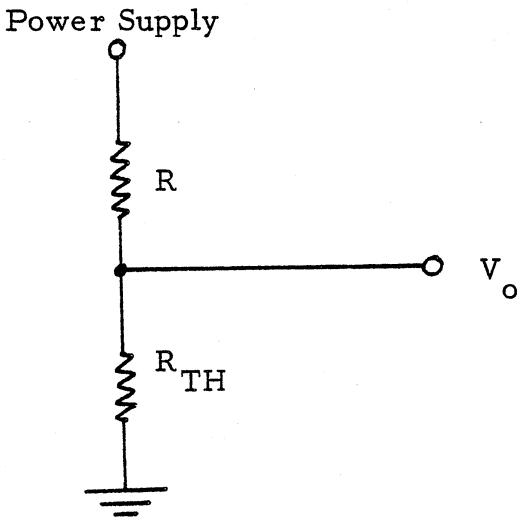

Figure 4.1.3. Typical Thermistor Circuit.

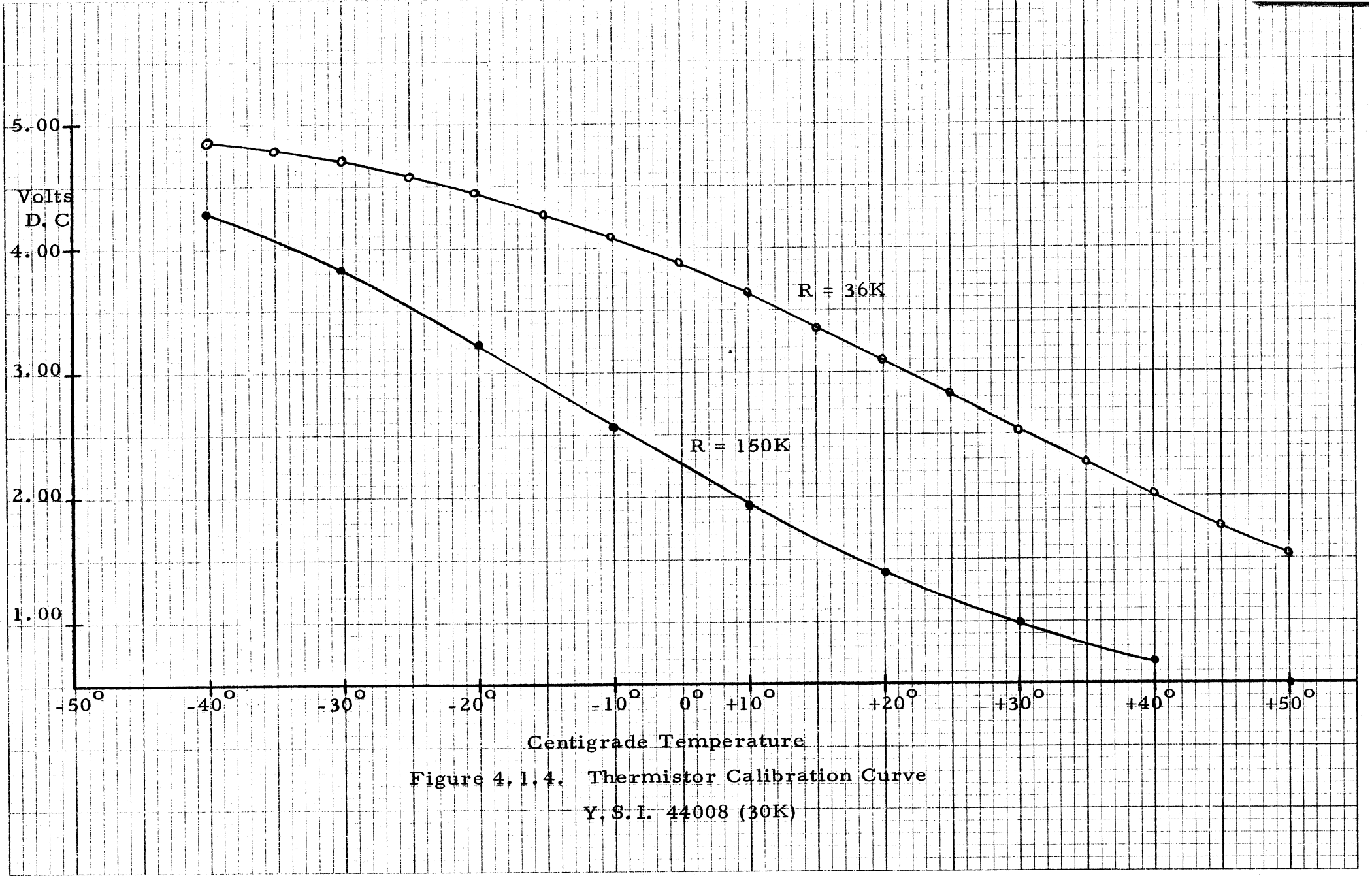

Figure 4.1.4. Thermistor Calibration Curve

Y.S.I. 44008 (30K)

The output voltage is the quantity that needs to be recorded by a recording device. After the data is received and stored in space, the voltage readings are then transferred to temperature readings on Earth by the use of a thermistor calibrations curve, which is specialized for each different type of thermistor used. A calibration curve for a Y. S. I. 44008 (30 kΩ) thermistor is shown in Figure 4. 1. 4. This curve is shown with two different values of R, 36 kΩ and 150 kΩ, for comparison. It is this R value which was shown in the circuit diagram of Figure 4. 1. 3. It can be seen that the two different curves are linear in different temperature regions. As the R value increases, this region of the curve gets shifted to the left. As the negative slope increases for these curves the sensitivity increases also, because for a small increase in temperature there is a corresponding large increase in voltage. Therefore, to get the highest degree of sensitivity on R value should be chosen which will place a steep section of the calibration curve near the middle of the expected temperature range.

By the use of simple calculations, we can solve for V_o in the circuit of Figure 4. 1. 3. as shown below in Figure 4. 1. 5.

From the chart of Figure 4.1.2., the resistance for certain temperatures is given in Figure 4.1.6. V_o is calculated by the use of the equation

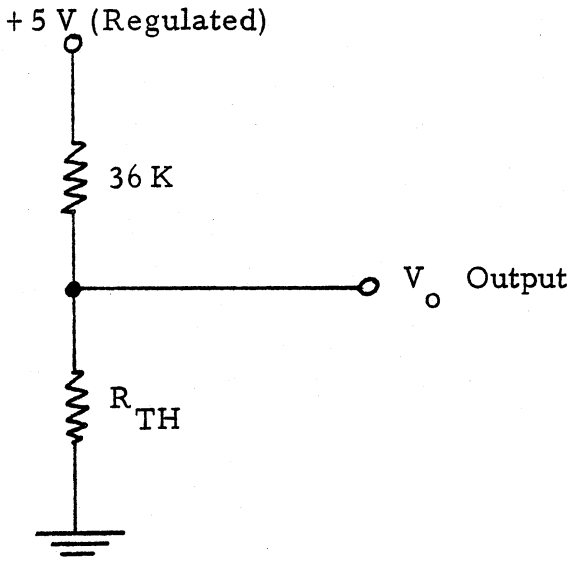

Figure 4.1.5. Solving for V_o in a Thermistor Circuit.

Certain Resistance Temperatures

$T(^oC)$	$R_{TH}(K\Omega)$	$V_o(V)$
0	94.98	3.63
25	30.00	2.273
50	10.97	1.17

Figure 4.1.6.

$$V_o = \frac{R_{TH}}{R_{TH} + 36\,K\Omega} \times 5\,V \qquad (4.1.1)$$

where the values 36 K Ω and 5 V are being used as examples and could vary from one case to another. There will be a small percentage of

error in the value for V_o due to the fact that any data recording device will have an input resistance. The error is calculated as follows: For example, if a recorder has a 1 megaohm input resistance and is at 25° C, the circuit of Figure 4.1.3 would look like Figure 4.1.7. below.

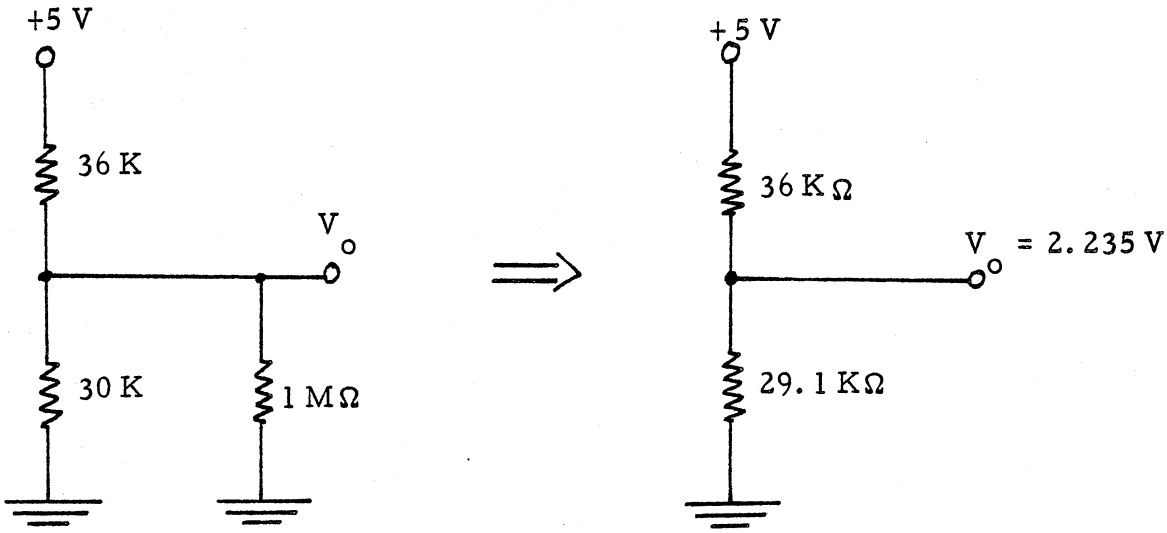

Figure 4.1.7. Thermistor Circuit at 25° C.

V_o is calculated by using Eq. 4.1.1. From Figure 4.1.4 for the same conditions (25°C and R_{TH} = 30 KΩ) the value for V_o equaled 2.273V. The difference between the V_o value for a circuit with a recording device attached and the one without is (2.273 - 2.235)V = .038V. Therefore, the percent error is E = .038V/ 2.273V x 100 = 1.67% .

4.1.4. Power. The power needed by the thermistor at a given temperature is calculated by using the equation

$$\text{Power} = \frac{[\text{ Power Supply (V)}]^2}{R + [\text{ resistance for given temperature }]}$$

So, at 25°C, the power needed is

$$P = \frac{5V \times 5V}{66K\Omega} = .38 \text{ milliwatts}$$

The maximum power that could ever be needed would be if R_{TH} equalled 0Ω in which case

$$P = \frac{5V \times 5V}{36K\Omega + 0\Omega} = .69 \text{ milliwatts}$$

4.1.5. Current. The current drawn by a thermistor circuit is calculated as follows. For instance, for N thermistor circuits linked together as shown in Figure 4.1.8., the current drawn would be $i = \frac{5V}{36K\Omega/N}$. So if N = 2, then i = 28 milliamperes. A number of thermistors would be liked together like this if just one circuit didn't want to be relied upon, or if widely varied temperature ranges were expected.

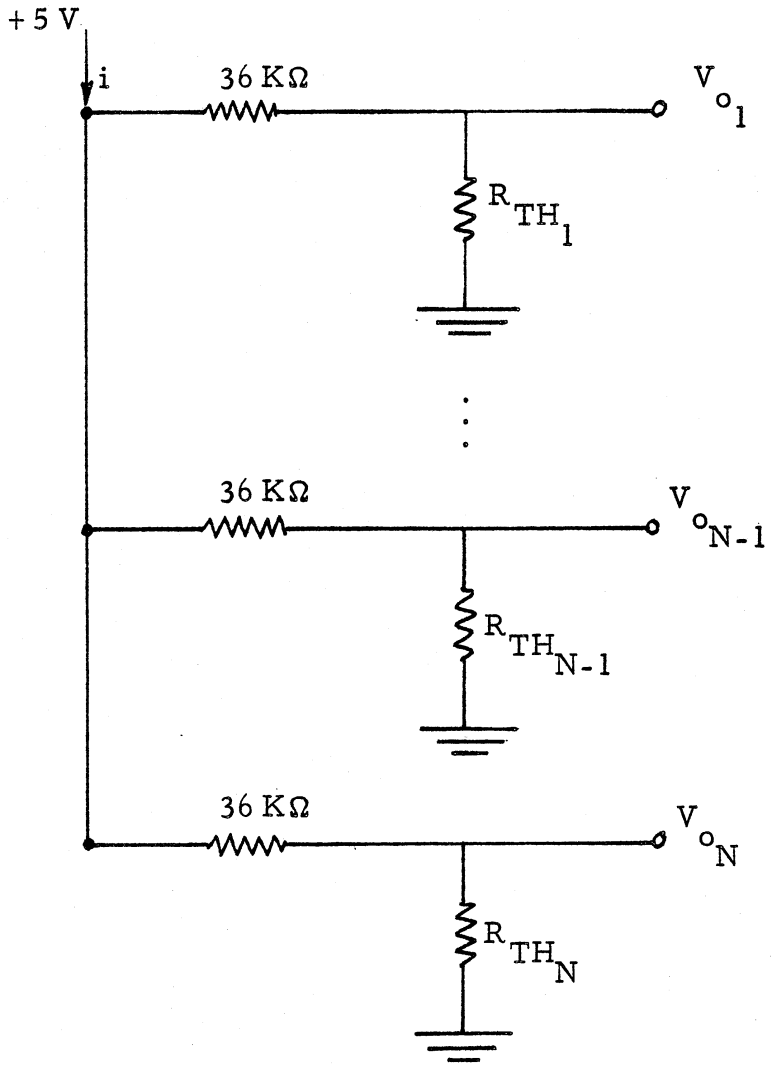

Figure 4.1.8. An N Thermistor Circuit.

The output values V_{o_1} thru V_{o_N} would be alternately read by the recording device through the use of a commutator. The commutator is a device which acts as an automatic switch such as that depicted in Figure 4.1.9. The commutator is linked in series with an A to D convertor and the data recorder itself. All three devices are available commercially as one complete unit whose size, weight and cost would depend upon the data handling capability and other options.

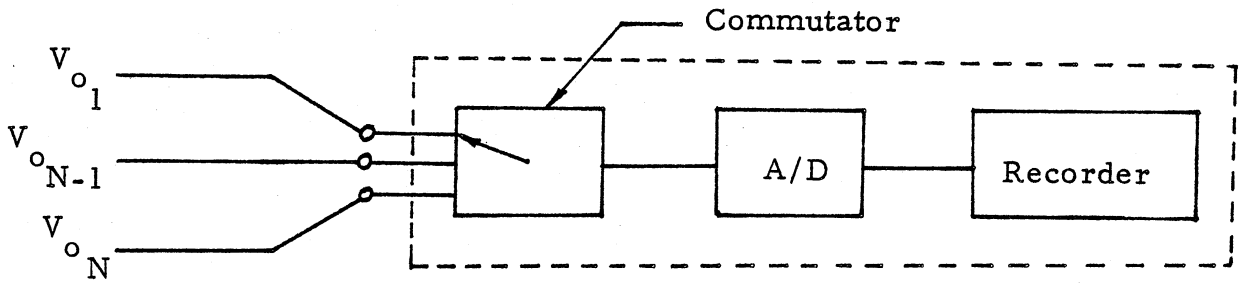

Figure 4.1.9.

4.1.6. Cost. The cost of setting up the remainder of the circuit would depend upon how many thermistors and resistors that are needed. The average price of a thermistor is $7.00. There are reductions in price as the quantity bought increases. The average price for a resistor is $1.00 and varies slightly with size. The given prices are based on available 1976 information from Allied Electronics [3].

4.1.7. Thermistor Attachment. An isolated thermistor in space cannot detect temperature due to the vacuum conditions. Therefore, thermistors are required to be attached to a nearby surface so that its temperature may be measured and used as that of the environment [1].

The thermistor(s) will have to be attached to an inner surface of the SCORE canister. Since the bottom and sides of the canister will be insulated, a thermistor would have to be attached to the canister top. A

thermistor is physically attached to a surface by applying a drop or two of epoxy to each and joining them. A thermistor may also be imbedded into a surface with the epoxy holding it in place.

References

[1] Sachse, Herbert B., Semiconducting Temperature Sensors and their Applications, 1975.

[2] Benedict, Robert P., Fundamentals of Temperature, Pressure and Flow Measurements, 1959.

[3] Allied Electronics 1976 Engineering Manual and Purchasing Guide, No. 750.

[4] Mr. John R. Caldwell, Sr. Research Associate Engineer, Space Physics Research Laboratory, The University of Michigan.

I would like to express special thanks to Prof. Caldwell from Space Research for his assistance in the writing of this chapter.

4.2. Linear Accelerometer -- Raymond T. Bush

4.2.1. Introduction. Acceleration of the Shuttle orbiter may vary from 10^{-7} g's to 5 g's. The steady-state acceleration in orbit is very small, typically in the 10^{-4} g range. This experiment proposes to measure the thrust acceleration (at launch) and the aerodynamic acceleration (during reentry) of the orbiter with a linear accelerometer. An accelerometer is a mechanical or electromechanical instrument that measures acceleration. The two general types of accelerometers measure either the translational or angular acceleration. Linear accelerometers are usually directional, measuring the acceleration along one axis or in one direction. Three of these accelerometers can be used together to form a triaxial accelerometer which measures the acceleration in three directions or components (X, Y, Z axes). Bendix Aerospace Systems Division in Ann Arbor is building an aerodynamic coefficient identification package (ACIP) for NASA which will be put on the Shuttle orbiter. This package will contain a triaxial accelerometer which will measure the orbiter's accelerations. An omni-directional accelerometer was developed in the late 1950's by the University of Michigan's Aerospace Engineering Department. This accelerometer was used in the falling sphere method to determine upper air densities. It measures the resultant linear acceleration.

4.2.2. Summary. An omni-directional accelerometer is available for use at no cost. Project SCORE can use an accelerometer that was developed here at the University for past experimentation. However, calibration and testing of the accelerometer will require a slight expense. The purchase of a triaxial accelerometer, though, would be very expensive. The omni-directional accelerometer can be used from .01 g's to 10 g's. It weighs about 2 pounds and has a volume of about 430 cm^3. The accelerometer will draw 19 watts of power for approximately 15 minutes. Considering the availability, cost, size, weight, and operational characteristics, the omni-directional accelerometer is the most effective instrument to use in this experiment. The results of this experiment can then be compared with NASA's flight profile of acceleration versus time. Since NASA is using a triaxial accelerometer, the resultant acceleration can be determined from the component or axial accelerations.

4.2.3. The Accelerometer System. The omni-directional transit-time accelerometer, as it is formally called, was developed at the University of Michigan's High Altitude Engineering Laboratory [1]. The system to be incorporated in the Getaway Special will include an intervalometer along with the accelerometer. The omni-directional accelerometer measures the resultant linear acceleration of a body. This is illustrated in Figure 4.2.1.

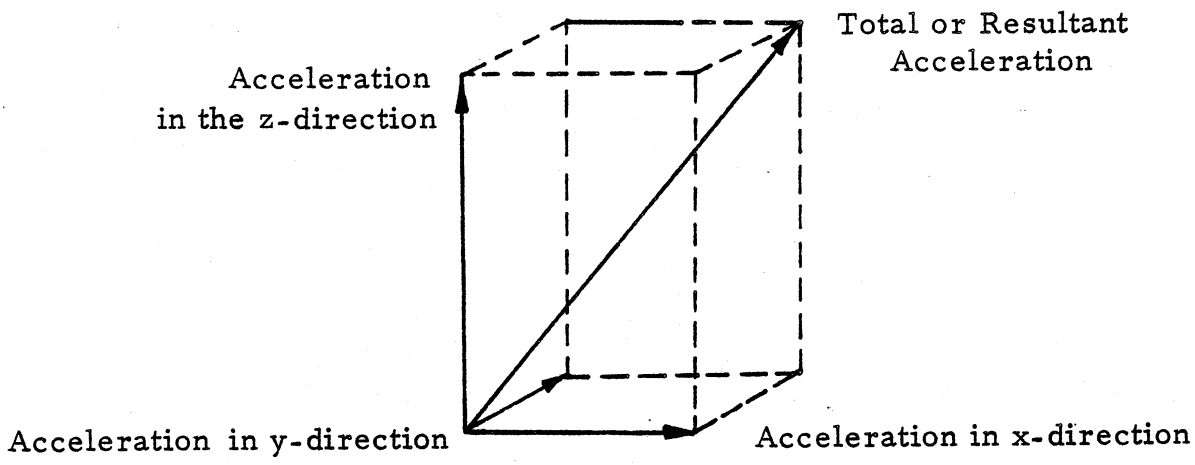

Figure 4.2.1. The Omni-Directional Accelerometer Measures the Resultant Acceleration.

This type of accelerometer will measure the thrust and aerodynamic acceleration of the orbiter by means of a drag-free falling reference mass in a cavity within the accelerometer. The reference mass is alternately centered and released, and the transit time required for it to move a known distance relative to the orbiter is recorded. Both the orbiter and reference mass are subject to gravity, and the relative acceleration, which is the propulsive or aerodynamic acceleration of the orbiter, is found from the transit-time by means of the falling body formula.

A simple schematic of the accelerometer is shown in Figure 4.2.2. The reference mass, or Bobbin, is centered by the pick-up or "caging" fingers, activated by the magnet coils.

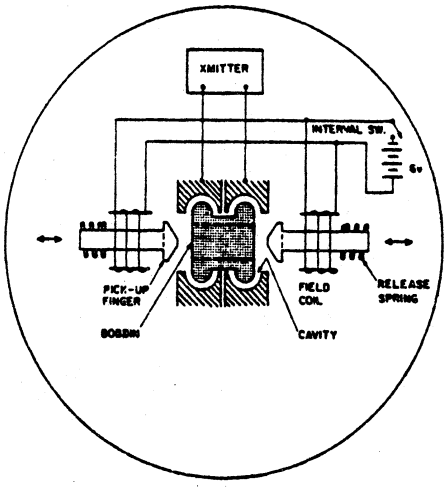

Figure 4.2.2. Simple Schematic of the Omni-Directional Accelerometer [1].

The release springs retract the caging fingers when the interval switch is opened, and the bobbin then falls freely in an essentially drag-free environment, accelerated with respect to the cavity by the relative acceleration, which is due to the thrust or aerodynamic force on the orbiter. A thin gold wire, the bobbin contact wire, circles the cavity. When the bobbin reaches the wall of the cavity, it touches this wire. A contact signal, which is capacitively induced by the wire, is then recorded. When centered, the bobbin is equidistant from the cavity wall in all directions, so that the transit time is independent of the orientation of the orbiter. A cut-away view of the accelerometer is shown in Figure 4.2.3. [1].

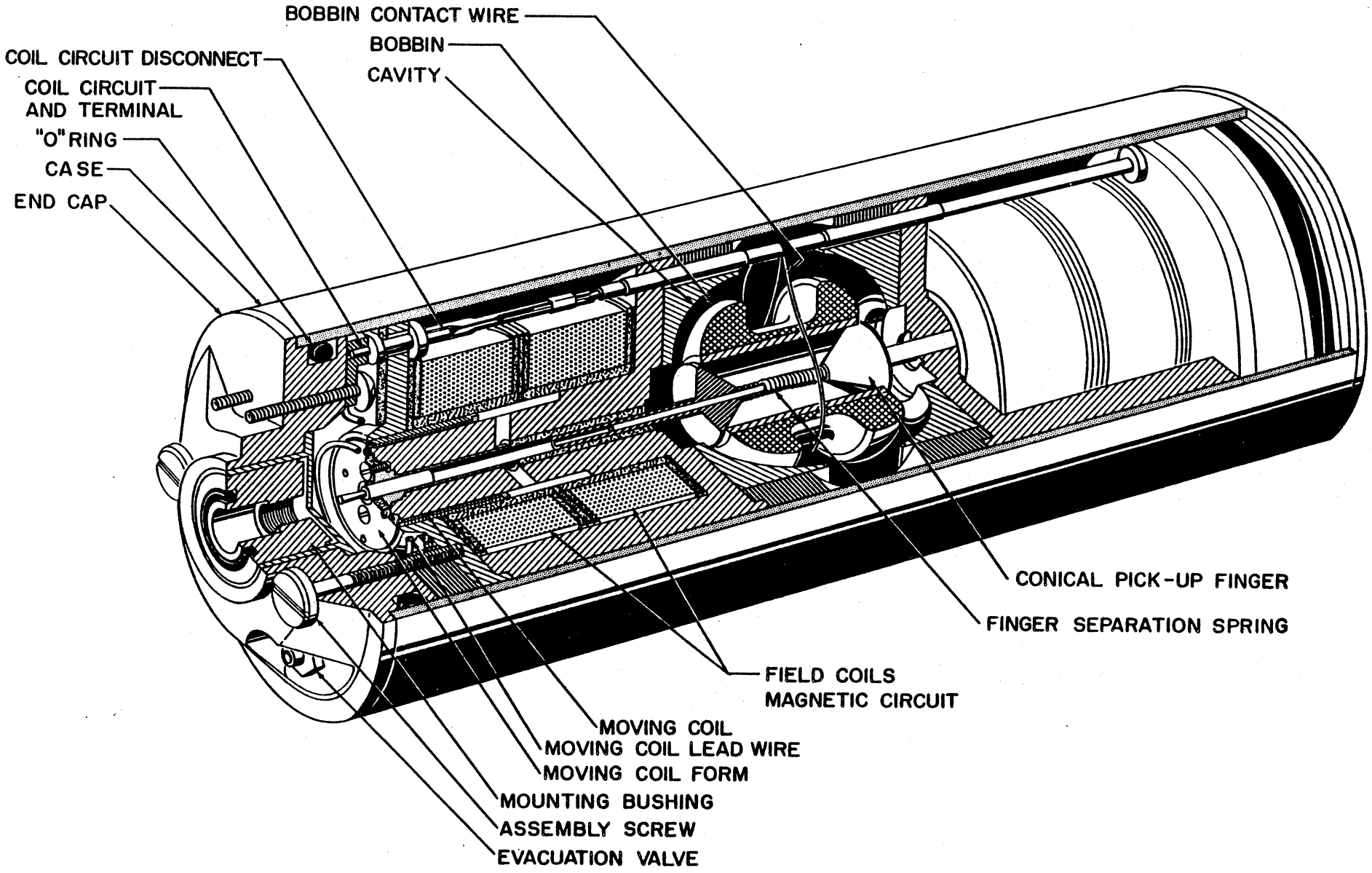

TRANSIT TIME ACCELEROMETER

The intervalometer energizes the accelerometer for a period of 150 msec. This occurs during every second that the intervalometer is on. The accelerometer drive circuit is used to energize the accelerometer solenoid coils used in recentering the bobbin. The 150 msec. pulse is amplified and applied as a drive signal to a high current transistor switch. When energized (the switch is closed), the transistor applied approximately 6 volts across the solenoid coils, 3 amperes flow for 150 msec., and the bobbin is centered in the accelerometer cavity. At the end of this 150 msec. period, the accelerometer drive circuit is de-energized (the switch is opened), and the bobbin is released. It is an essential requirement that no velocity be imparted to the bobbin during release. If the velocity is not approximately zero, the calculated acceleration will be incorrect. A sketch of the intervalometer is shown in Figure 4.2.4. Once again, the intervalometer is responsible for periodically caging or centering the bobbin in the cavity and releasing it [1].

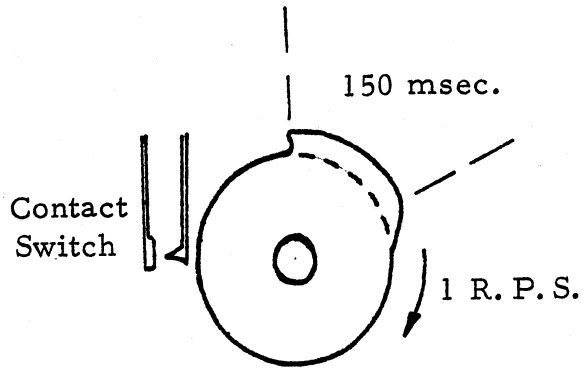

Figure 4.2.4. Representation of Intervalometer .

The accelerometer is dimensioned in Figure 4.2.5. Temperature requirements restrict its operation between -10°C and 50°C approximately. The accelerometer can measure acceleration from .01 g's to 10 g's. It weighs approximately 2 pounds and draws 18 watts of power when on. Since the accelerometer will probably be drawing the most power of any of the experiments, the accelerometer circuit should have its own batteries as to avoid failure in other circuits. As a final point, the omni-directional accelerometer is independent of pressure.

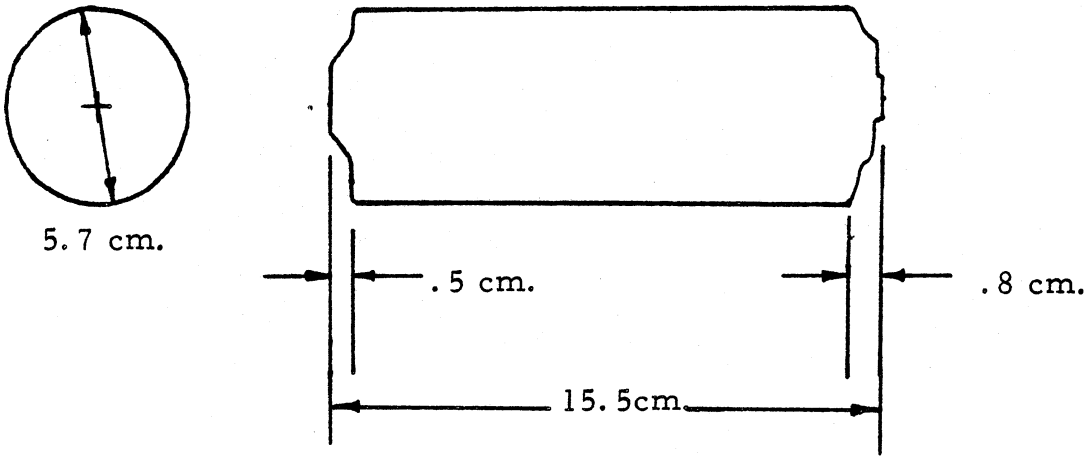

Figure 4.2.5. Approximate Dimensions of the Accelerometer Cylinder (not to scale).

4.2.4. Data. The basic data consists of bobbin release times, when the bobbin is at the center of the accelerometer cavity, and bobbin contact times, when the bobbin touches the cavity walls. The difference between release time and contact time is the transit time which will range from .001 to .312 seconds approximately. The accelerometer gap

(distance between centered bobbin and cavity wall) is 3/16 of an inch. An idealized picture of the data is shown in Figure 4.2.6. Once the transit time is known, the acceleration can be found from the falling body formula,

$$s = 1/2\, a\, t^2 + V_o t \qquad (4.2.1)$$

where V_o, the initial velocity, is assumed very small and neglected, then

$$s = 1/2\, a\, t^2$$

and

$$a = 2s/t^2$$

where a is the acceleration, s is the accelerometer gap, and t is the transit time measured.

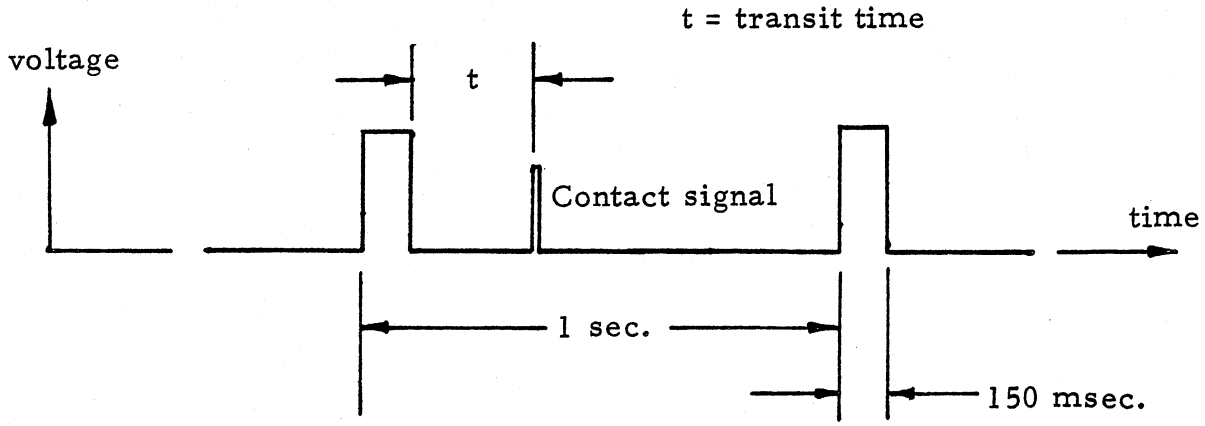

Figure 4.2.6. Idealized Picture of the Data .

The acceleration will be measured during the launch and reentry phases since the steady-state acceleration in orbit is too small to be measured. Steady-state acceleration is typically 10^{-4} g's. Powered flight

is approximately 12 minutes maximum while reentry (deorbit to landing) is 80 minutes maximum [2]. Thus, the accelerometer is to be operational for 92 minutes. To correct for deviations, an average value of the acceleration should be used. This can be achieved by running the accelerometer for 5 seconds (obtaining 5 data points) and then shutting off for 3 seconds. A timer/ sequencer would be needed to turn off and on the intervalometer in 5 and 3 second intervals. Each set of 5 data points would be averaged into a single value after the data was retrieved. This procedure would draw 18 watts of power for approximately 9 minutes. If the accelerometer was on for the entire 92 minutes, 14 minutes of power would be required, since the accelerometer draws power for 150 msec. during every second of operation. This data could be compared to NASA's data by using their flight profile of acceleration versus time.

4.2.5. Signals. The accelerometer system will require 3 signals: turn-on at launch, turn-off after insertion into orbit, and turn-on at the beginning of reentry. If the accelerometer is turned on 5 minutes before launch, turned off 5 minutes after orbit insertion, and turned on 5 minutes before deorbit, the accelerometer will be required to be on for an additional 15 minutes. Additional power would then be needed. It is also possible that a g-switch can be used to activate turn-on at launch and at the start of reentry. However, the acceleration of the orbiter can be as low as 1.5 g's at lift-off. The g-switch would have to be very sensitive.

4.2.6. Testing and Calibration. The accelerometer will have to be tested prior to launch. Errors can be discovered in centering, under and over caging, dimensions, and in operational malfunctions. Experience has shown that accelerometers operating correctly at 1 g will do so at higher and lower accelerations as well. The 1-g "bench test" can also take into account the .8 msec lag time between the opening of the switch and the release of the fingers. The initial velocity imparted to the bobbin at release, either by off-center caging or inaccurate construction, is the biggest source of error at low accelerations [1]. The low acceleration operation of the accelerometer may be tested by the bullet-drop procedure. This test measures .01 g's and can be conducted at the University of Michigan.

Since it is readily available, the omni-directional accelerometer is very practical for this experiment. If the accelerometer proves to be defective, a new one can be manufactured at the University of Michigan for approximately $3000 to $5000. However, if any accelerometer is to be purchased, serious attention should be directed toward other accelerometers available to us which might be more desirable (triaxial vs. omni-directional).

References

[1] L. M. Jones, 'Falling Sphere Method for Upper-Air Density, Temperature and Wind," Feb. 1967,pp. 50-82.

[2] NASA, "Gas Experimenter Handbook," December 1978, pp. 1 - 83.

[3]

4.3. Vibrations -- David M. Pitera

4.3.1. Recent Advances. Recent advances in technology have evolved much new and sophisticated electronic equipment, at the same time the environment to which this equipment is being subjected is getting increasingly hostile. In the post World War II years, however, with the development of jet and rocket engines a new problem was found The vehicles equipped with these engines experience what is termed random vibration. It differs from normal sinusoid vibration in that it cannot be exactly predicted. At any one time one cannot be exactly sure what amplitude and frequency of vibration your equipment might be subjected too. To add to the problem, most random vibration is at a greater amplitude than sinusoidal vibration.

When this was first encountered. it seemed reasonable to use some type of probability function to describe what to expect at a certain time. An early "shock spectral" was a graph of peak motion and the duration of the applied transient. The present method is to plot frequency vs. power. A shock spectral graph for the environment of our project in the Space Shuttle is shown in Fig. 4.3.1.

4.3.2. A shock is defined as a mechanical vibration capable of exciting resonances in a structure. Random vibration may be looked at as a large number of irregularly times small shocks. As an example, suppose that a typical piece of equipment like the capacitor shown in

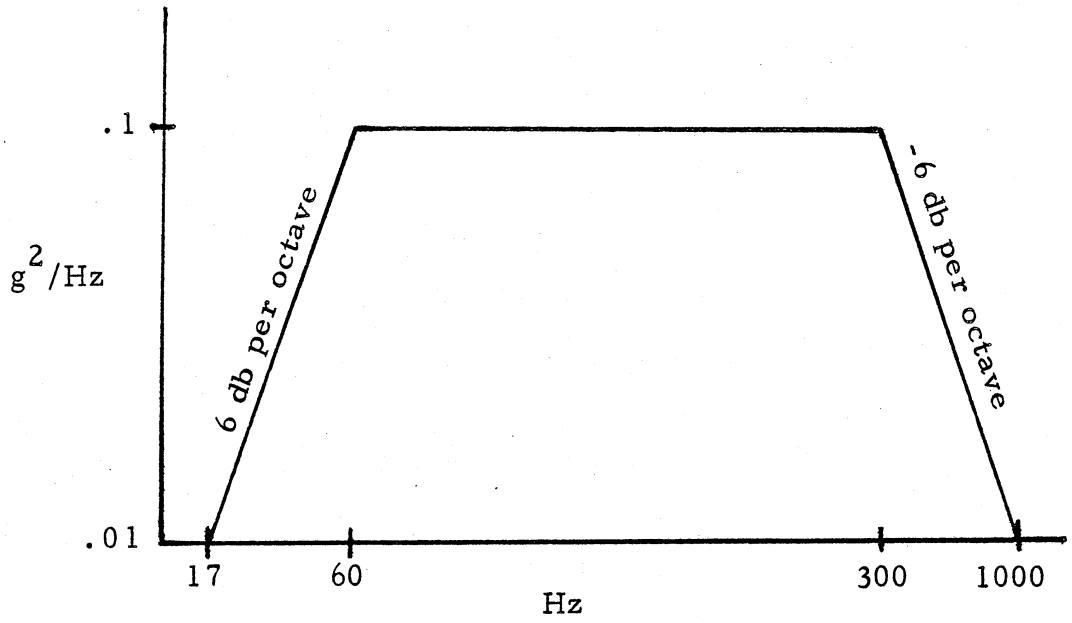

Figure 4.3.1. [6]

Figure 4.3.2, is subjected to a vibration. The most damaging part of vibrations is the accelerations they cause. As the capacitor is moved back

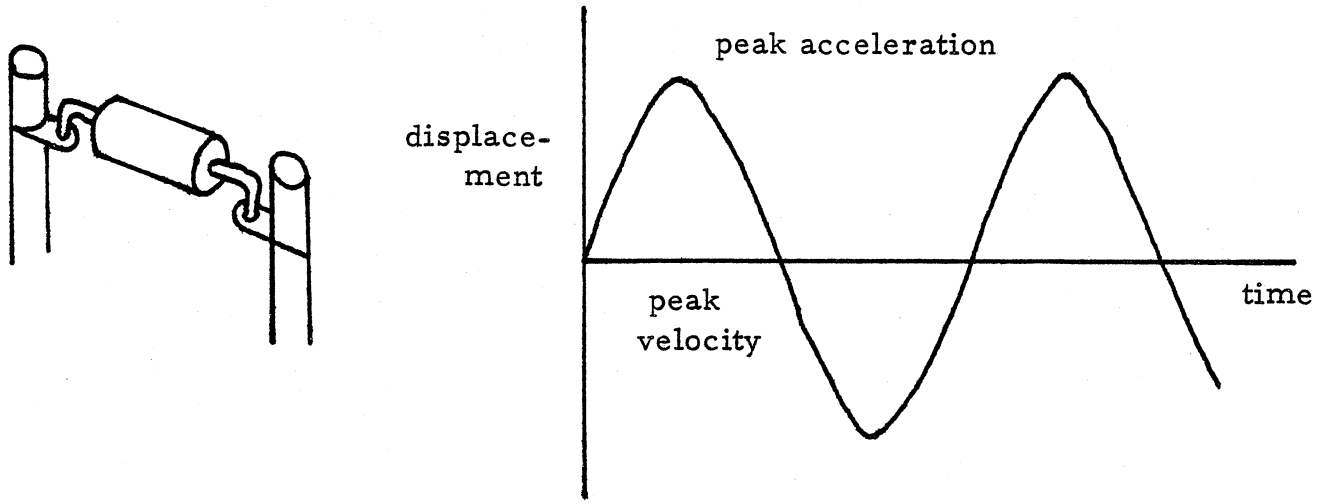

Figure 4.3.2. [3]

and forth it is continuously under changing accelerations. If we assume the vibration to be sinusoidal, we may visualize the problem as shown in Figure 4. 3. 2. At a peak point the acceleration is maximum, but the part is not moving. As the capacitor passes its equilibrium position, the acceleration drops to zero while the velocity increases to a maximum. As it moves to the lower peak the velocity drops to zero while the acceleration again increases to a maximum in the opposite direction.

In random vibration, because of the different frequencies and amptitudes, exact accelerations cannot be predicted. However, using probability analysis the root mean square (RMS) value can be found .

This is done by integrating under the power spectral density curve (Fig. 4. 3. 1) and then taking the square root. If the power input at a particular frequency is low, it will be a low point on the spectral diagram. If there are no vibrations at a particular frequency there is no power at this point. As an example, Figure 4. 3. 3 shows a graph of F(t), a randomly varying vibration function having many differing frequencies and amplitudes. In Figure 4. 3. 3 (b) the spectral density is shown. The spectral density varies slowly but shows some power across a broad band of frequencies. Next is a figure (Fig. 4. 3. 4) of G(t), a random vibration of close to one frequency but varying amplitude. The sepctral density diagram for this function has a single peak at the frequencies present in G(t). There is no power at other frequencies.

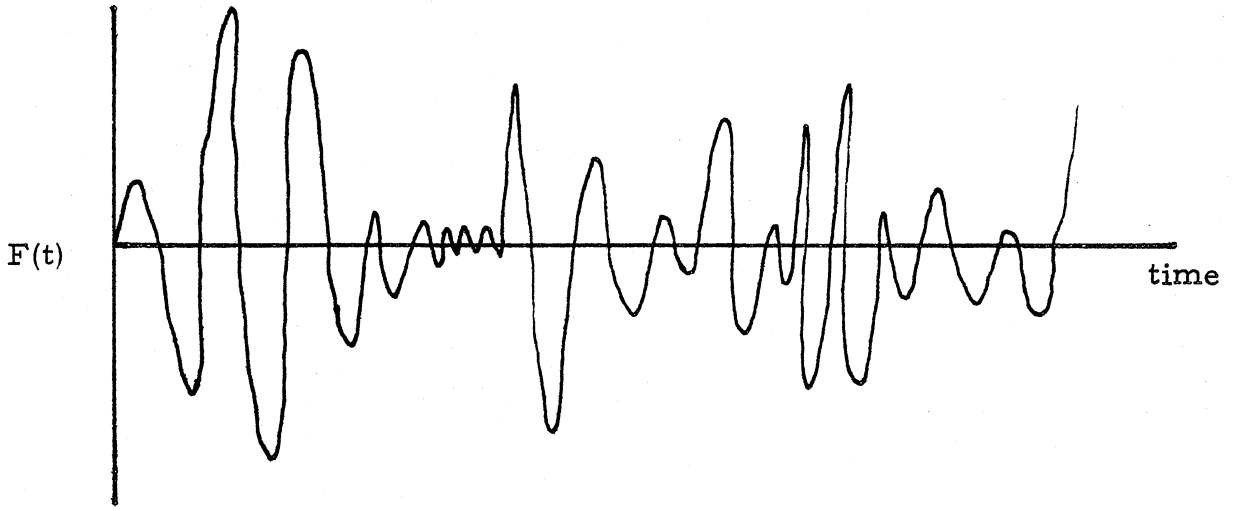

Figure 4.3.3. (a) [5]

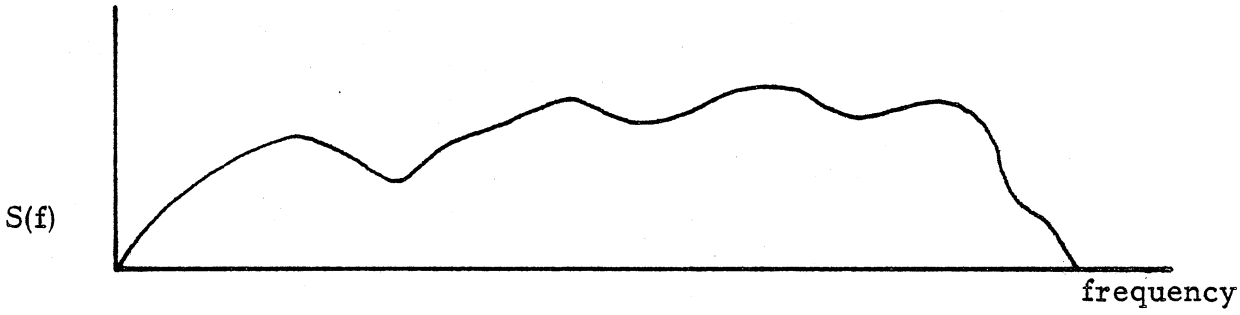

Figure 4.3.3. (b)

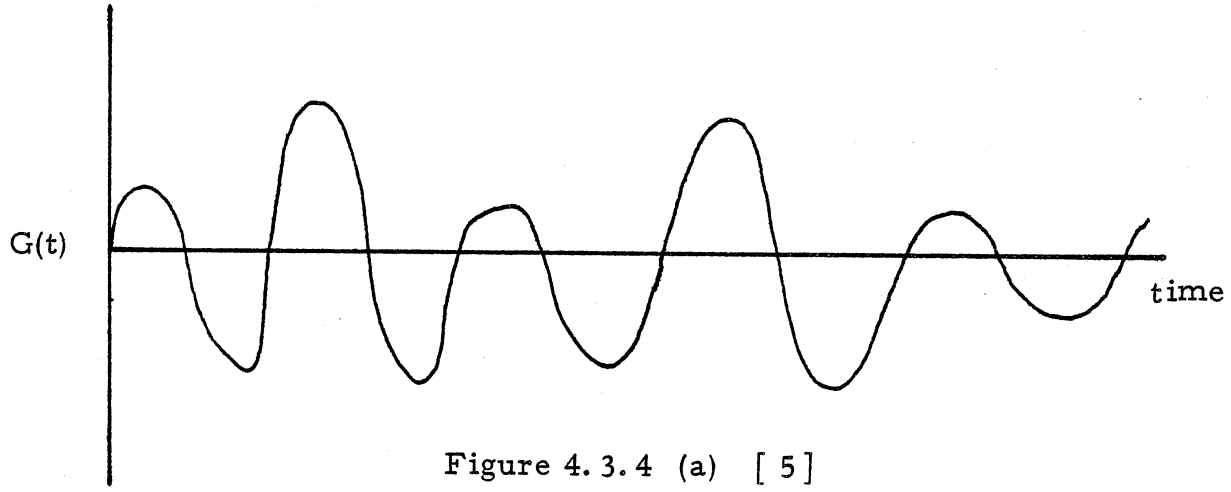

Figure 4.3.4 (a) [5]

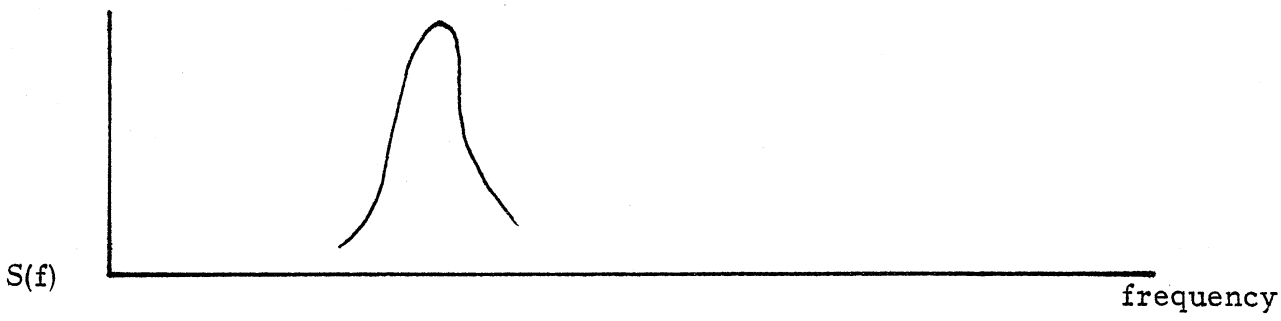

Figure 4.3.4 (b)

4.3.2.1. Detailed Discussion. In order to talk more specifically about random vibrations we must first define what type of random vibrations we will discuss. Suppose that we record the random vibrations of a railroad car moving over a certain stretch of track. To get an accurate picture of the vibrations present we must make many recordings. If the average amplitude of the vibration at a certain time T is identical to the average at a time $T + \tau$, then the random vibrations are termed stationary. If each recording is averaged and is equal to another recording average, the vibrations are said to be ergodic. In the following discussions, the vibrations are both stationary and ergodic.

The time average for a particular function is defined as

$$\bar{X}(t) = \langle x(t) \rangle = \lim_{T \to \infty} \frac{1}{T} \int_0^T x(t)\, dt \qquad (4.3.1)$$

The mean square value is

$$\bar{X}^2 = \lim_{T \to \infty} \frac{1}{T} \int_0^T x^2\, dt \qquad (4.3.2)$$

4.3.2.2. As stated earlier the spectral density diagram is a plot of the energy or power of the vibrations at each particular frequency. To understand this better, first consider a periodic function F(t) which contains many discrete frequencies. It can be represented by the real part of the series

$$F(t) = \mathrm{Re} \sum_n F_n\, e^{in\omega_o t} \qquad (4.3.3)$$

F_n is a complex number and R_e stands for the real part of the series.

We could write this equation in terms of its complex conjugate as

$$F(t) = \frac{1}{2}\left\{ \sum_n F_n e^{in\omega_o t} + \sum_n F_n^* e^{-in\omega_o t} \right\} \qquad (4.3.4)$$

and determine its mean square value as

$$\overline{F}^2 = \lim_{T\to\infty} \frac{1}{T} \int_o^T \frac{1}{4} \left\{ \sum_n F_n e^{in\omega_o t} + \sum_n F_n^* e^{-in\omega_o t} \right\}^2 dt$$

$$= \sum_n \frac{F_n F_n^*}{2} = \sum \frac{1}{2} |F_n|^2 = \sum_n \overline{F}_n^2 \qquad (4.3.5)$$

Thus the mean square value of the multifrequency wave is simply the sum of the mean square values of each harmonic component present, the result being a discrete frequency spectrum shown in Figure 4.3.5.

Next examine the mean square contribution in the frequency interval $\Delta\omega$.

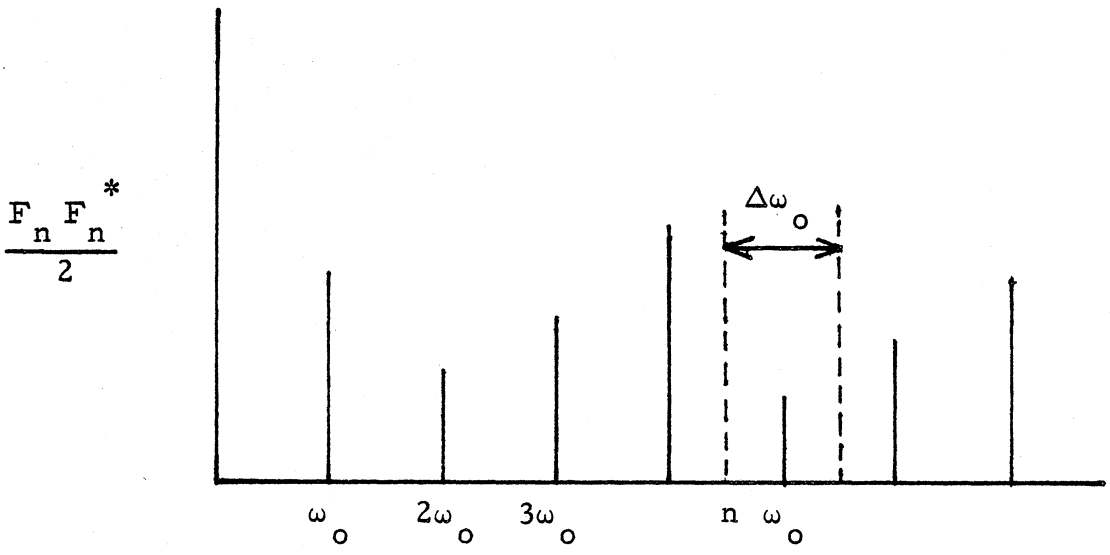

Figure 4.3.5 [5]

To do this let $S(n\,\omega_o)$ be the density of the mean square value in the interval $\Delta\,\omega$ at the frequency $n\,\omega_o$. This becomes

$$s(n\,\omega_o)\,\Delta\,\omega = \frac{F_n F_n^*}{2} \tag{4.3.6}$$

$$s(n\,\omega_o) = \frac{F_n F_n^*}{2\Delta\omega} \tag{4.3.7}$$

It is evident that when F(t) contains a very large number of frequency components, the descrete density function $S(n\,\omega_o)$ becomes nearly a continuous spectral density function $s(\omega)$ as shown in Figure 4.3.6.

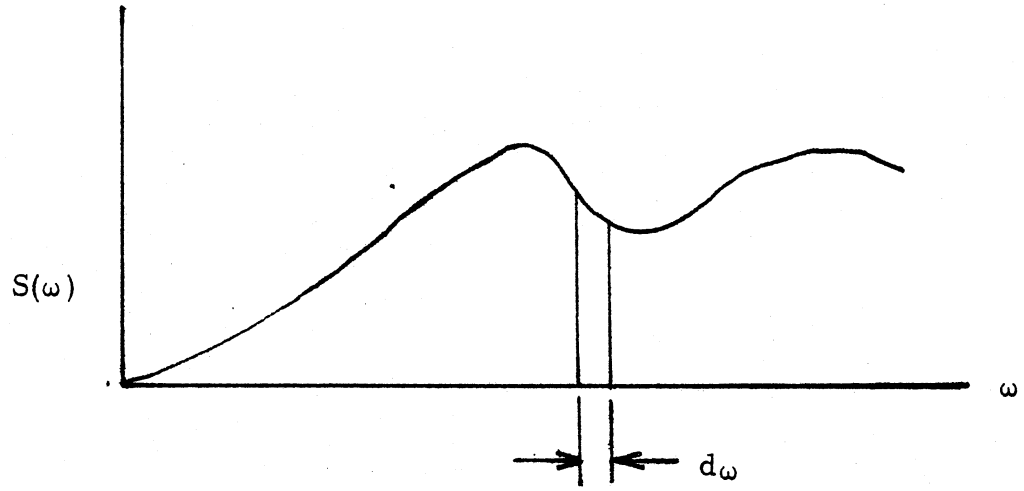

Figure 4.3.6. [5]

The mean square value of F is then

$$\overline{F}^2 = \int_0^\infty S(\omega)\ d\omega \tag{4.3.8}$$

or

$$\overline{F}^2 = \int_0^\infty S(f)\ df \tag{4.3.9}$$

4.3.2.3. Probability Distribution. A random time function is shown in Figure 4.3.7. What is the probability of its instantaneous value being less than (more negative than) some specified value X_1 ?

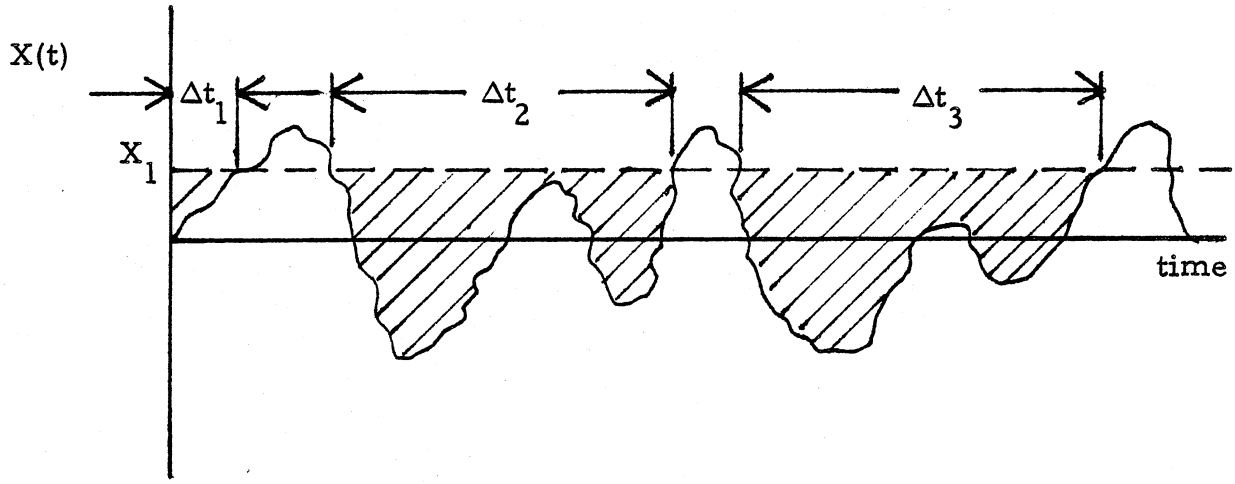

Figure 4.3.7. [5]

To answer this, draw a horizontal line at the specified value X_1 and sum the time intervals Δt_i during which X(t) is less than X_1 . This sum divided by the total time represents the fraction of the total time that X(t) is less than X_1 or the probability that X(t) will be found less than X_1 .

$$P(X_1) = \text{Prob}\,[\,X(t) < X_1\,] = \lim_{t \to \infty} \frac{1}{t} \sum \Delta t_i \quad . \qquad (4.3.10)$$

If a large negative number is chosen for X_1 none of the curve will extend below X_1 so $P(X_1 \to \infty) = 0$. On the other hand, if X_1 is moved up all of the curve will eventually be below X_1. Hence, $P(X_1 \to \infty) = 1$. A plot of $P(X_1)$ or $P(X)$ vs X would have to increase monotonically from 0 at $X \to -\infty$ to 1 as $X \to \infty$. This curve is

called the cumulative probability distribution function P(x).

If we wanted to determine the probability of X(t) lying between the values X_1 and $X_1 + \Delta X$ all we need to do is to subtract $P(X_1)$ from $P(X_1 + \Delta X)$. The probability density function is defined as

$$p(X) = \lim_{\Delta X \to 0} \frac{P(X+\Delta X) - P(X)}{\Delta X} = \frac{dP(X)}{dX} \qquad (4.3.11)$$

It is clear from calculus that p(X) is the slope of the cumulative probability distribution P(X). Therefore, we can also write the above equation as

$$P(X_1) = \int_{-\infty}^{X_1} p(X)\, dX \qquad (4.3.12)$$

From Figure 4.3.8, the area under the probability density curve between the two values of X represents the probability of the variable being in this interval. Since the probability of X(t) being between $\pm \infty$ is certain

$$P(\infty) = \int_{-\infty}^{+\infty} p(X)\, dX = 1.0 \qquad (4.3.13)$$

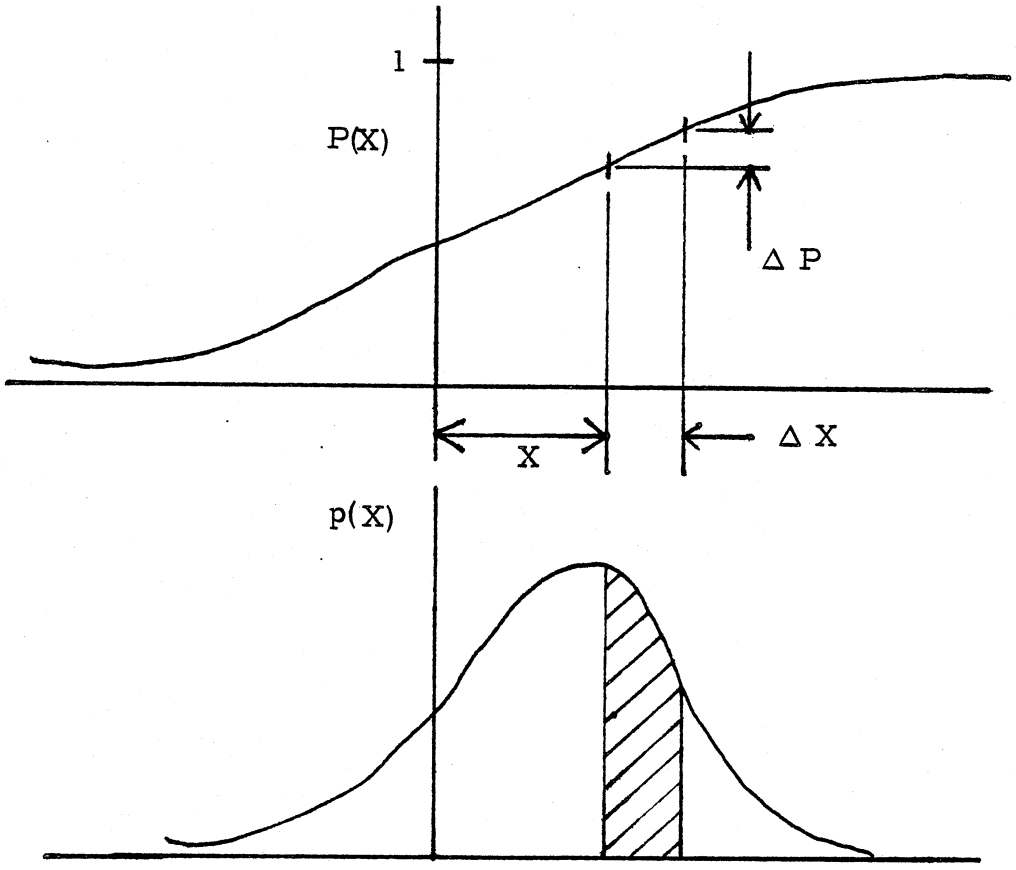

Figure 4.3.8 [5]

4.3.2.4. The mean and mean square value are related to the probability density function in the following manner. The mean value $\overline{X}$ coincides with the centroid of the area under the probability density curve p(x) as shown in Figure 4.3.9. We can, therefore, use the first moment to determine it.

$$\overline{X} = \int_{-\infty}^{\infty} X\ p(X)\ d\,X \qquad (4.3.14)$$

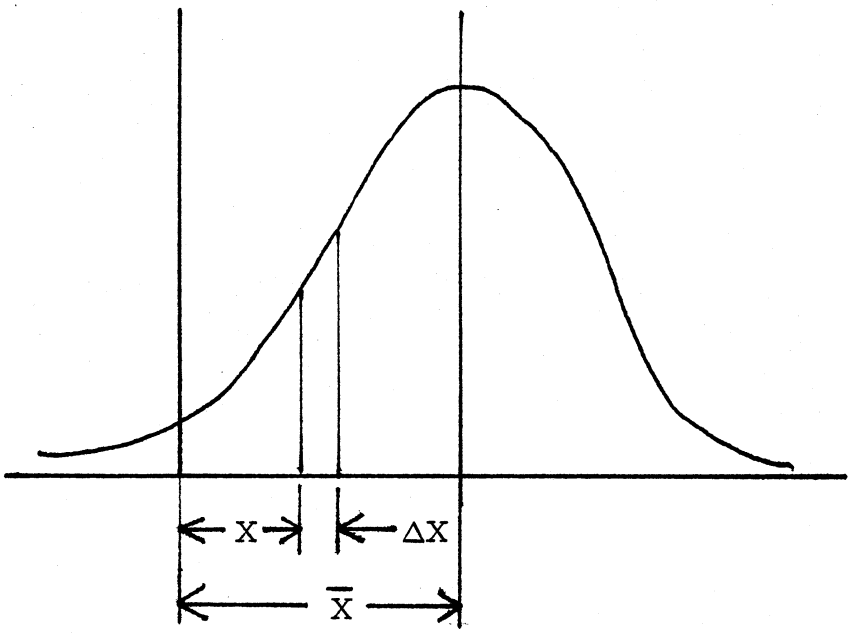

Figure 4.3.9. [5]

The mean square value is determined in the same manner from the second moment

$$\overline{X}^2 = \int_{-\infty}^{\infty} X^2 \, p(X) \, dX \qquad (4.3.15)$$

which is analogous to the mo ment of inertia under the probability density curve about X = 0. Another term, the variance σ^2, is defined as the mean square value about the mean or

$$\overline{\sigma}^2 = \int_{-\infty}^{\infty} (X - \overline{X})^2 \, p(X) \, d X$$

$$= \int_{-\infty}^{\infty} X^2 \, p(X) dX - 2 \overline{X} \int_{-\infty}^{\infty} X \, p(X) \, dX + (\overline{X})^2 \int_{-\infty}^{\infty} p(X) \, dX$$

$$= \overline{X}^2 - 2(\overline{X})^2 + (\overline{X})^2 \qquad (4.3.16)$$

The standard deviation is the positive square root of the variance. When the mean value is zero $\sigma = \sqrt{\overline{X}^2}$ and the standard deviation is equal to the root mean square value.

Two types of probability distributions occur frequently in nature: Gaussian and Rayleigh. Gausian is more important to us because random vibration is distributed in this manner.

Gausian distribution is the well known bell shaped curve. It can be represented by

$$p(x) = \frac{1}{\sigma\sqrt{2\pi}} \quad e^{-(x^2/2\sigma^2)} \tag{4.3.17}$$

The standard deviation, σ, is a measure of the spread about the mean value. In Figure 4.3.10 the Gausian distribution is plotted non-dimensionally in terms of X/σ. The probability of x(t) being between $\pm \lambda\sigma$ (where λ is any positive number) is found from the equation

$$\text{Prob}\,[\, -\lambda\sigma \leq x(t) \leq \lambda\sigma \,] = \frac{1}{\sigma\sqrt{2\pi}} \int_{-\lambda\sigma}^{\lambda\sigma} e^{-x/2\sigma^2} \, dx \tag{4.3.18}$$

The following is a chart of probabilities at different values of λ

λ	Prob$[\, -\lambda\sigma \leq x(t) \leq \lambda\sigma \,]$
1	68.3%
2	95.4%
3	99.7%

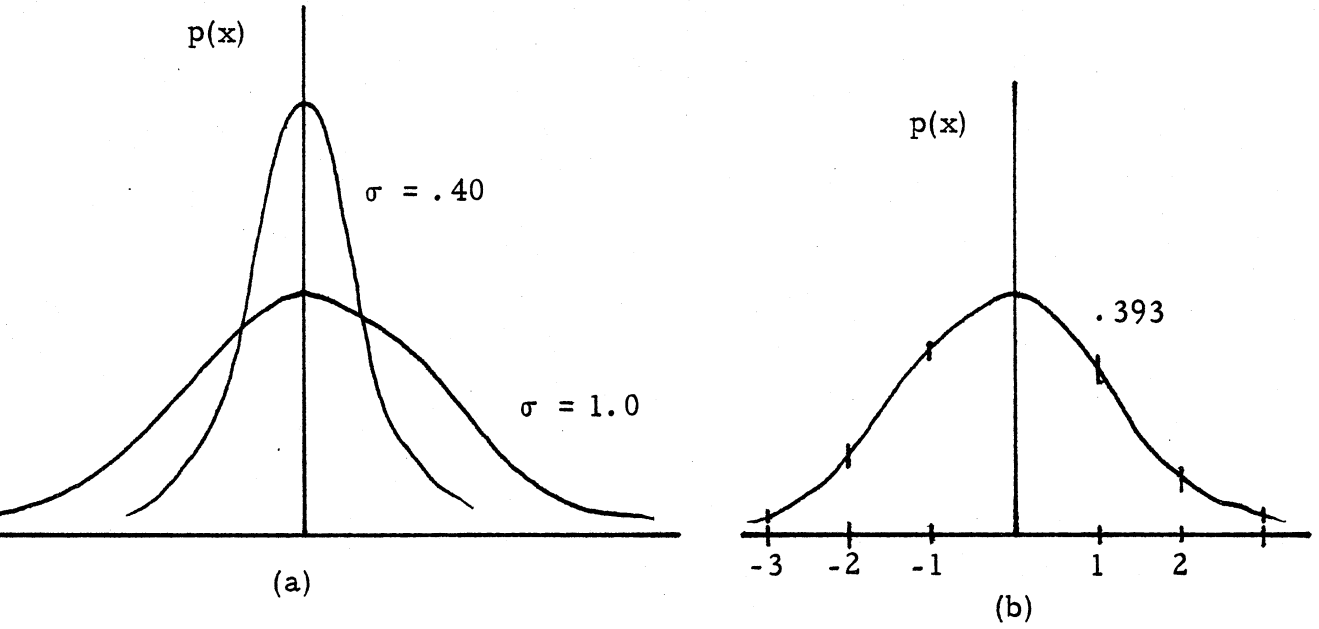

Figure 4.3.10 [5]

These ideas are now clarified by the following examples.

4.3.2.5. Example I. (Taken from Thompson).

A random signal has a spectral density which is constant

$$s(f) = 0.004 \text{ in}^2/\text{cps}$$

between 20 and 1200 cps, and zero outside this frequency range. Its mean value is 2.0 in. Determine its standard derivation and its rms value.

Solution: If the mean value is not zero, we must use

$$\overline{X}^2 = (\overline{X})^2 + \sigma^2 .$$

The standard deviation is found from

$$\sigma^2 = \int_0^\infty s(f)\, dt = \int_{20}^{1200} 0.004\, df = 4.72$$

and the mean-square value is

$$\overline{X}^2 = 2^2 + 4.72 = 8.72 .$$

The rms value is then

$$\text{rms} = \sqrt{\bar{X}^2} = \sqrt{8.72} = 2.95 \text{ in.}$$

The problem is graphically displayed by the Figure 4.3.11..

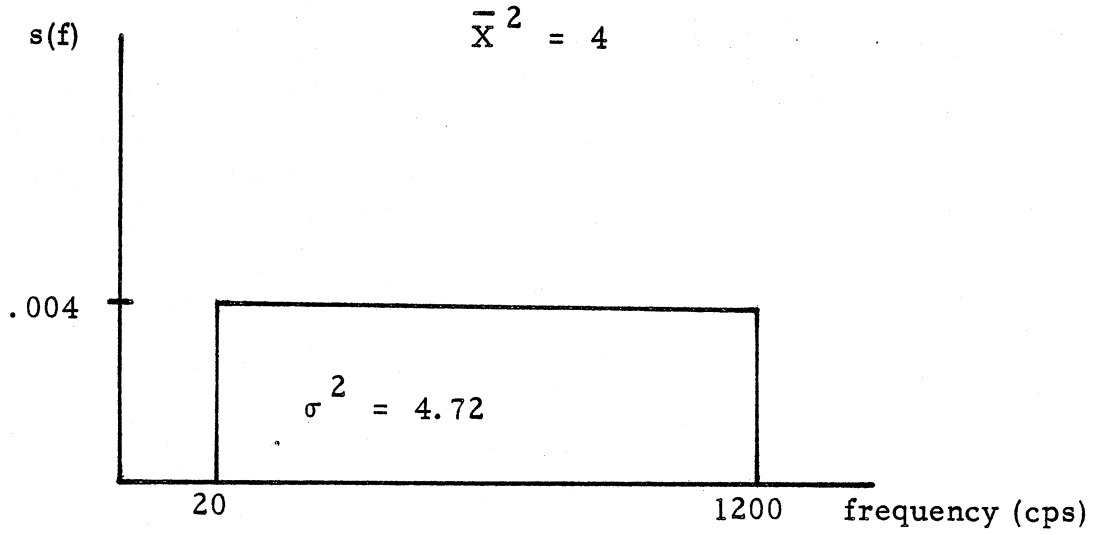

Figure 4.3.11 [5]

Example II. Calculation of G_{RMS} for our data on the Space Shuttle. (See Figure 4.3.1). Note: The slope indicates the rate of energy change. A 6 db per octave slope implies that the energy change per octave is proportional to the frequency squared. A 3 db slope would imply that the energy change per octave is proportional to the frequency. A slope of -6 db per octave is proportional to f^{-2}. For our problem the mean value is zero so $\sigma^2 = \bar{X}^2$. The mean square value is found from the following formula:

$$\bar{X}^2 = \int_{\omega}^{\omega + \Delta\omega} S(f)\ df \quad .$$

For the first section, 17 to 60 Hz

$$\bar{X}^2 = \int_{17}^{60} A f^2 \, df \quad .$$

The constant, A is determined by picking a known point on the diagram such as f = 60 Hz , $g^2/Hz = .1$

$$.1 = A \; 60^2 \implies A = 2.776 \times 10^{-5}$$

$$\bar{X}_1^2 = \int_{17}^{60} (2.778 \times 10^{-5}) f^2 \, dt = \frac{2.778 \times 10^{-5}}{3} \left[f^3 \right]_{17}^{60} = 1.95 \; g^2$$

Over the second interval from 60 to 300 Hz

$$\bar{X}_2^2 = \int_{60}^{300} .1 \, df = .1 \left[f \right]_{60}^{300} = 24 \; g^2$$

and the third interval 300 to 1000 Hz

$$\bar{X}_3^2 = \int_{300}^{1000} B f^{-2} \, df \quad .$$

Picking a known point

$$.1 = B \; 300^{-2} \implies B = 9000$$

$$\bar{X}_3^2 = \int_{300}^{1000} 9000 f^{-2} \, df = -9000 f^{-1} \Big|_{300}^{1000} = 21 \; g^2$$

$$\bar{X}^2 = \bar{X}_1^2 + \bar{X}_2^2 + \bar{X}_3^2 = 46.95\ g^2$$

$$\bar{X} = \text{rms}_g = 6.85\ g\ .$$

4.3.1. Vibration Measurement

One possible experiment that might be performed as part of our project could be the measurement of these vibrations. In talking to various people about this issue, it is continuously brought up that the spectral density diagram is too high. Most people feel that the engineers at NASA who developed the data for random vibrations decided to be sure that experiments both large and small would survive. To be conservative, they raised the minimum intensity that a package had to be test at. This caused a problem when the first equipment was designed for the Shuttle. Not realizing the intensity of the vibrations, packages were literally shook to pieces when tested. Part of our project is to determine what vibrations are actually present on the Shuttle.

Early vibration measurements were done with a series of reeds, each reed would be tuned to a different frequency. In order to cover a large amount of frequencies there would have to be many reeds. The modern method is to use small accelerometers mounted on the specimen and then use a computer to reduce the data into a useful form. In Figure 4.3.12 a random input is fed into a bandpass filter that only allows certain

frequencies to go through.

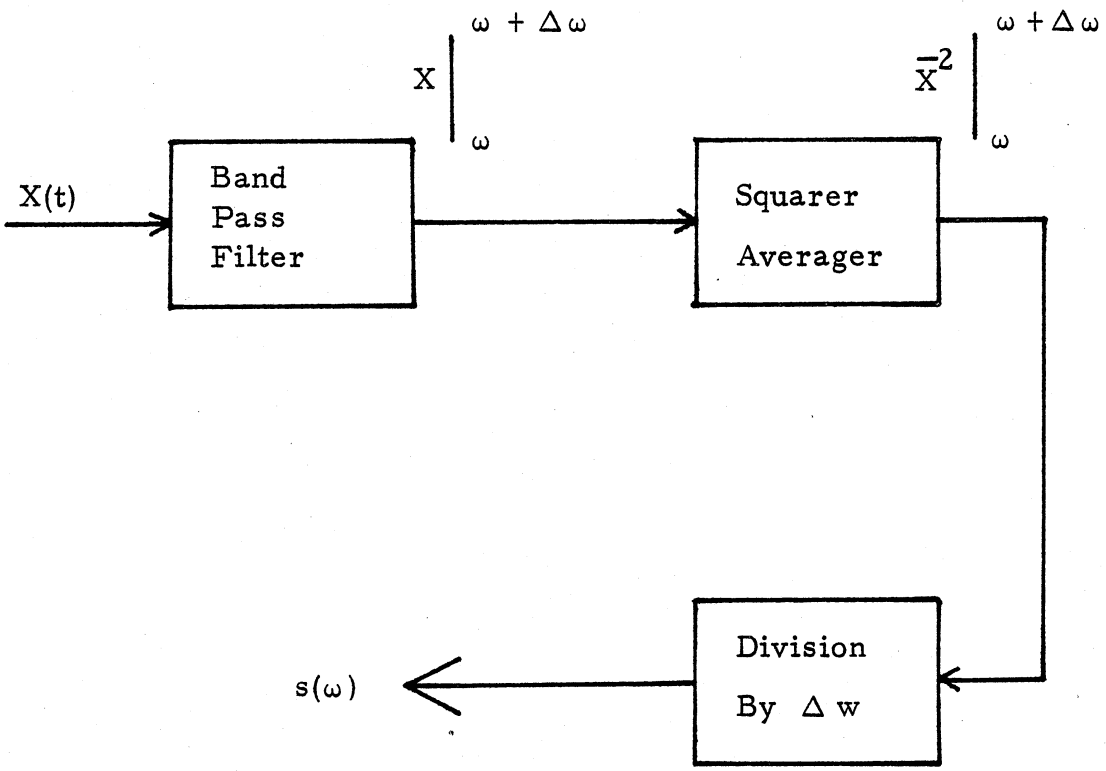

Figure 4.3.12 [5] .

This allows only frequencies from ω to $\Delta\omega$ to be picked up. Another device squares and averages the input. Then the mean square value is divided by the bandwidth. The result is a value of power spectral density.

For high resolution the bandwidth should be made as narrow as possible but the band pass filter cannot be reduced indefinitely or there will be a loss in the reliability of the measurement. Also, to insure an accurate picture of the vibrations present a very long record is required. This, of course, is impossible for our experiment. However, to insure enough data for varifying stationarity, mean square values, etc, two or three accelerometers could be used.

Random vibrations is a relatively new field. It was not investigated in great detail until recently. This makes finding books (or experts) in the field quite a challenge. Most books dealing with random vibrations are greatly concerned with probability analysis. One observation that can easily be made is that when our project is designed, the resonant frequency of a particularly delicate part cannot be in the zone from sixty to three hundred hertz, (see Figure 4.3.1), where the maximum spectral density is. It should either be stiffened to increase it's resonate frequency or it should be protected by vibration absorbers to lower the resonant frequency. Many areas still need further study.

References

The following is a list of reference books, as well as companies involved in vibration instrumentation.

[1] Dinca Florea , Non-Linear and Random Vibrations, Academic Press, 1973.

[2] Meirovitch, Leonard, Elements of Vibration Analysis, McGraw-Hill, New York, 1975.

[3] Marrow, Charles T., Shock and Vibration Engineering, Vol. 1, The Aerospace Corporation, Los Angles, California, John Wiley & Sons, Inc., New York, 1963.

[4] Lyon, Richard H., Random Noise & Vibration in Space Vehicles, Bolt, Beranek & Newman, Inc., U. S. Government Printing Office, Washington, D. C. 1965.

[5] Thomson, William T., Prentice-Hall, Inc., Englewood Cliffs, New Jersey 1972.

[6] Experimenter Handbook, National Aeronautics and Space Administration, Goddard Space Flight Center, Sounding Rocket Division, December 1978.

Endevco
Depat. G, Rancho Veijo Road,
San Juan Capistrano, California 92675
TX: 714/493-8181

Setra Systems
12 Huron Drive
Natick, Massachusetts 01760
TX: 617/655-4645

Conrac
330 G Madison Avenue
New York, New York 10017
TX: 313/687-3330

Entran Devices, Inc.
775 Avenue of Americas
New York, New York 10001
TX: 212/242-7889

Systron Donner
Dept. G
1711 S. Mountain Avenue
Monrovia, California 81016
TX: 213/358-4571

Validyne
18819 NAPA Street
Northridge, California 81324
TX: 213/886-8488

BBN Instruments
50 G Moulton Street
Cambridge, Massachusetts 02138
TX: 617/491-0091

Consolidated Controls Corporation
15 Durant Avenue
Bethel, Connecticut 06801
TX:203/743-6721

Process Control Division
1601 Trapelo Road
Waltham, Massachusetts 02154
TX: 617/890-2000

4.4 Cosmic Rays -- Gregory J. Ruselowski

4.4.1. Introduction. Cosmic rays from all parts of the galaxy bombard us everyday. Fortunately, our atmosphere acts as a protective shield to dissipate effectively the intense energy in cosmic rays. This energy loss renders cosmic rays relatively harmless to us.

In spaceflights, however, there is no protective atmosphere to shield space vehicles from high energy cosmic energy. Such radiation presents a hazard not only to astronauts and other living organisms in the spacecraft, but also to electronic equipment and instruments.

Presently, information about cosmic rays is scarce. This report provides a basic background of cosmic rays so that, in the future, an experiment can be implemented by our design group to analyze cosmic rays in outer space.

4.4.2. Summary and Conclusions. The payload of project SCORE will encounter an environment in which energetic cosmic rays move about freely. These particles can be tested many different ways. If the project is to take advantage of the experimental opportunity afforded by cosmic rays, a basic understanding of such rays is essential. This section provides the necessary background by systematically covering six (6) major aspects of cosmic rays. They are description, effects, origin, detection, past experiments, and proposed experiments.

Project SCORE is interested in primary galactic cosmic rays. These are the type of cosmic rays which exist at the orbital altitude of the orbiter.

These particles are very energetic and can damage instruments on board the Shuttle and in our package. Cosmic rays also affect living organisms by ionizing their cells.

Cosmic rays are though to gain their energies by an electromagnetic process similar to those at work in solar flares. The electromagnetic process is believed to occur in galaxies like the Milky Way.

Some means must be employed to detect cosmic rays. Five possible detection devices are discussed and of these, the Geiger-Müller counter, photographic emulsions, and Lexon plastic are the most practical and merit further study for use with our experiment.

In previous space missions, experiments to analyze the effects of cosmic rays have included pocket mico, bacterial spores, seeds, and eggs. In some studies, astronauts themselves have been used. These experiments give insight to possible biological experiments which could be performed on SCORE. Possible experiments for our package might analyze the degredation of solar cells by cosmic radiation or measure the amount of cosmic rays in space.

The purpose of this section is to introduce cosmic rays to the design team. Ultimately, this section will provide the groundwork for a future cosmic radiation experiment aboard the Space Shuttle.

4.4.3. Description of Cosmic Rays. Almost everyone has heard of cosmic rays, but not many people know what cosmic rays are or how they act. This section will give a general description of cosmic radiation and then discuss the two types of rays found: primary and secondary cosmic rays.

4.4.3.1. General Description. Cosmic rays are high energy, positively charged particles (ions). These particles travel at velocities near the speed of light and can be found in the Earth's atmosphere and throughout the galaxy.

Cosmic rays are very energetic with energies ranging between 10^9 and 10^{19} electron-volt (10^{19} eV equals the energy required to lift a mass of one kilogram to a height of one meter). Figure 4.4.1. shows the energy spectrum of cosmic rays as a function of particles/ cm^2.

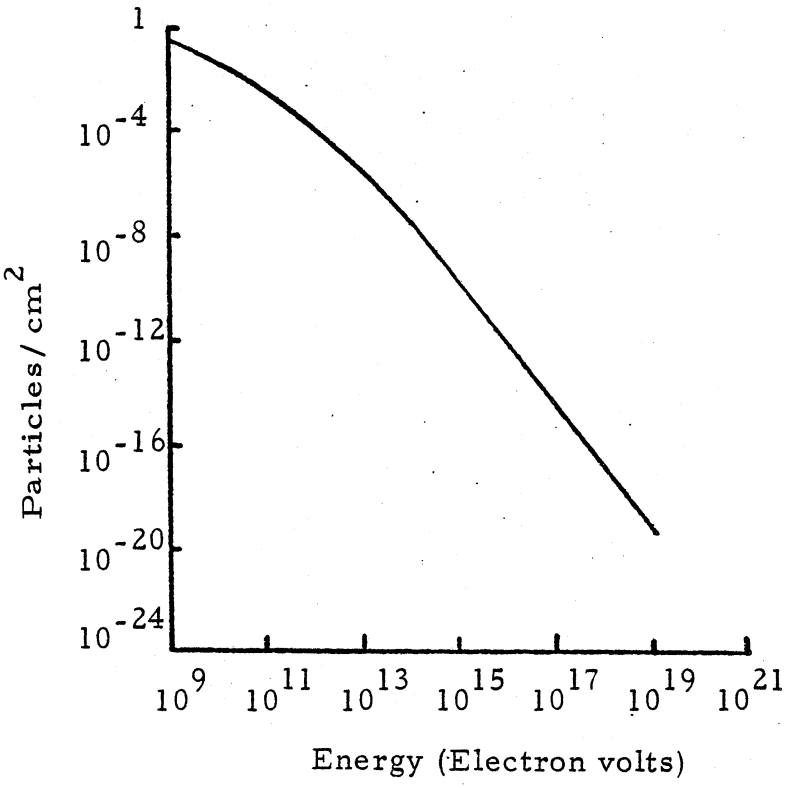

Figure 4.4.1. Energy Spectrum of Cosmic Rays.

Cosmic rays have a very short wavelength. The wavelength of cosmic rays is about one thousand times shorter than the wavelength of x-rays. Table 4.4.1 compares the wavelength of cosmic rays with x-rays and normal visible violet light:

	Wavelength(Angstroms)
Cosmic Rays	.0003 - .0006
X-Rays	.1
Violet Light	3000

Table 4.4.1. Comparison of Wavelengths [3].

High energy and short wavelength enable cosmic rays to penetrate virtually all substances with little absorption. Many cosmic particles pass right through spacecrafts and higher energy particles can penetrate 6 ft. of lead. The higher energy particles are usually primary cosmic rays.

4.4.3.2. Primary Cosmic Rays. Primary cosmic rays are stable particles found throughout outer space, but rarely on Earth. Physicists are convinced that practically all primary cosmic rays are nuclear-active and positively charged particles. Primary rays are composed of protons and bare nuclei of heavier elements. Table 4.4.2. shows the composition of primary cosmic rays per 100,000 protons.

The primary cosmic rays made up of the heavy nuclei contain the highest energies. These particles are called high Z(Z symbolizes atomic number), high energy particles or HZE particles. HZE particles are the most damaging cosmic rays to biology and instruments. The effects of these rays will be discussed in Section 4.4.5.

Nuclei	Z(atomic number)	Relative number in Space
Hydrogen ($-\rho$)	1	100,000
Helium (α)	2	6,770
Light Nuclei	3-5	146
Medium Nuclei	6-9	430
Heavy Nuclei	10	246

Table 4.4.2. Primary Cosmic Ray Composition[2].

All cosmic particles approaching the Earth are deflected by the Earth's magnetic field: the slow light particles are deflected more than the fast, heavy ones. The Earth's magnetic field acts somewhat like a large bar magnet or "magnetic dipole." There is a region around the Earth where a compass needle will point along the magnetic lines of force, represented by the dashed lines in Figure 4.4.2. The Earth's magnetic field causes many cosmic rays (like the ray in Figure 4.4.2) to be deflected downward into the Earth. The magnetic deflections of particles produces the "latitude effect"; more cosmic radiation is found at high latitudes (North and South) than near the equator.[1]

Other cosmic particles are deflected into an area called the Van Allen radiation belt (see Figure 4.4.2). The Van Allen belt is an intense region of radiation produced by the accumulation of cosmic and other charged particles. There are no sharp boundaries to the belt, but the whole Van Allen belt is between 320 and 32400 kilometers altitude and extends all around the Earth. The Space Shuttle Orbiter will orbit our payload between 270 and 380 kilometers which is not in an intense cosmic radiation area of the Van Allen belt.

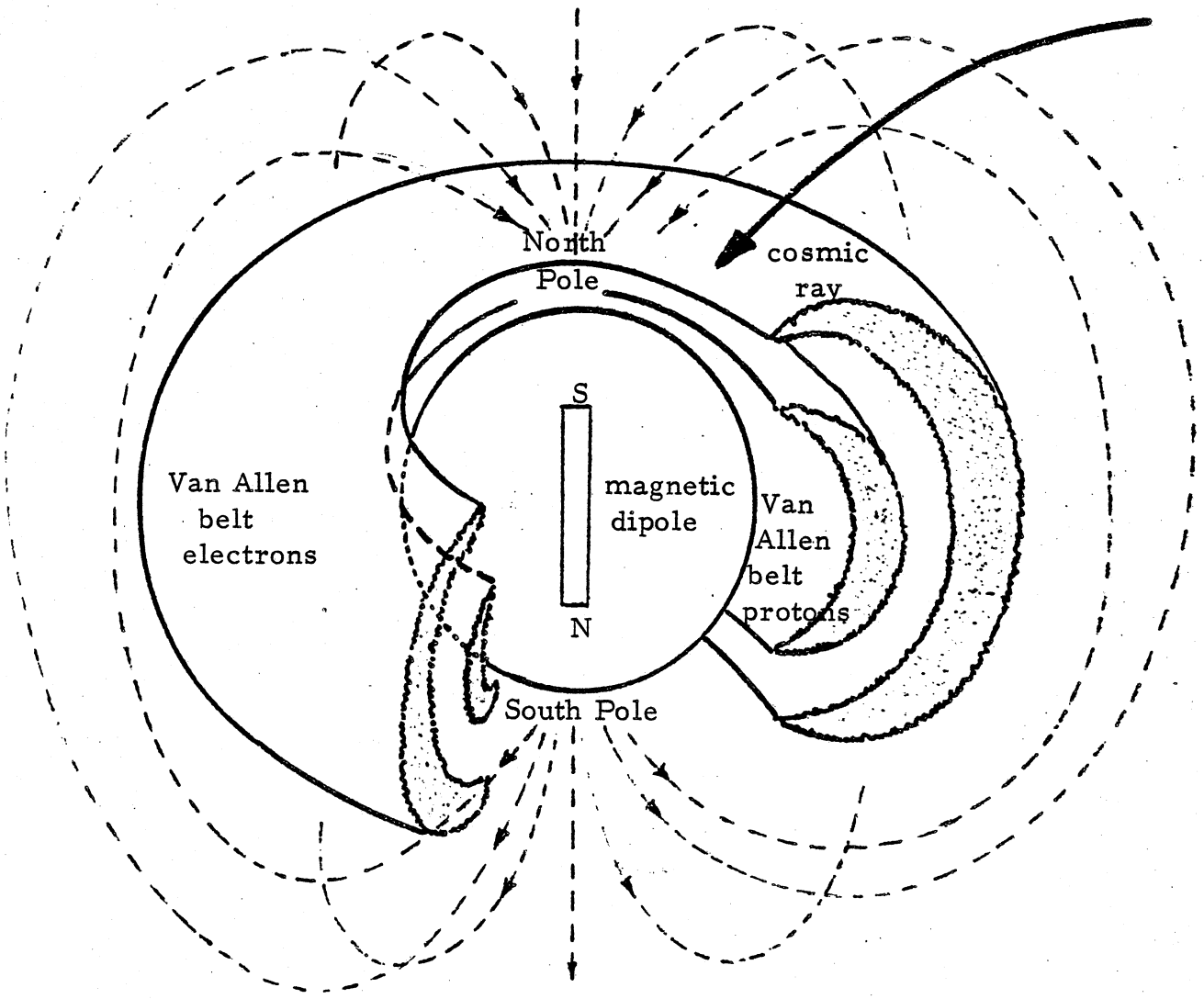

Figure 4.4.2. Schematic Diagram of the Earth and the Van Allen belt. (The dashed lines represent magnetic lines of Force.)

4.4.3.3. Secondary Cosmic Rays. While primary rays are found mostly in outer space, secondary rays are found mainly in the atmosphere of the Earth. Secondary cosmic rays are created when primary cosmic rays collide with the nuclei of gases in our atmosphere. The primary ray and the nucleus of the gas disintegrate into secondary cosmic particles. Secondary cosmic rays are unstable short-lived (less than 1 second) particles called, "π-mesons, heavy mesons, and hypersons." Other particles are also formed which are not as abundant as these. [2]

Often, secondary particles contain sufficient energy to collide with other nuclei in the atmosphere to create even more secondary particles. Thus, when one primary particle enters our atmosphere, it starts a chain reaction of collisions which may produce hundreds or thousands of secondary particles. These collisions continue to multiply, dissipate energy, and form other secondary cosmic rays until a maximum cosmic ray production is reached. Production falls off when there is not enough energy to form more secondary cosmic rays.

Using a Geiger counter to detect cosmic rays, Figure 4.4.3. shows the steady level of count due to primary particles until secondary production begins when the altitude decreases to about 60 km. Maximum secondary production occurs at about 30 km. The counting rate then decreases below 30 km as insufficient energy slows the formation of secondary particles:

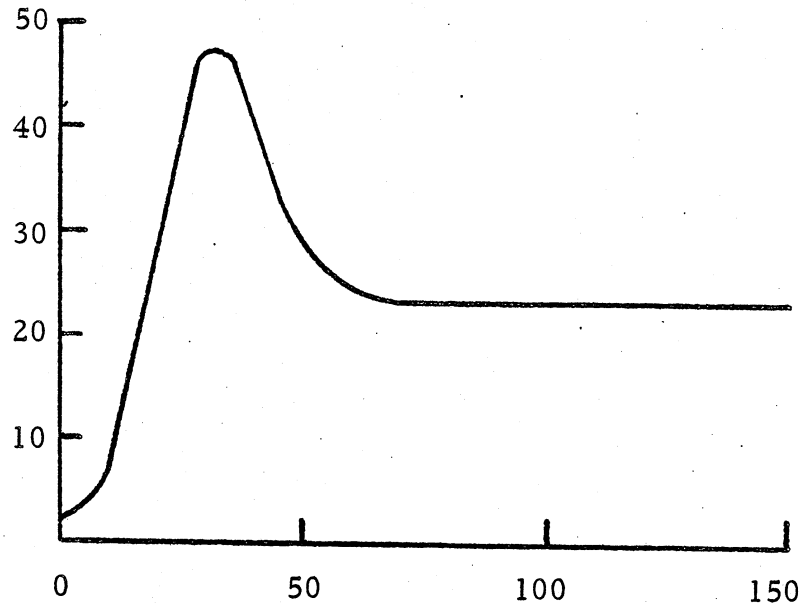

Figure 4.4.3. Counting Rate of a Single Geiger counter as a Function of Altitude .

Since the Orbiter will be orbiting our payload at an altitude of 270-380 km, it is obvious the main concern for our payload will be the primary cosmic rays.

4.4.4. Origin of Cosmic Rays . Our experimental package will be subjected to primary cosmic rays. To understand these particles more fully, it is necessary to consider the origin of cosmic rays. This section considers two sources of cosmic rays: solar and galactic.

4.4.4.1. Solar Cosmic Rays. Solar cosmic rays originate from the sun and make up a small portion of all cosmic rays. Solar cosmic rays have less energy and move at slower velocities than galactic rays. Scientists believe that solar cosmic rays are blown out of the sun by violet explotions. [1]

This report will not be concerned with solar cosmic rays since the Solar Radiation Group is studying this problem.

4.4.4.2. Galactic Cosmic Rays. Galactic cosmic rays are high energy protons and nuclei of heavier elements coming from all directions. Since protons and nuclei of the heavier elements are found everywhere in the universe, the problem is not to explain the presence of these particles, but rather, the problem is how these particles might have acquired their tremendous energies.

Physicists theorize that cosmic ray particles gain their energies by being accelerated by electromagnetic processes more or less like those at work in solar flares. Scientists believe that there are enormous clouds of ionized gas, mostly hydrogen, wandering through space. Energy is exchanged between these wandering clouds and fast moving individual particles. On the average, the individual particles gain energy in the excahnge, thus creating cosmic rays. [2]

Interstellar matter is not distributed uniformly throughout the universe, but rather, is condensed in galaxies. Because of this nonuniformity, the electromagnetic energizing process is though to be condensed in galasies. Thus, it can be assumed that the cosmic rays striking the Earth's surface were created in our own Milky Way Galaxy. However, scientists also believe that a few extremely energetic cosmic rays (10^{19} eV) could possibly be of extragalactic origin. [2]

Other theories, such as cosmic rays originating from stars or supernovae, have also been postulated. These theories explain the origin

of some cosmic rays, but they cannot account for all particles or the high energy radiation witnessed. In summary, there is no absolute concensus on where cosmic rays come from, but electromagnetic acceleration of particles in our Galaxy is the most popular and convincing theory.

4.4.5. Effects of Cosmic Radiation. Cosmic radiation damages both electronic equipment and living organisms. In particular, HZE particles cause the most damage due to their high energy. This section presents an overview of cosmic damage to equipment and organisms so that project personnel can become aware of these effects when designing a cosmic ray experiment.

4.4.5.1. Radiation Effects on Instruments. Cosmic rays affect photographic film in cameras, most of the electronic equipment in spacecraft, and sensitive instruments designed to detect x-rays or far-ultraviolet light. Photographic film is fogged by radiation. Electronic parts, such as semiconductors or discharge tubes, may give unwanted pulses of current (false counts) when cosmic rays or high-speed protons pass through them. Long exposure can permanently damage some electronic parts and can also fog photographic film so that it is unusable. Damage can partially be prevented by shielding equipment with thick metal sides (like a bank vault). [1]

Shielding, however, can also contribute to damaging equipment. The primary rays will hit the shield, causing the metal to absorb the ray,

and thus create secondary particles. The formation of "secondaries" makes calculating the incidence and effect of cosmic particles very complicated.

4.4.5.2. Radiation Effects on Biology. When radiation is absorbed in living cells, it ionizes atoms or molecules in the cell and may disorganize or kill the cell. The loss of a few cells in a large organism such as a human usually has no effect. Long exposure, however may cause harm and more visible damage. Overall biological damage is measured in "rads." One rad (radiation absorbed dosage) is equivalent to 10^{-5} joules of energy absorbed per gram of tissue. For humas, the lethal dose is about 400 rads. Astronauts on long space missions have so far accumulated only 3 or 4 rads, which has no significant effect. However, on future missions of longer duration, cosmic ray dosage may be a serious matter.[1]

In summary, cosmic rays affect instruments and life in varying degrees. The results of any cosmic ray experiment implemented by our group would probably be most beneficial to planners of longer duration space missions.

4.4.6. Detection of Cosmic Rays. Any experiment involving cosmic rays will require some means to detect these rays. Detecting cosmic rays in space should be simple, easy, and accurate. This section describes and makes recommendations concerning five detection devices

used today: the electroscope, Geiger-Müller counter, Wilson "cloud expansion" chamber, photographic emulsions, and Lexon plastic.

4.4.6.1. Electroscope. The electroscope was the first instrument to detect the presence of cosmic rays some seventy-five years ago. The electroscope consists of two bits of gold leaf hung alongside one another at the lower end of an insulated metal rod (See Figure 4.4.4). When a charge of either positive or negative electricity is placed on the leaves, they diverge from one another , taking the shape of an inverted V. If cosmic rays are present in the air, those of the opposite sign to the charge on the electroscope will be attracted to it, neutralize its charge, thus causing the leaves to collapse and hang vertical once again. [3]

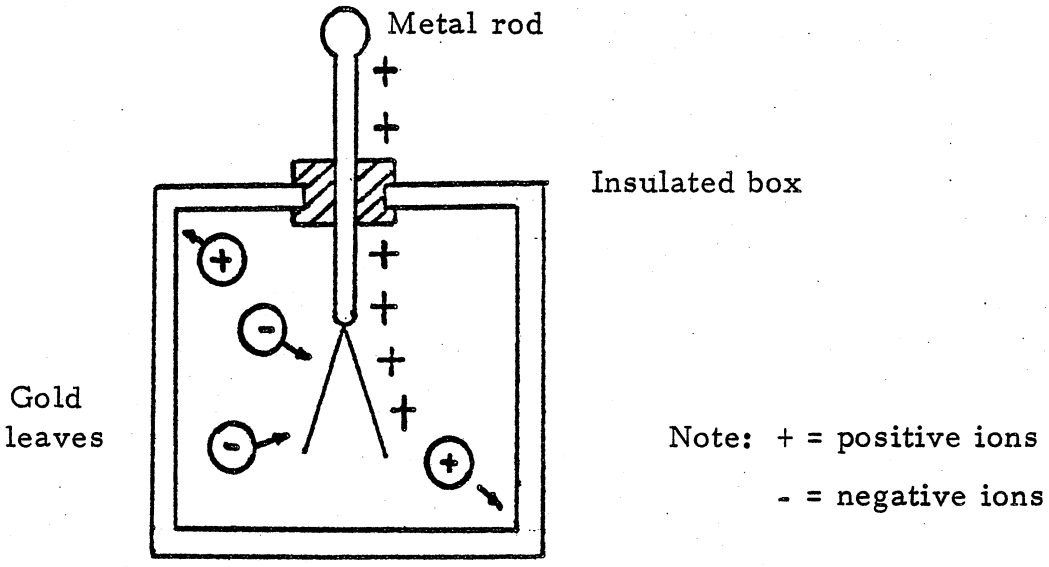

Figure 4.4.4. Schematic of an Electroscope.

The electroscope is a cruide and inaccurate method of detecting cosmic radiation. Therefore, the electroscope is not recommended for our needs.

4.4.6.2. Geiger-Müller Counter . The Geiger-Müller counter or Geiger counter consists of a hollow metal tube with a fine wire stretched along the central axis of the tube. The wire and tube are insulated from each other. The apparatus is sealed in a glass tube containing a neutral gas (usually argon) at a pressure of about 10 cm. of Hg [6] . The wire and the tube are then highly charged with opposite types of electricity almost to the point where a spark will flash between them. If cosmic rays pass through the tube and produce ions, then the gas in the tube will become conductive. A current of electricity will then flow from the wire to the tube momentarily discharging the device and causing a click or count (see Figure 4.4.5)[3] .

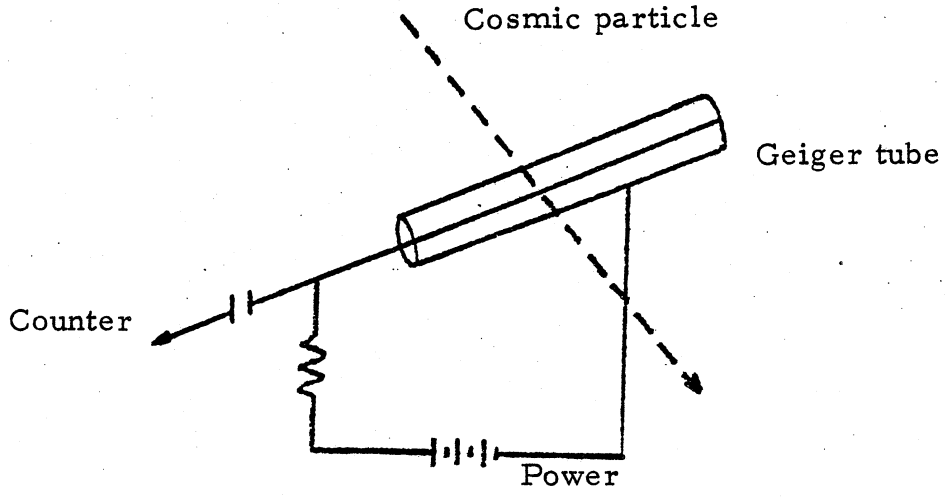

Figure 4.4.5. Schematic of a Geiger-Müller Counter.

The useful qualities of the Geiger counter are its light weight, small volume, insensitivity to temperature and humidity, and ease of use [6] . Shortcomings are its lack of discrimination (it is impossible to identify the type of particle triggering the discharge) and the relatively long "dead time" (10^{-4} sec.) that must elapse after a discharge has occurred before the counter is ready to be triggered again, which prevents very fast counting. Despite these disadvantages, it is recommended the Geiger-Müller counter be studied for further possible use.

4.4.6.3. Wilson "Cloud Expansion" Chamber . Another type of ionization detector is the Wilson cloud chamber. The Wilson chamber is a glass container in which there is plenty of water so that the enclosed air will become saturated (humidity = 100%). To the chamber, there is attached a small piston so that the volume of the chamber can be suddenly expanded. This expansion cools the air slightly and causes a supersaturated state. A fog will then be produced, only if dust or ions are present in the chamber. If all of the dust in the air has been removed, then droplets of fog form only on the ions. By this means, the location of every ion in the chamber can actually be made visible under an intense illumination that shows up every water drop. Photographs can be made for a permanent record [3] .

The Wilson cloud chamber is perhaps the most useful device of all for viewing and detecting cosmic rays. However, there are several

disadvantages including the chamber's sensitivity to temperature and pressure. Therefore, it is recommended that the Wilson cloud chamber be eliminated from consideration for space use.

4.4.6.4. Photographic Emulsions and Lexon Plastic. In the photographic emulsion technique, specially manufactured emulsions must be used. These emulsions are very thick - sometimes as thick as 1mm. - and require very delicate developing and fixing. Such emulsions have no glass support and have a very high concentration of silver bromide crystals, making them sensitive to even minimum ionization due to fast cosmic particles carrying unit charge. The emulsions are examined for cosmic ray tracks by means of a microscope.

Another similiar method which has been recently developed is called "Lexon plastic nuclear detectors." These detectors consist of thin wafers of Lexon plastic. Like photographic emulsions, cosmic particles leave tracks in the plastic, which are then examined by a microscope. Lexon plastic is relatively insensitive and only measures high energy (HZE) cosmic particles, with atomic numbers in the range $8 \leq Z \leq 26$. These detectors were developed for the Apollo missions, and were placed on various parts of the astronauts body to detect cosmic radiation [8].

Both the photographic emulsion and the Lexon plastic methods have many advantages. They are light weight, small bulk, require no electrical power, and can differenciate between different cosmic particles.

The major disadvantage is the time-consuming and delicate microscopic examination procedure required when the experiment is completed. Despite this disadvantage, these techniques are also recommended for further study.

In summary, all five methods measured cosmic radiation by detecting ionization of particles by cosmic rays. However, the Geiger-Muller counter, photographic emulsion, and Lexon plastic methods held distinct advantages over the other detectors devices and merit further study for use in our project. It may even be possible to place a combination of two or three of these detectors in our package.

4.4.7. Previous Cosmic Ray Experiments. Cosmic rays present health hazards to humans and other living organisms in outer space. For this reason, much experimentation with cosmic rays has undertaken in previous Apollo and Skylab missions. Scientists have tested pocket mice, bacterial spores, seeds, and eggs for possible biological damage due to cosmic rays. Astronauts have also been tested. This section gives an overview of these experiments to gain insight on the types of cosmic ray experiments that can be performed in outer space.

Perhaps the most interesting cosmic ray experiments have involved the light flashes in the eyes of astronauts (NASA Experiment MA106). It appears that flashes of light appear in astronauts eyes when they close their eyes. These light flashes take on various shapes and appear in the

eye with a frequency anywhere from 2 flashes/ minute to 8 flashes/ minute. It has been attempted to relate these flashes with the occurence of cosmic rays by placing cosmic ray detectors around the astronauts head. These detectors were sensitive to energies greater than 4×10^{15} electron volts. Results have indicated that there are at least three cosmic particle causes of light flashes, [1]. They are:

1. Ionization in the retina by high-mass cosmic rays.
2. A "shock wave of light" emitted when a cosmic particle moving near the speed of light enters the eyeball whose speed of light is slower than that of the particle.
3. Ionization in the retina by alpha particles produced by nuclear collisions with high energy protons.

Experiments with cosmic radiation have also been used with pocket mice aboard Apollo XVII. These experiments were called, "Project BIOCORE (NASA Experiment M212, Biological Cosmic Ray Experiments)." The primary objectives of the experiments were to determine whether high Z-high energy (HZE), ZZ6, particles can produce microscopically visible injury of brain and eye tissue. Results on the pocket mice showed no visible eye damage, but small lesions on the brain were observed.[9]

Other experiments on Apollo-Soyuz were conducted to determine the damage caused by HZE cosmic rays on small living organisms such as bacterial spores, seeds, and eggs (NASA Experiment MA-107). These spores, seeds, and eggs were stacked between sheets of Lexon plastic to detect cosmic rays. Results showed that the bacteria and eggs showed

serious damage (deformities, inability to reproduce) by the cosmic rays. The plant seeds, however, showed little damage at all.

These experiments give a brief overview of the type of cosmic ray experiments that have been executed in outer space. Note that scientists seem particularly concerned about damage cuased by HZE primary galactic cosmic particles. Hopefully, SCORE can implement a worthwhile experiment to investigate the damaging HZE particles.

4.4.8. Proposed Experiments. Cosmic rays effect instruments, as well as living organisms. As mentioned previously, instruments can be damaged or ruined by cosmic rays. Since our project is designed by aerospace engineers, it is natural that SCORE explore the cosmic particle effects on instruments rather than on biology. One such experiment could be to analyze the damage due to HZE particles on silicon photovoltaic solar cells.

4.4.8.1. Solar Cell Degredation. Many satellites and Skylab have used solar cells to supply electrical power. It has been generally known that solar cells degrade in space due to cosmic radiation and photons. Degredation of solar cells in space is an important consideration because it is essential to know the power output of the cell at all times, although SCORE personnel could find no actual test results of solar cell degredation in outer space, a few computer codes have been written which compute such degredations as power decreases and resistence increases[10].

A solar cell experiment abroad the Shuttle could be surprisingly simple. All that would be required would be a few small solar cells and a cosmic ray detector such as Lexon plastic or photographic emulsions. The Lexon plastic and the photographic emulsions could be stacked on the solar cell. The entire arrangement would be placed on top of the canister (this procedure may have to be cleared by NASA). Control solar cells would be maintained on the ground while the Shuttle is in orbit. When the mission is completed, the SCORE solar cells would be compared to the ground solar cells by such parameters as power output and resistance differences. The cosmic ray detectors would then be counted for cosmic particle tracks. Relations between cosmic particles and solar cell power and resistance would then be sought. Counting the cosmic particles would most likely be the most difficult phase of the experiment since a microscope would be required.

Clearly, this experiment proposal is a very rough preliminary design and much work will be required and many questions need to be answered if it is ever to be flown. However, the main objective of this proposal is to demonstrate the type of instrument experiments which could be performed with cosmic rays.

4.4.8.2. Measurement of Cosmic Rays. In keeping with the measurement theme of project SCORE, it would be possible to just measure the amount of cosmic rays that bombard the Orbiter. This is

a simple experiment which would be easy to set up, execute, and receive data from. All that is required is a Geiger-Muller counter.

The Geiger counter would be placed in the canister (or outside the canister if NASA agrees). The batteries in the package would supply electrical power to the Geiger counter and "clicks" or counts would be recorded on magnetic tape. When the mission is completed, the tape would be read into a computer to get instantaneous results. This set up eliminates the costly microscopie examination period required if photographic emulsions or Lexon plastic were used.

In general, Geiger counters are fairly cheap in price and a spare Geiger counter might possibly be found in the Space Physics Research Laboratory. Volume of weight would not be a problem since Geiger counters are relatively small. A typical Geiger tube is 7 to 8 inches long and about 3/4 inches in diameter. The electronics of the counter can be compared to a small transistor radio in size and weight. More detailed information on Geiger counters is surprisingly scarce.

Much more information on Geiger counters will need to be found if this experiment is to be implemented. Details such as size, weight, counting rate, recharge time, power consumption, temperature limites, and pressure limits need to be considered to integrate the Geiger counter with SCORE. These requirements can be met and they provide a suitable challenge to design and execute an experiment to measure cosmic rays.

References

1. "Apollo-Soyez Pamphlet No. 6 - Cosmic Ray Dosage," NASA-EP138, October 1977.

2. Cosmic Rays, Bruno Rossi, McGraw-Hill Book Co., 1964.

3. Cosmic Rays Thus Far, Harvey Brace Lemon, W.W. Norton & Co., Inc., 1936.

4. The Story of Cosmic Rays, W.F.G. Swann, Sky Publishing Corp., 1955.

5. Cosmic Rays, J.G. Wilson, Wykeman Publications LTD, 1976.

6. Cosmic Rays, Andre Cachon, Alice Daudin and Louis Jauneau, Walker and Co., 1965.

7. "Origin of Ultra High Energy Cosmic Rays," P. Kiraly, NATURE, Vol. 255, June 19, 1975, pp. 619-620.

8. "Heavy Cosmic Ray Exposure of Apollo Astronauts," E. V. Barton and R. P. Henke, Science, Vol. 187, pp. 263-265.

9. "Project BNCORE/MZ12/, A Biological Cosmic Ray Experiment: Procedures, Summary, and Conclusions," Aviation, Space and Environmental Science, Vol. 46, April 1975, pp. 467-481.

10. "Space Radiation of Solar Cells," A.H. Kalma and C.J. Fischer, IEEE Transactions on Nuclear Science, Vol. NS-23, No. 6, December 1976.

4.5 Solar Radiation Experiment (Infrared Measurement) -- Edward A. Thomas

4.5.1. Introduction

The Sun, our nearest star, is the principal cause of life on Earth. The energy radiated from it in the form of electromagnetic radiation, solar wind, gravity, sound, and magneto-hydro-dynamic (MHD) waves provides the energy needed to support and maintain life on our planet. The sun radiates 3.8×10^{33} ergs (energy) every second in the form of electromagnetic radiation alone--of which all the planets and their respective satellites of our solar system combined receive only .000001%. This tremendous amount of energy is created at the Sun's core by a thermo-nuclear fusion process involving hydrogen, whence it takes one million years to reach the solar surface. The overall energy flux density reaching a mean distance of 93,000,000 miles from the sun averages 1367 ± 7 watts/m^2 (a 1976 measurement) [1]. This is called the solar constant, and our climate would disasterously change if that value fluctuated as little as 1%. The value of the solar constant can be obtained from careful measurement of the rate of radiation received in the form of x-rays, ultraviolet radiation, light, infrared radiation, and radio waves outside the atmosphere of the Earth. The importance of the non-fluctuation of this constant is reflected in the fact that, even though continuous monitoring has shown no observable variation, NASA has decided to use instruments aboard the Solar Maximum Mission (SMM) and spacelab to continuously monitor the constant within an accuracy of 0.1 % [1].

The results of a measurement of the solar constant can be combined

with similar laboratory measurements to obtain an estimate of the sun's temperature. Using a black body assumption model of the sun, provides a close approximation of the measurement of infra-red radiation to a coresponding measurement of the temperature of the sun. According to experimental data, an ideal emitter of electromagnetic radiation (a black body) radiates energy at a rate proportional to the fourth power of its temperature. Because the Sun is visible, energy is flowing out of it from hotter to cooler regions (see Fig. 4.5.1.), and so it cannot be uniform in temperature. And since most of the electro-magnetic radiation from the sun is in the form of light, the region associated with the temperature obtained from the black body assumption is that of the photosphere (see Fig. 4.5.1.). This temperature is called the effective temperature and is around 5800° K.

In selecting the topic of "Solar Radiation Measurement," the original plan involved the measurement of the entire spectrum from x-rays to radio waves (see Fig. 4.5.2). It was soon learned that, due to weight and space limitations, a proposed experiment should be limited to one of the types of electromagnetic radiation (since it was found that skylab had measured the entire spectrum, but their experiment took up a whole wall full of equipment). Thus the range was narrowed down to three choices: ultraviolet, infrared, and optical. Concerned with the problems of having to use a port (which meant a depressurized canister) to obtain the ultraviolet and infrared measurements instead of a window in the canister (because it

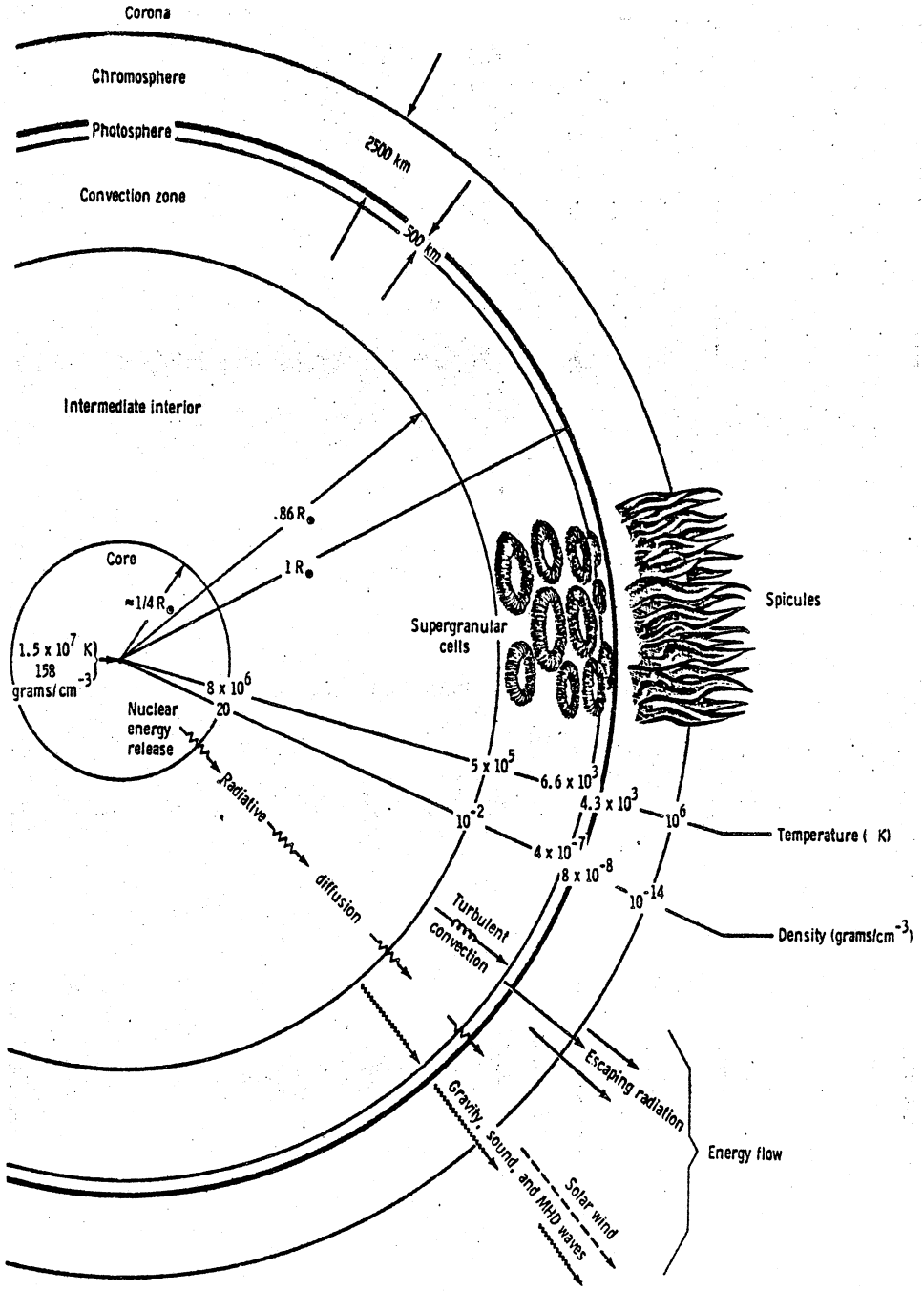

Figure 4.5.1. Idealized general solar properties (not drawn to scale). [2]

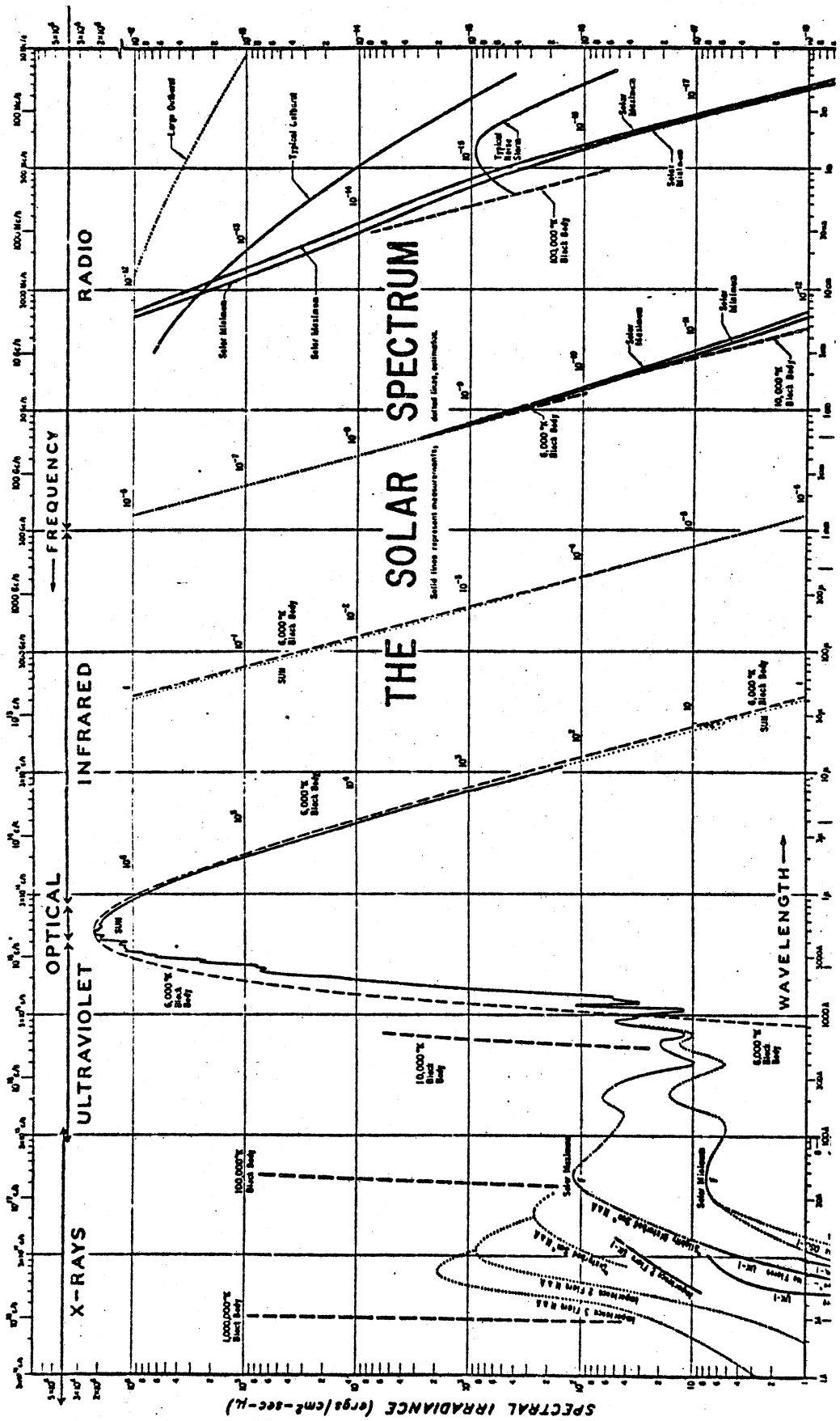

Figure 4.5.2. The Solar Spectrum. [7]

Explanation of Figure 4.5.2.

The units of spectral irradiance read, in unabbreviated form, "ergs per square centimeter per second in a wavelength interval of one micron." Because of the enormous range of energies charted here, it was necessary to fold this logorithmic scale thrice in the infrared and radio regions [7]. The folded sections are accompanied by the appropriate numerical labels. A continuous spectrum would look like this:

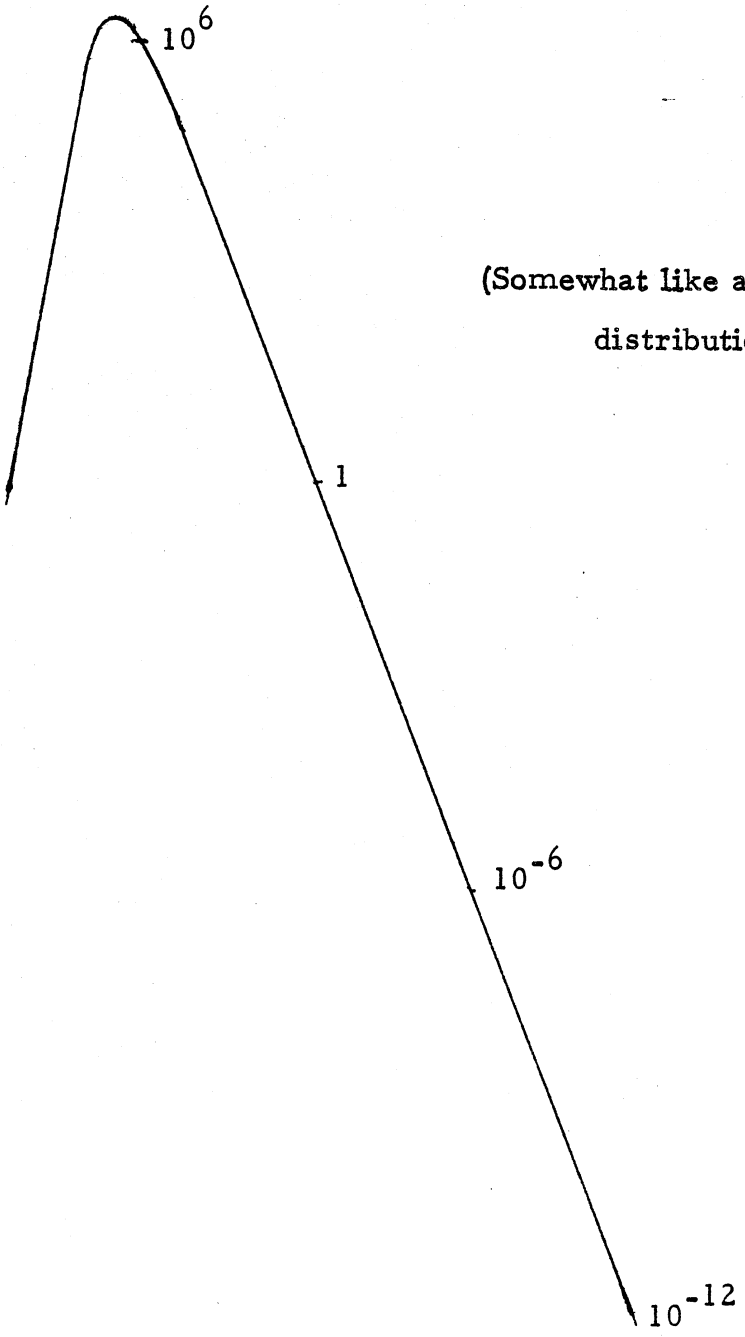

Table 4.5.1.

The Electromagnetic Spectrum

Frequency	Type	Wavelength
beyond 3×10^{18} c/s	γ rays	beyond 1 A
3×10^{18} c/s to 3×10^{16} c/s	X-rays	1 A to 100 A
3×10^{16} c/s to 9×10^{14} c/s	Ultraviolet	100 A to 4000 A
9×10^{14} c/s to 5×10^{14} c/s	optical	4000 A to 8000 A
5×10^{14} c/s to 300 G c/s	infrared	8000 A to 1 mm
300 G c/s to less than 30 M c/s	radio	1 mm to greater than 10 meters

was thought the UV and IR would be altered by the glass, whereas the consensus was that the visible would not be), the problem was investigated until a suitable answer was found. The answer to this problem was a product called IRTRAN (to be used for the canister window), which has very well known absorption properties and also transmits infrared very well. So it was decided that the proposed experiment would measure the infrared spectrum of the Sun.

From the preceding discussion about solar radiation and the reasons why one is interested in measuring it, a statement of the purpose of this proposed experiment is forthwith. It is hoped that the proposed experiment will enable future project SCORE personnel to extrapolate from measurement of the infrared radiation of the Sun the following: (1) the infrared spectrum of the sun, (2) the solar constant, and (3) the approximate temperature of the photosphere of the Sun.

4.5.2. Summary and Conclusions

This experiment is going to measure the infrared spectrum somewhere between 1μ and 300μ (to be determined by subsequent project SCORE designers). It will be aimed at making three determinations: (1) the solar spectral intensity, (2) the solar constant, and (3) the approximate temperature of the photosphere of the sun. Use will be made of a metal (or possibly a thermistor) bolometer with an a. c.

response obtained by using a mechanical "chopper." There are two critical considerations involved with this experiment, the first is a sun oriented flight profile and the second is a special IR filter glass for the proposed window called, "IRTRAN."

4.5.3. Discussion

Since the discovery of the infrared region by Sir William Herschel in 1800, the informational and technological knowledge of the infrared and its detection has evolved slowly but steadily to the early 1900's. With the input of military interest since World War II, the detection and measurement of infrared has matured to the highly technical engineering operation it is today. Because of the many variables inherent in infrared measurement, there is opportunity for great variations in detection type and hence there is no one "best" detector. First, four of the most important variables will be defined; then, the different types of detectors will be discussed.

Infrared detectors are characterized by four major quantities: wavelength response, time constant of response, responsivity, and equivalent noise input. The wavelength response of thermal detectors is usually a wide band of wavelengths, whereas the wavelength response of photon detectors is usually some characteristic wavelength. The time constant of response is given by the equation

$$\tau = \frac{C}{G} = RC \,, \qquad (4.5.1)$$

where C is the thermal capacity of the element and G is the thermal conductance of the element (or R is the thermal resistance). Responsivity is characteristic of a given detector and the units are volts per watt incident radiation. Equivalent noise input is the amount of background "noise" the detector has and is due to thermal effects, resistance of the detector, etc. With any given detector, one wants a high responsivity with a fast response ($\tau \rightarrow 0$). Unfortunately, this presents a dilemma, for to get a high responsivity, one needs a longer time of incident radiation which means a slower time constant, and for a fast time constant, the detector doesn't have enough time to "warm up," i.e., low responsivity[3].

There are two main branches of infrared detectors: photon detectors (which are independent of temperature change), and thermal detectors (which are temperature dependent). Photon detectors are almost always made of semi-conductor material, and are noted for the fact that they respond only to select wavelengths of incident radiation. There are three main types of photon detectors: photovoltaic-- where the incident radiation produces a voltage across the p-n junction of a semiconductive material, photoconductive-- where the incident radiation changes the semi-conductor's electrical conductivity, and photoemissive--where the incident radiation excites electrons in the semiconductor crystal to the extent that they are emitted and become free to be collected by an external anode. Thermal detectors are non-selective

of the radiation incident upon them; that is, they are not wavelength dependent. There are four main types of thermal detectors: thermocouple--where the radiation incident upon a thermoelectric junction of two different metals develops a characteristic voltage, Golay cell--where the radiation incident upon a pneumatic chamber filled with a certain gas expands a membrane stretched across one end of the cell and this distortion is detected by a complicated means of mirrors and lenses, pyroelectric--where the incident radiation increases the temperature of a material and hence its electrical charge, and the bolometer. There are two types of bolometers, the thermistor bolometer and the metal bolometer. Both detectors use a change of electrical resistance with increase in temperature as their mechanism of detection, but the thermistor bolometer uses a semi-conductor material, whereas the metal bolometer uses a metal, usually nickel or platinum, coated with a special "black" to increase its detection capabilities [3].

The type of detector finally recommended for use in the UM/ SCORE package is the bolometer. Since the experiment is to obtain the infrared spectrum over a range of wavelengths, that cut out the photon detectors because they are wavelength selective. That left the thermal detectors. Of the thermal detectors, the Golay cell was out because of weight and complexity considerations, while the pyroelectric type was out due to a lack of sufficient information. Between the thermocouple and the bolometer, the bolometer was chosen because much more information about the bolo-

meter type was on hand. Of the bolometer type, there are two kinds, and, although the rest of this report deals with a detector system as pertaining to a metal bolometer, room for choice between the two is left for subsequent SCORE personnell to choose.

The flow diagram given in Fig. 4.5.3 shows how a typical infrared detection system might be developed, from the operational requirements to completed product. It is included in this report for future reference. The remainder of this section deals with the detector system that is proposed, starting from the detector unit itself and building up, like an automobile on an assembly line, to the complete system package.

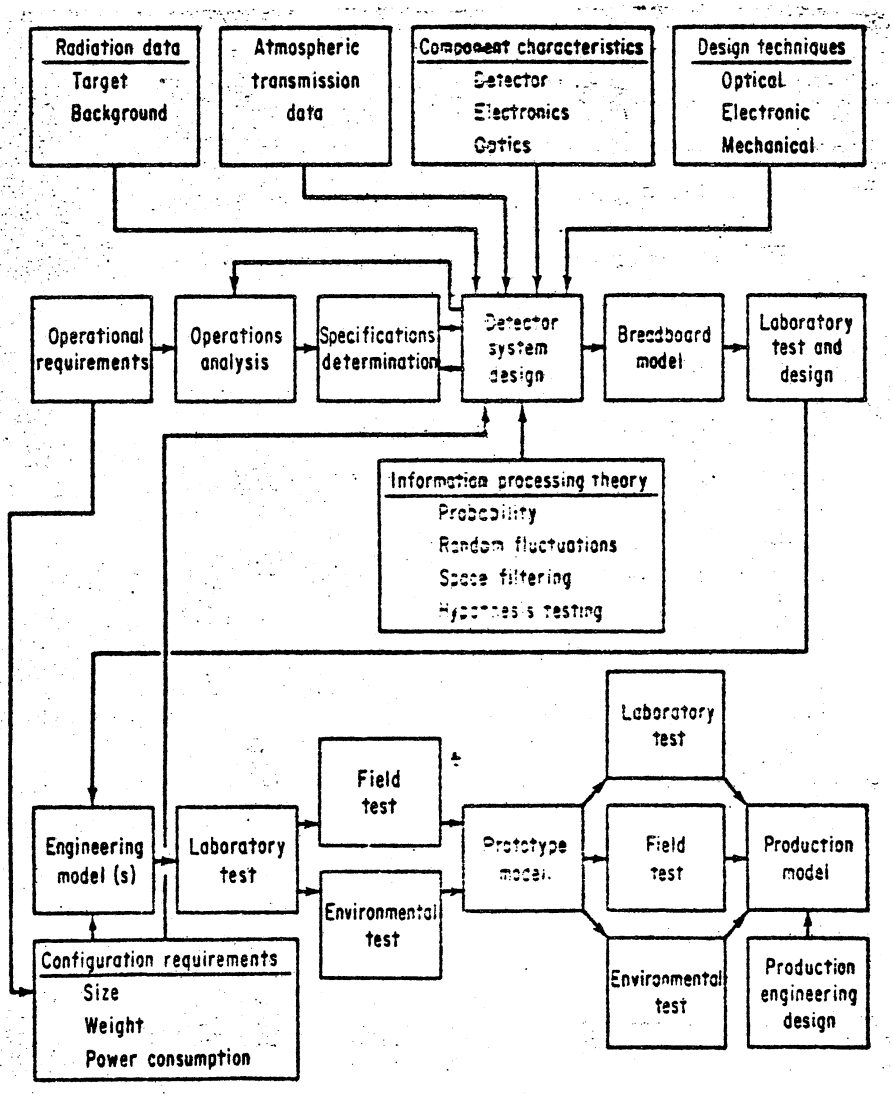

Figure 4.5.3. [4].

The basic bolometer circuit consists of a Wheatstone bridge type arrangement with a d.c. voltage source (in series with a calibration resistor) across two points of the bridge and the output terminals as the other pair of points of the bridge. As the bolometer resistance increases due to the incident radiation, the voltage drop across the output points of the bridge changes and this is what you are measuring (see Fig. 4.5.4).

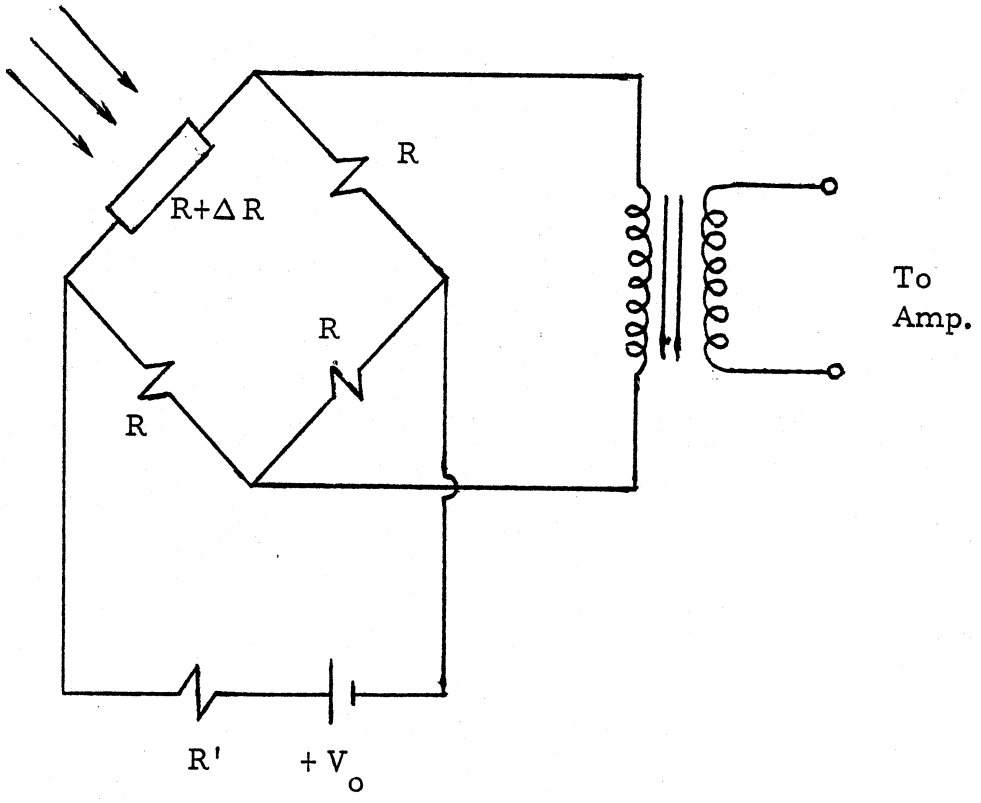

Fig. 4.5.4. Typical Bolometer Circuit.

For all bolometers, there is a complication of this polarizing voltage (V_o). This voltage must be very steady and this can be a troublesome point. Since the variation of the voltage output is very small, before it can be hooked up to a recorder, it has to be amplified. Here we run into another problem in that because the resistance of the metal strip bolometer is usually very small (on the order of 20Ω), it has to be hooked up to a step-up transformer (to bring the resistance up to about 2MΩ) before it can be hooked up to the amplifier.

The detector signal is turned into an a. c. signal before getting to the transformer and amplifier by "chopping" the radiation incident on the detector by a mechanical means. Chopping will be discussed in a subsequent section. The frequency to be amplified is dependent upon the chopping frequency, because, in order to keep noise to a minimum, the amplifier must be tuned to accept a small bandwidth about the chopping frequency. The noise introduced into the signal by the amplifier may be expressed as a resistance R, where R is equivalent to the Johnson noise (to be discussed later) introduced by a resistance R [3] .

The next element of the circuit is a voltage rectifier (see Figure 4. 5. 5.), and from there the output is finally recorded. The R-C circuit shown in Fig. 4. 5. 5 has the effect of smoothing out the rectified output and reducing the bandwidth of the signal talked about in the preceding paragraph to the value $(4RC)^{-1}$, where R(= R') is the resistance of the recorder.

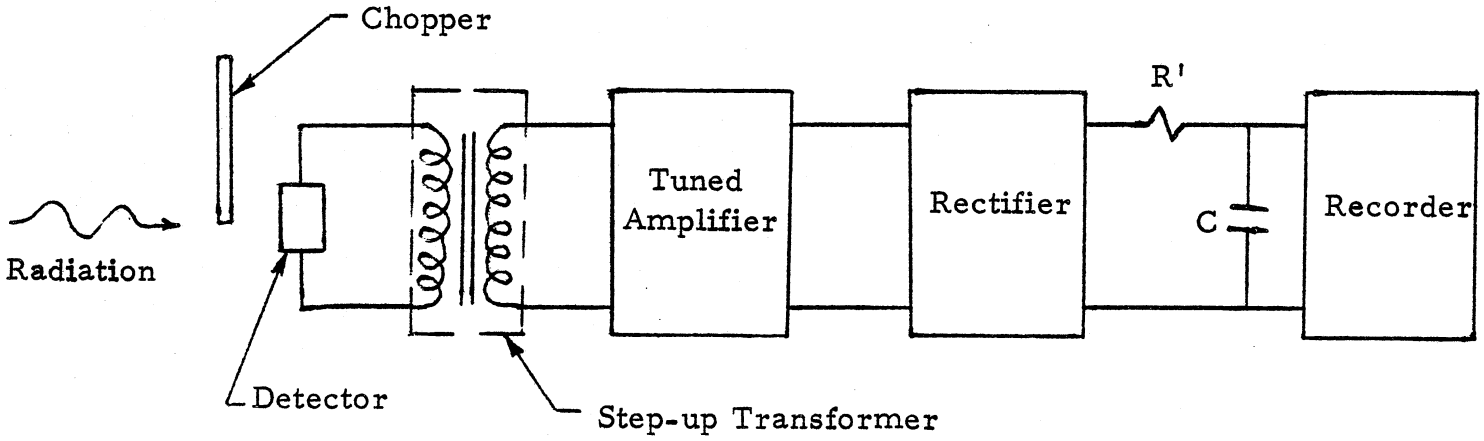

Fig. 4. 5. 5. Detector Electrical System. [3]

The disadvantage of this system is that, although the bandwidth of the signal has been smoothed, the noise passing through the amplifier will be present, smoothed and rectified, as will be the signal.

The next stage to be discussed is the chopper. The chopper will be run by a small d. c. motor powered by the main power supply. The chopper will be a rotating disc with missing sections. The frequency of chopping is determined by two things; the time constant of the detector, and the rate at which information is required from the incident signal. Thermal detectors normally have chopping frequencies of 5, 10, and 13 c/s [3]. Chopping is advantageous because it helps you get rid of unwanted radiation. Chopping is also helpful because a. c. signals are easier to amplify, and noise is reduced by using a high chopping frequency.

The final total detector package should look as pictured in Fig. 4. 5. 6. Next, some special considerations necessary to the operation of this particular experiment will be noted. First of all is the window consideration. The window we will be provided with has to have a special type of glass that will filter out all but the infrared radiation. This glass is available upon request from NASA (for a fee) and it is called IRTRAN. The IRTRAN types range from IRTRAN 1 to IRTRAN 6 [4 and 6]. The IRTRAN should be matched up with the wavelengths this experiment will evaluate. The second consideration is the mission profile. This experiment requires a mission profile that spends some

amount of time with the bay doors pointed toward the sun. A third consideration is the on/ off switch. This consideration is not as imperative as the other two, but at this time there seems to be no way in which a timing sequence will be able to do the job, i. e., to know when the bay doors are pointed toward the sun. So it is recommended that we use one of the three available on/ off signals from the astronauts as the "on" switch for this experiment.

The "noise" in a detector is related to its characteristic resistance by the following equation

$$E^2 = 4kTR(f_2 - f_1) \qquad (4.5.2)$$

where E is the rms voltage value for the Johnson noise, k is Boltzman's constant, f_1 and f_2 are the upper and lower limits of the bandwidth of frequencies that were passed by the measuring system, R is the detector resistance, and T is the absolute temperature. Amplifiers also produce noise according to the same equation. As a matter of fact, the main reason why a step-up transformer is placed between the two is to raise the detector noise (as a function of its resistance) to a value several times greater than that produced by the amplifier. These noise voltages are added in the following fashion: if E_1 is the noise given by the detector and E_2 is the noise from the amplifier, then the total noise (E) is given by the equation $E^2 = E_1^2 + E_2^2$. For a more complete discussion, see Infrared Instrumentation and Techniques (Ref. [5] , pgs. 24 and 25).

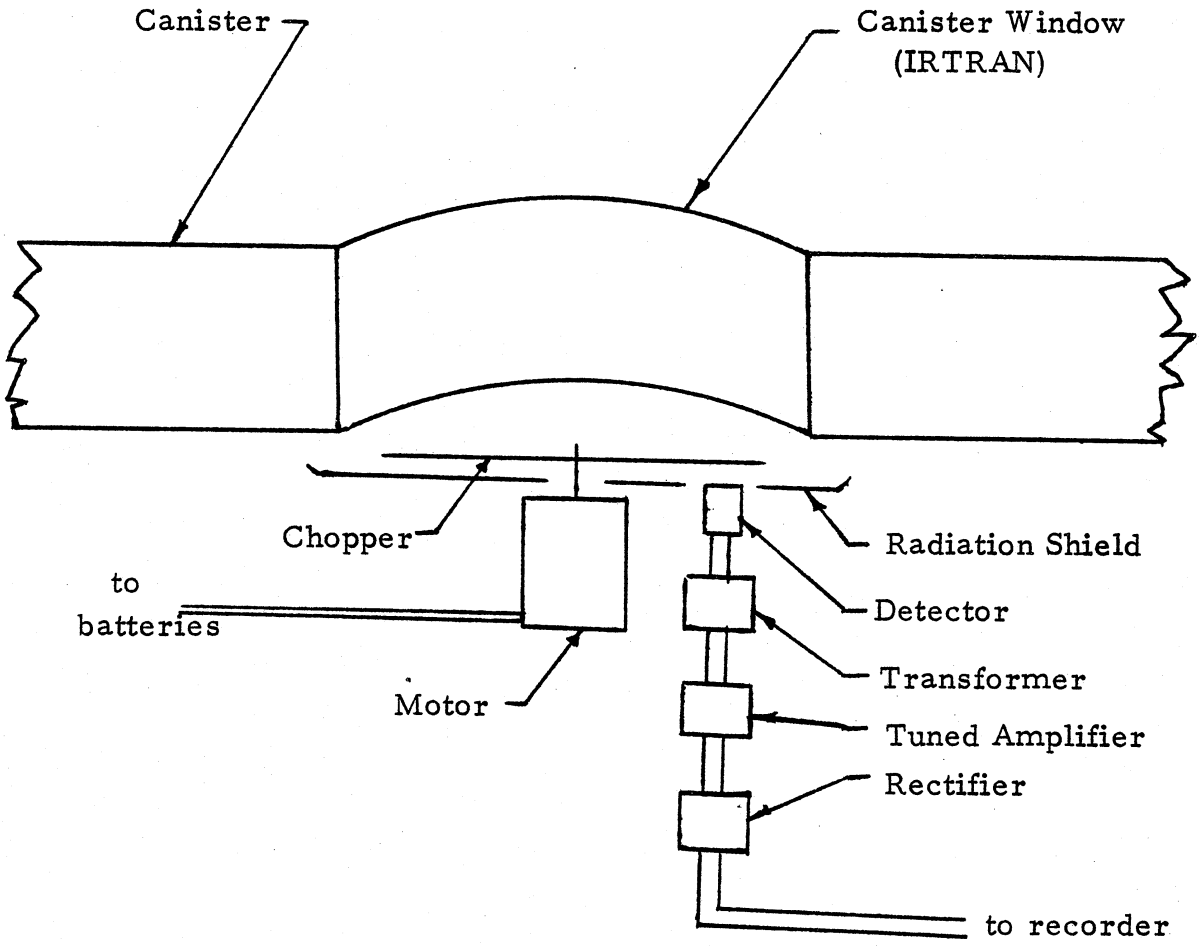

Fig. 4.5.6. Total System Package .

There are two more types of noise present in most detectors, current noise and thermal noise. For pure metals, current noise is negligible and shall not be considered further because we will be using a metal bolometer. The thermal noise in a detector is given by the equation

$$\omega^2 = 16\, A\, k\sigma\, T^5 (f_2 - f_1) \qquad (4.5.3)$$

provided the only contact it has with its surrounding is thru radiation alone. In the above equation, ω is the average thermal noise power value for the detector, A is its area, σ is the Stefan-Boltzman constant, and the rest of the symbols are as described for the same symbols in the equation for the Johnson noise. See Infrared Physics, (Ref. [3]) for the derivation of the above expression and a thorough explanation of Thermal noise.

Afterword

I was originally thinking of measuring the infrared between 30 μ and 300μ , because, to my knowledge, it has never been done before. It could be attempted using the new pyroelectric detectors that have been developed for use with lasers. But since I could obtain no information about these new detectors, and since the energy levels irradiated by the sun in this region are so low, we will have to be conventional and measure the near infrared.

References

[1] Solar Terrestrial Programs, David P. Stern, NASA Publications, August 1978.

[2] The Quiet Sun, by Edward G. Gibson, NASA Publication SP-303, 1973.

[3] Infrared Physics, Houghton and Smith, Oxford University Press, London, 1966.

[4] Infrared Physics and Engineering, Jamieson, et. al., McGraw-Hill, New York, 1963.

[5] Infrared Instrumentation and Techniques, by A. E. Martin, Elsevier Publishing Co., Amsterdam, 1966.

[6] Infrared Radiation, Antonin Vasko, CRC Press, Cleveland, OH, 1968 (translated).

[7] Graph of the Solar Spectrum compiled by H. H. Malitson, Goddard Space Flight Center, Greenbelt, Maryland, August 1964.

5. OPERATIONS

5.1. Safety -- Raymond T. Bush

5.1.1. Introduction

Any mishap in a Getaway Special (GAS) payload could jeopardize the primary payloads or the orbiter and the crew. The purpose of the safety program is to eliminate or reduce to a minimum any hazardous functions which could result in damage to property or injury to personnel. GAS payloads will have to conform to NASA's safety regulations.

5.1.2. Summary

Safety requirements for GAS payloads are not definitive at this time [1]. These requirements will be more fully developed in the near future. At the earliest, the first GAS will be flown in late 1981. The basic shuttle safety policy applies to Getaway Specials. This does not affect GAS payloads very much unless explosives or toxic gases are carried in the experiment. NASA will give safety reviews to design proposals which will eventually lead toward safety certification of the GAS.

5.1.3. Basic Shuttle Policy

The basic shuttle safety policy is stated in the following two NASA documents: "Safety Policy and Requirements for Payloads Using STS" [2] and "Launch Site Accomodations Handbook for STS Payloads" [3]. In case of conflict between these two documents, "Safety Policy" takes precedence. These documents are primarily concerned with

explosives, propellants, radiation, toxic/combustible/corrosive materials, pressure vessels, electrical hazards, offgassing, and outgassing. It appears that Project SCORE would be concerned with pressurization, electrical hazards, and outgassing from the batteries. The electrical circuit should be protected against possible short-circuit and fire hazards. If the canister is pressurized, the design burst pressure level will have to be found. In general, safety factors must be equal to or greater than 1.4. This value is slightly higher for pressure vessels.

5.1.4. Safety Reviews

Implementation of the safety requirements has been delegated to the Johnson Space Center (JSC), which has accepted Goddard Space Flight Center (GSFC) as the GAS payloads representative. GSFC will publish safety guidelines to inform GAS users of their responsibilities. Formal safety reviews will be conducted by the Payload Safety Review Panel which includes representatives of JSC and Kennedy Space Center (KSC). In order to make an informed presentation at these reviews, GSFC, the GAS representative, must receive some basic information from GAS users. Since design iterations are anticipated, GSFC requires only informal information at the time of payload conception. More formal information will be required when the experimenter decides on a "Design Freeze" [4].

Safety compliance and basic design information will be needed by GSFC. A safety compliance data package shall precede the delivery of the payload to the launch site by 30 days. This package generally states that all safety requirements have been met. Project SCORE might have to be concerned with the following two items contained in the package:

1. A log book maintained on each pressure vessel/system showing pressurization history, fluid exposures and other pertinent data shall be delivered with the payload.

2. Summary of the tests, analyses, and/or inspections performed to show verification of the related safety requirements [2] .

In addition to this data, each experimenter must send to GSFC detailed design, operations, and descriptive data for evaluation. This data must include drawings, electrical and mechanical schematics, chemical and biological balance equations showing heat flow, assembly, and handling procedures for all payload systems [4] .

5.1.5. Testing and Final Certification

GSFC has final safety certification responsibility and therefore must be able to perform pre-flight payload inspection and test, if necessary. NASA reserves the right to inspect and/or test any and all materials, components and elements of the payload at any time. At present, NASA is considering the advisability of shake-testing experiments to establish the structural integrity of the package [5] . Unless

our design incorporates shock mounting, our experiment will probably need this vibration test. NASA will charge GAS users a nominal fee for pre-launch testing and/or servicing. The safety procedures are summarized in Figure 5.1.1. A safety matrix is also included for reference as Figure 5.1.2. During the year before launch, NASA wants final input data to support a safety certification and to permit a final technical/ thermodynamic check. Roughly two months before the scheduled flight, the package must be delivered to NASA. It should be delivered in person to KSC. The GAS user is responsible for the cost of shipping the payload to NASA. The payload should be shipped only after the design has been given safety certification by NASA. Once at KSC, the payload will be given a final safety inspection, and then installed in the flight container or canister.

GET AWAY SPECIAL
SMALL SELF-CONTAINED PAYLOADS

SAFETY PROCEDURES

1. EXPERIMENTER PROVIDES DESCRIPTION AND PRELIMINARY ELECTRICAL, MECHANICAL, AND CHEMICAL SKETCHES TO GSFC.
2. GSFC SUGGESTS MATERIALS, PYROTECHNICS, STRUCTURES, ETC,: SENDS PAYLOAD SAFETY MATRIX TO EXPERIMENTER.
3. EXPERIMENTER COMPLETES DESIGN, FILLS IN SAFETY MATRIX EXPLAINING HOW HAZARDS ARE MINIMIZED, AND SENDS FINAL DRAWINGS AND SCHEMATICS TO GSFC.
4. GSFC REVIEWS SAFETY ANALYSIS AND WORKS WITH EXPERIMENTER TO FINALIZE IT.
5. GSFC PRESENTS THE PERTINENT DATA TO THE JSC/KSC SAFETY REVIEW BOARDS.
6. REITERATE 3, 4, AND 5 UNTIL APPROVED. TWO OF THESE SAFETY REVIEW CYCLES ARE A STANDARD SERVICE. ALL SAFETY REVIEW CYCLES AFTER THE SECOND MAY BE CHARGEABLE TO THE EXPERIMENTER.
7. PAYLOAD IS INSPECTED IN DETAIL AND TESTED IF NECESSARY BY GSFC FOR COMPLIANCE WITH SUBMITTED MATERIAL BEFORE INSTALLATION INTO FLIGHT CONTAINER. ANY TESTING REQUIRED IS A CUSTOM SERVICE CHARGEABLE TO THE EXPERIMENTER.

Figure 5.1.1. [4] .

PAYLOAD SAFETY MATRIX

PAYLOAD:	PAYLOAD ORGANIZATION:	DATE:	PAGE:

SUBSYSTEM \ HAZARD GROUP	COLLISION	CONTAMINATION (TOXICITY, ETC.)	CORROSION	ELECTRICAL SHOCK	EXPLOSION	FIRE	INJURY AND ILLNESS	LOSS OF ENTRY CAPABILITY	RADIATION	TEMPERATURE EXTREMES		
BIOMEDICAL												
HAZARD DETECTION AND SAFING*												
CRYOGENICS												
ELECTRICAL												
ENVIRONMENTAL CONTROL												
HUMAN FACTORS												
HYDRAULICS												
MATERIALS												
MECHANICAL												
OPTICAL												
PRESSURE SYSTEMS												
PROPULSION												
PYROTECHNICS												
RADIATION												
STRUCTURES												

NOTE: Hazard groups and subsystems are defined and described in JSC 11123, STS Payload Safety Guidelines Handbook. The subsystems list may be added to or modified to relate to a specific payload. The intent of this form is to assist the Payload Organization in scoping the task of identifying hazards associated with the payload.

*REFERENCE SECTION 3.2 "CAUTION AND WARNING" IN JSC 11123.

Figure 5.1.2. [4] .

References

[1] Telephone conversation with Gene McCoy, Chief of Payload Integration, Kennedy Space Center, March 1, 1979.

[2] "Safety Policy and Requirements for Payloads Using the Space Transportation System (STS)," NASA , Washington, D. C., March 1979.

[3] "Launch Site Accomodations Handbook for STS Payloads," Section VI, Kennedy Space Center, March 14, 1978.

[4] "GAS Experimenter Handbook," NASA , Goddard Space Flight Center, December 1978.

[5] "Small Self Contained Payload Program 'GAS'," Chester M. Lee, August 1978.

5.2. Administrative Matters -- Gregory J. Ruselowski , Raymond T. Bush

As with any project of this size and scope, other non-technical areas must be addressed. Presently three areas have been considered: launch site processing, offers of technical assistance, and insurance.

5.2.1. Launch Site Processing

The Get Away Special (GAS) has limited interfaces with the orbiter and will not be processed as a standard payload. Presently, NASA plans to send project SCORE a shipping container which has the exact dimensions as the actual canister that SCORE will be flown in. The SCORE package will be transferred from the shipping container to the flight canister at a Receiving and Build-Up Center whose location has yet to be determined. The GAS will then be installed in the Orbiter at the Orbiter Processing Facility (OPF) at Kennedy Space Center (KSC). At the OPF, the GAS payloads will be built-up, attached to a special bridge beam, and installed in the Orbiter much like any other bridgebeam.

A Launch Site Support Plan (LSSP) will be prepared upon completion of the coordination and negotiation between the Space Transportation System (STS) User Organization and the Launch Site Support Manager (LSSM). The plan is a commitment of launch site facilities, support equipment, and services to the STS User for a given time period. A generic (or substitute) LSSP will be prepared by KSC for GAS users and will be approved by KSC and Goddard Space Flight Center (GSFC). Additions to the generic LSSP will be prepared as necessary for each GAS payload.

5.2.2. Offers of Technical Assistance

Through the GAS coordinating office at GSFC, several companies have obtained our name as a GAS participant. Subsequently these companies have written to us offering their resources, technical expertise, and facilities to project SCORE. Obviously, some sort of payment will most likely be charged if SCORE decides to accept any of these services. Thus far, four companies have expressed interest in helping us and their brochures are available in the Aerospace Engineering 482 Library. A list of these companies can be found in Appendix F.

5.2.3. Insurance

Much time, effort, and expense is involved with project SCORE. When completed, the package will constitute a substantial investment and there will be a potential for loss.

To alleviate the pain of possible package loss, two insurance companies have written to the SCORE team indicating that they are developing special programs to insure GAS users. Information about the companies can be found in the Aerospace Engineering 482 Library. The addresses of the companies are listed in Appendix G.

APPENDIX A

Power Conditioning Circuits and Information

CALCULATING VOLTAGE REQUIREMENTS FOR

Power-Supply Transformers

By WILLIAM J. BATES,
Special Products Div.,
Zenith Radio Corp.,
Chicago, Ill.

TRANSFORMER OUTPUT VOLTAGES required to achieve given d-c output voltages can be determined accurately by a simple, rapid method. In a full-wave capacitor-input filter circuit for a d-c power supply, the magnitude of the d-c output voltage, as related to the rms value of the a-c input to the transformer, is a function of four independent variables: capacitance of the input capacitor, C, in farads; powerline frequency, ω, in radians; load resistance, R_L, in ohms; and series resistance, R_s, in ohms.

If the product of $\omega R_L C$ exceeds a certain value, it may be considered a constant, and a system of mathematics may be employed that simplifies computation. Such errors as arise from this approximation are negligible in practical applications owing to the tolerance variation in components.

The plot assumes $\omega R_L C \geqq 100$. With the availability of silicon rectifiers and high-capacitance electrolytic capacitors, the product of $\omega R_L C$ can be made $\leqq 100$, that is, variations in R_L may be compensated for by C.

The load resistance of the circuit is determined by the voltage and current requirements so it cannot be changed to achieve this end. Also, power-line frequency cannot be changed readily.

The series resistance is the sum of transformer resistance and rectifier forward resistance. With silicon rectifiers, the rectifier forward resistance is usually negligible compared to the transformer resistance. Transformer resistance, determined by the turns ratio and wire size, can be predicted accurately if the transformer output current and approximate a-c voltage are given.

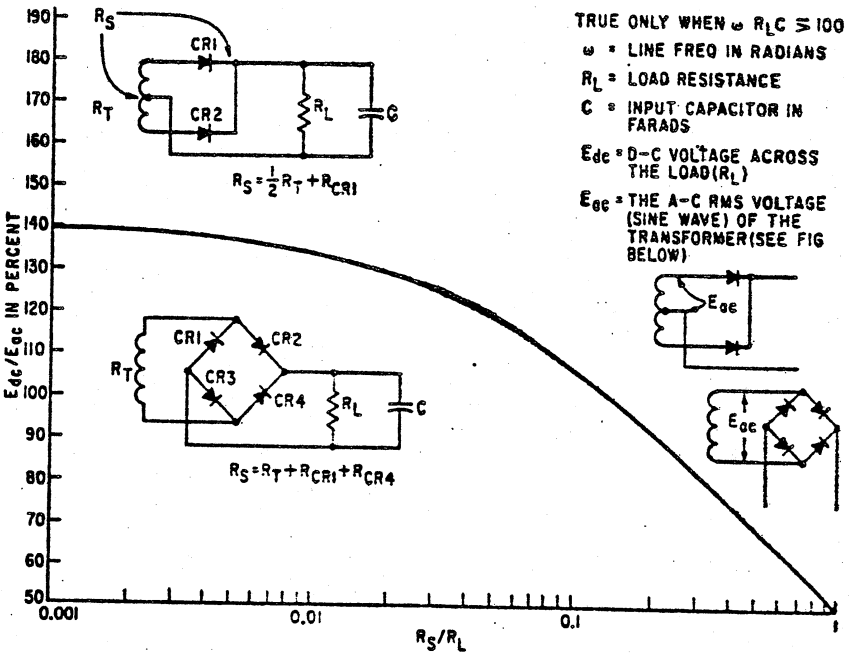

How E_{d-c}/E_{a-c} varies with R_s/R_L for full-wave rectifiers

With the above information and with the aid of the curve, the a-c output voltage of the transformer can be specified.

Example 1: A 250-v, 50-ma source voltage is required for the unregulated portion of a regulated power supply. It is to be operated from a 60 cps source. Therefore $R_L = 250/(50 \times 10^{-3}) = 5{,}000$, $\omega = 2\pi \times 60 = 377$, Minimum $C = 53$ μF so that $\omega R_L C = 377 \times 5{,}000 \times 53 \times 10^{-6} = 100$. Experience predicts a series resistance of 40 to 80 ohms. This means R_s/R_L will vary between 0.008 and 0.06. The E_{dc}/E_{ac} ratio will vary between 1.35 and 1.31, which means that the rms transformer voltage required will be between 185 and 191 v rms. This is about 2 percent accuracy — a typical transformer tolerance. Therefore, the center value of 188 volts would be chosen.

Example 2: Given a rectifier filter circuit with a series resistance (R_s) of 100 ohms, an output voltage of 250v at 50 ma, and with $\omega R_L C \geqq 100$, what is the percent of regulation if the load is reduced to 25 ma?

$$R_{L1} = \frac{250}{(50 \times 10^{-3})} = 5{,}000 \text{ ohms}$$

$$R_{L2} = \frac{250}{(25 \times 10^{-3})} = 10{,}000 \text{ ohms}$$

The R_s/R_L ratio would vary between 0.02 and 0.01. On the curve, E_{dc}/E_{ac} will vary between 1.29 and 1.34. If transformer voltage is 188v, the d-c voltage will be $188 \times 1.34 = 251.9$ or $188 \times 1.29 = 242.5$. The regulation would be 3.7 percent with the 50 percent load change.

BIBLIOGRAPHY

O. H. Schade, *Proc IRE*, 31, p. 341, 1943.

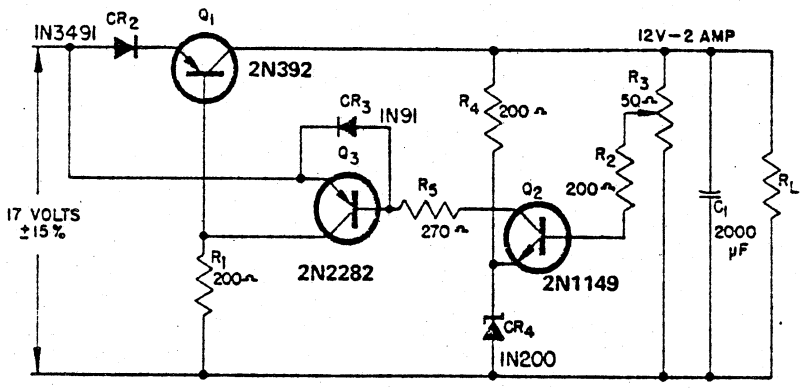

1.1.14 Delco proportional voltage regulator. A voltage proportional to the output voltage is compared to the voltage of reference diode CR4. The differential signal is then amplified by transistor Q3. The output signal of this transistor is used to control the current in the series transistor Q1 in such a way that the voltage across the load remains constant.

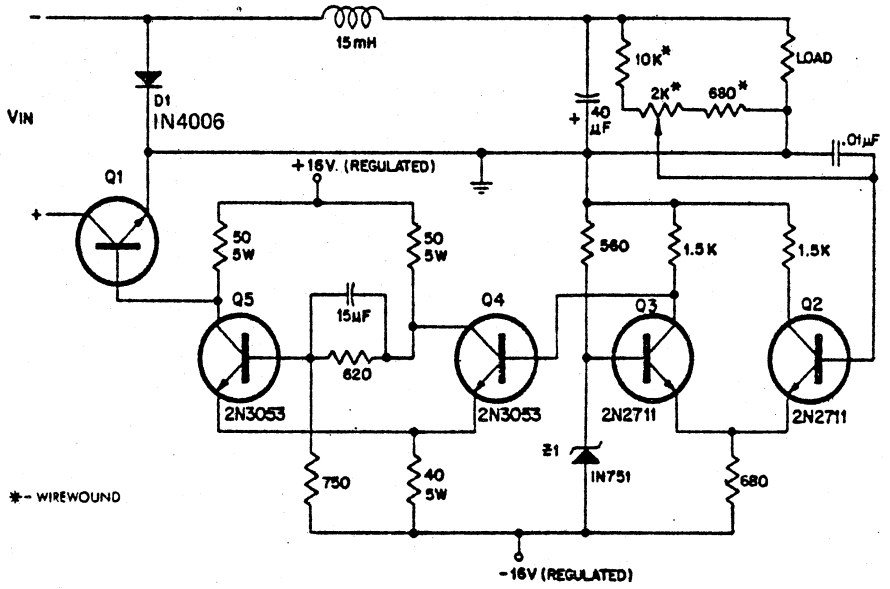

1.1.15 Delco pulse-width-modulated switching regulator uses a single high-voltage silicon transistor as a series element. The output voltage is manually adjustable within the range of the potentiometer in the error voltage divider. This method of voltage regulation has several definite advantages over conventional regulation:

1. Higher efficiency.
2. Fewer series elements.
3. Less heatsink area.

By using a transistor (for Q1) from the Delco DTS-410, DTS-411, DTS-423, DTS-430, or DTS-431 series, various combinations of output voltages and currents may be obtained. The following table shows the maximum regulator conditions for these devices.

Q1	Max Input	Max Output	
DTS-410	200V	150V,	2A
DTS-411	300V	225V,	2A
DTS-423	325V	250V,	2A
DTS-430	300V	225V,	3A
DTS-431	325V	250V,	3A

Efficiencies as high as 92% can be obtained under full load. Total regulation for minimum-to-maximum inputs and minimum-to-maximum loads is less than 0.6%, and ripple is 0.75V peak at full load.

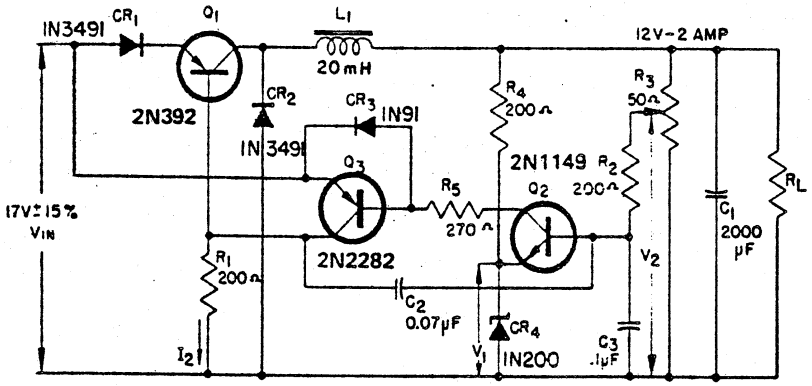

1.1.16 Delco pulse-width-modulated voltage regulator is a series regulator operating in the switching mode. High efficiency is the outstanding advantage to be gained from this mode of operation. Efficiencies as high as 80% can be realized even with the input voltage several times larger than the output voltage. The main disadvantage, poor frequency response, may be lessened by using a higher switching frequency.

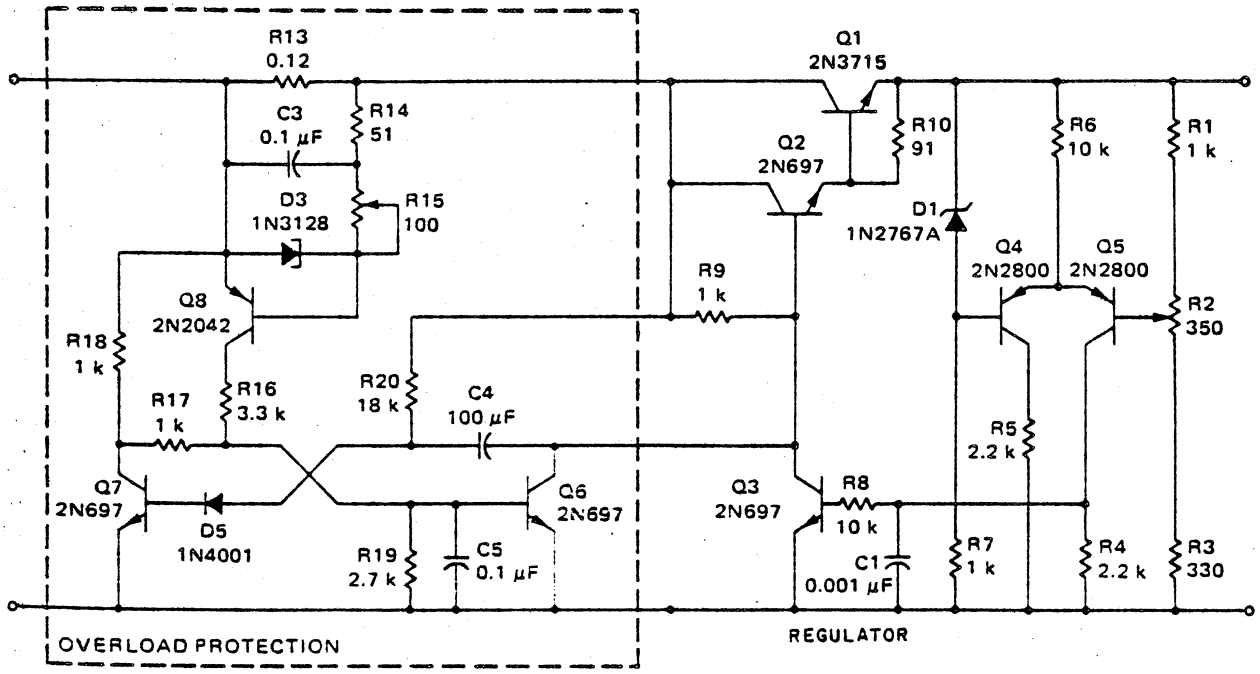

1.1.17 Motorola series regulator with overload protection. Overload sensing circuit triggers the monostable multivibrator, which in turn removes the drive from the series-pass driver transistor. This turns the regulator circuit off until the monostable multivibrator resets. If the overload still exists after reset, the regulator is again turned off. This type of protection would be adequate for resistive loads; however, for large capacitive loads, the surge current charging the capacitor would cause the overload circuit to turn the regulator off.

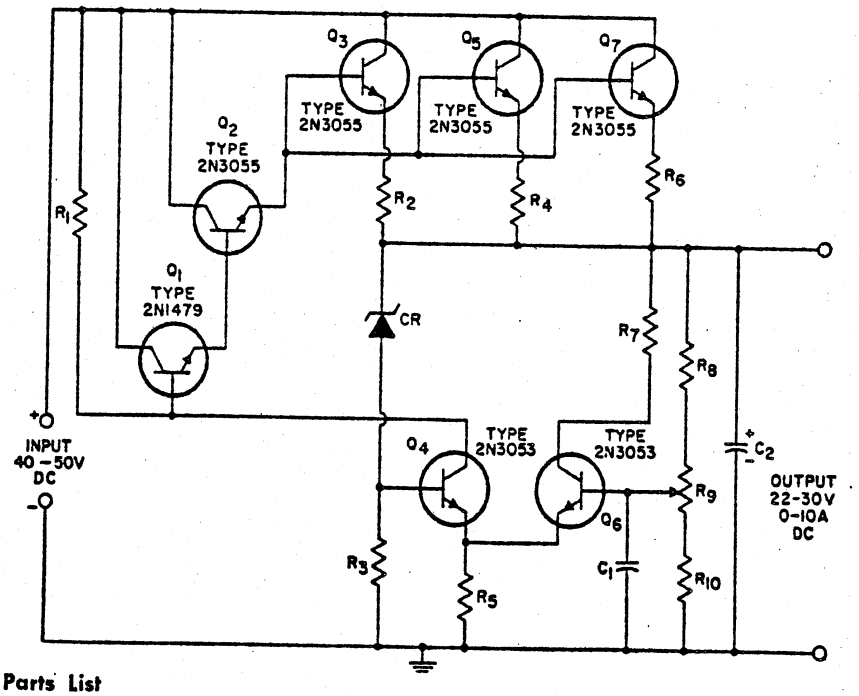

Parts List

C_1 = 1 μF, paper, 25 V
C_2 = 100 μF, electrolytic, 50 V
CR = reference diode, 12 V, 1 watt
R_1 = 1200 ohms, 0.5 watt
R_2, R_4, R_6 = 0.1 ohm, 5 watts
R_3 = 2000 ohms, 0.5 watt
R_5 = 570 ohms, 0.5 watt
R_7 = 270 ohms, 0.5 watt
R_8 R_{10} = 1000 ohms, 0.5 watt
R_9 = potentiometer, 1000 ohms, 0.5 watt

1.1.18 RCA series voltage regulator has adjustable output, line regulation within 1.0%, and load regulation within 0.5%. Regulation is accomplished by varying the current through three parallel 2N3055 transistors connected in series with the load. A zener provides the reference voltage for the circuit.

If the output voltage tends to rise for any reason, the total increase in voltage is distributed across bleeder resistors R8, R9, and R10. If R9 is set to midpoint, half the increase in output voltage is applied to the base of the 2N3053 transistor Q6. This increased voltage is coupled to the base of Q4 by R5, the emitter resistor for the two transistors. Because the voltage drop across CR remains constant, the full increase in voltage is developed across R3 and thus is applied directly to the base of Q4. Because the increase in voltage at the base is higher than that at the emitter, the collector current of transistor Q4 increases.

As the collector current of Q4 increases, the base voltage of Q1 decreases by the amount of the increased drop across R1. The resultant decrease in current through Q1 causes a decrease in the emitter voltage of this transistor. The resultant decrease in current through Q1 causes a decrease in the emitter voltage and thus in the base voltage of Q2.

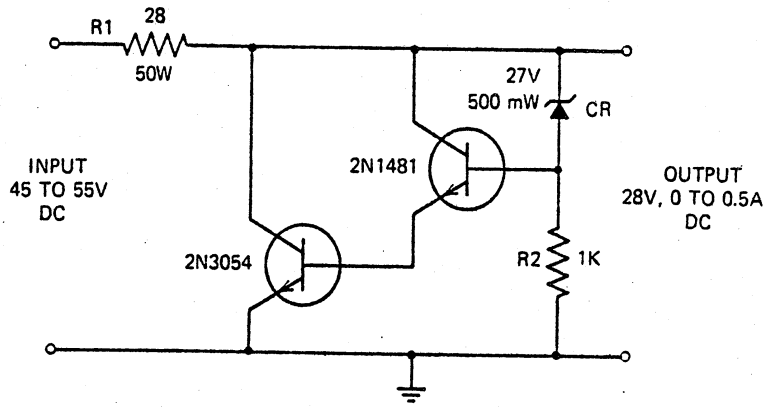

1.1.19 Simple two-transistor shunt voltage regulator can provide a constant (within 0.5%) dc output of 28V for load currents up to 0.5A and dc inputs from 45 to 55V. The two transistors operate as variable resistors to provide the output regulation. A 27V zener is used as the control element.

The output voltage tends to rise with an increase in either the applied voltage or the load-circuit impedance. The current through R2 and CR then increases. However, the voltage drop across CR remains constant at 27V and the full increase in the output voltage is developed across R2. This increased voltage across R2 is direct-coupled to the base of the 2N1481 transistor and increases the forward bias so that the 2N1481 conducts more heavily. The rise in the emitter current of the 2N1481 increases the forward bias on the 2N3054, and the current through this transistor also increases.

As the increased currents of the transistors flow through resistor R1, which is in series with the load impedance, the voltage drop across R1 becomes a larger proportion of the total applied voltage. In this way, any tendency for an increase in the output voltage is immediately reflected as an increased voltage drop across R1 so that the output voltage delivered to the load circuit remains constant.

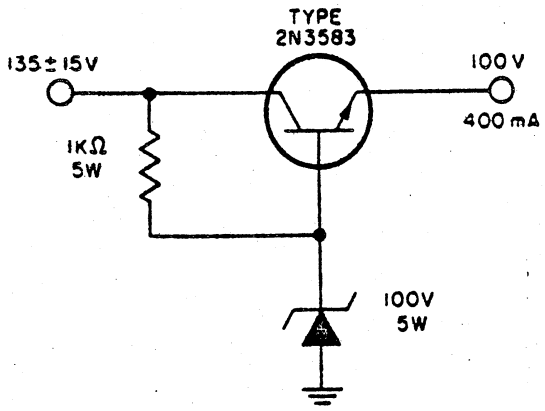

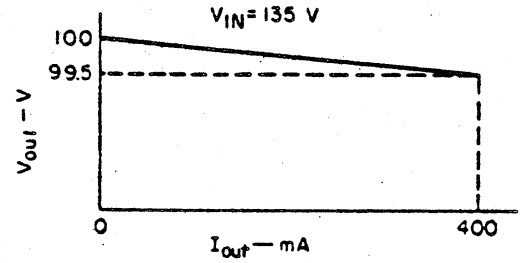

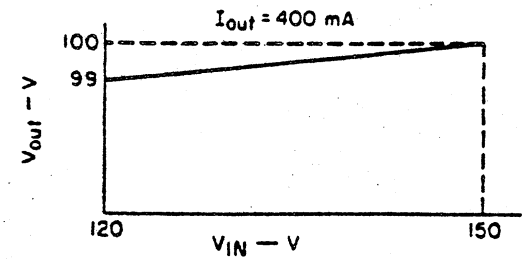

1.1.20 RCA simple transistor voltage regulator.

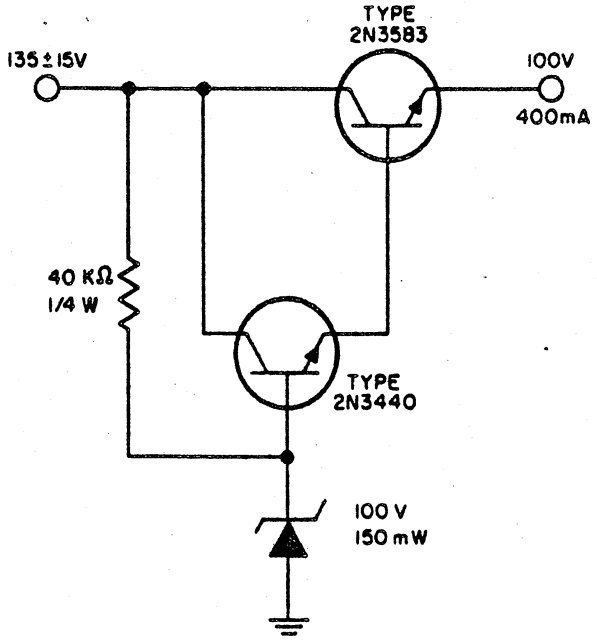

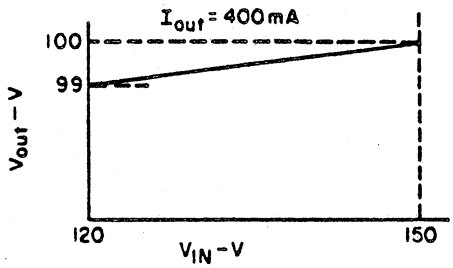

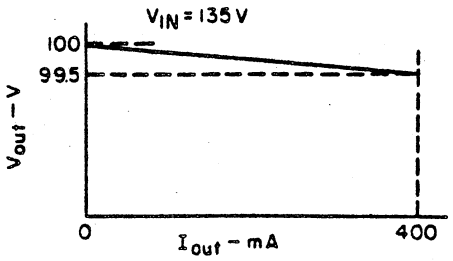

1.1.21 RCA series voltage regulator using the Darlington driver.

1.3 Direct-Current Converters

Since dc cannot be transformed from one voltage value to another for power applications, when a load requires a higher or a lower value of direct current than our dc source can provide, we must employ some form of dc conversion. Most generally, this involves inversion or commutation of the dc into a string of pulses, which we can then feed into an appropriate transformer whose output can be rectified and filtered like that of any power supply.

In the process of conversion, however, we try to get the fastest possible commutation possible, since we know that the size of a power transformer (which governs its cost) is inversely proportional to the frequency of the commutated input signal.

The owner of an expensive piece of entertainment equipment designed for operation from the U.S.-standard 60 Hz power line is usually dismayed to find that the unit overheats considerably when he tries to use it in a country that has a 50 Hz standard. He learns the hard way that lower line frequencies mean heavier, bulkier transformer cores.

A dc-to-dc converter requires ac for only a small portion of the total circuit, and it doesn't really matter to anyone whether the switching frequency is fast or slow, since the stage following ac transformation involved rectification of the ac anyway. Designers who care about package size and weight, component cost, and ease of filtering will select a high-frequency converter circuit every time. But that doesn't mean that there are no disadvantages with this approach.

There are two disadvantages worth considering: the sound wave created by the system switching at an audio rate and the interference that is likely to result from the nonsinusoidal waveform of the switching transistors. Both these anomalies can be corrected with simple engineering efforts, however. Various sound-deadening techniques can be employed to curtail the radiated wave from the converter unit, from use of special chassis mounts for mobile applications to packing the chassis (or wrapping it) with sound-absorbing material. Conventional shielding techniques can overcome the signal-radiating problem when it causes objectionable interference to other equipment.

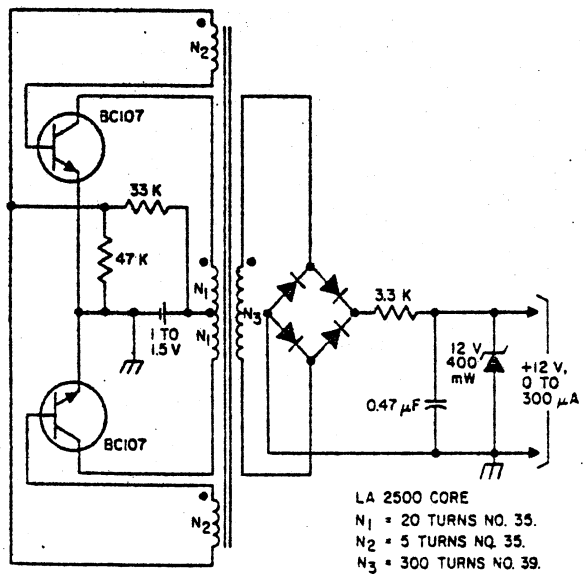

1.3.1 RCA dc-to-dc converter for powering CMOS from a single cell.

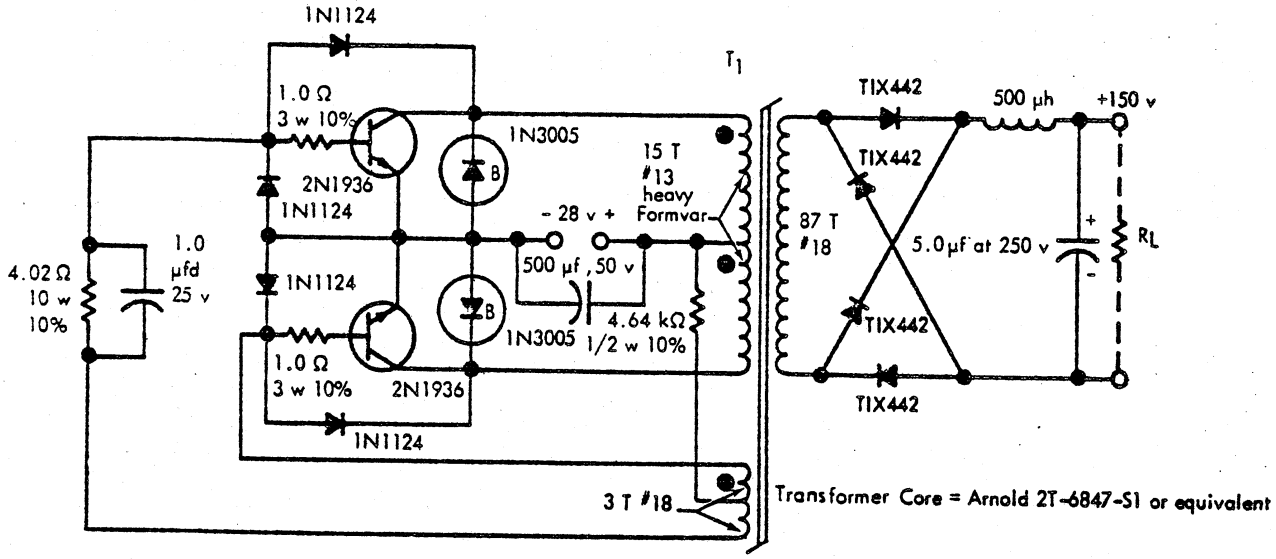

NOTE: Minimum usable h_{FE} = 10 at V_{CE} = 3v, I_C = 10a, T_A = 25°C
Both transistors use heat sinks, $\theta_{C\text{-}HS} + \theta_{HS\text{-}A} \leq 2°C/w$ each. All diodes must have adequate heat sinks.

TYPICAL PERFORMANCE AT T_A = 25°C
Efficiency = 80%
Output ripple 1.0 volt

1.3.2 225W, 10 kHz dc-to-dc converter operates from −55 to +125°C. Semiconductors are Texas Instrument devices.

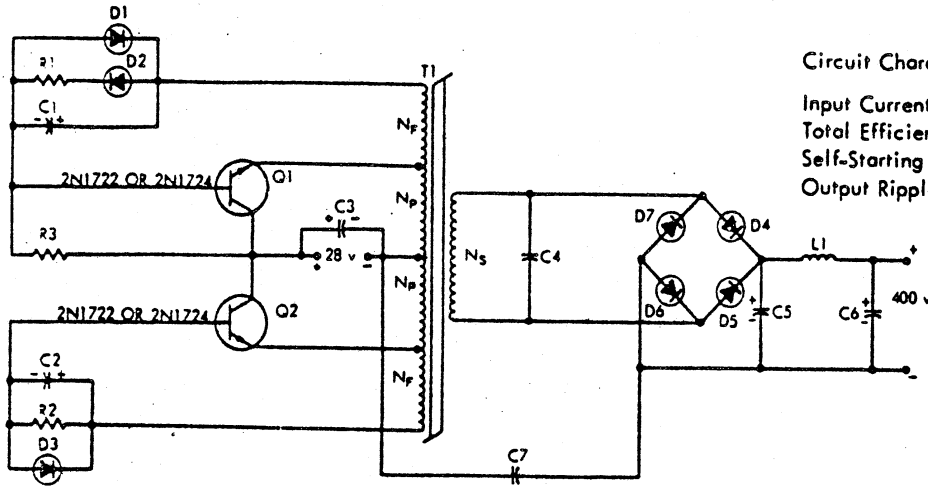

Circuit Characteristics at 120 w Power Output:

Input Current - 5a
Total Efficiency - 85%
Self-Starting and Short-Circuit Protected
Output Ripple - 0.6 v max.

Q1 & Q2 - TI 2N1722
OR TI 2N1724
D1 - D3 - TI 1N645
D4 - D7 - TI 1N1096
C1 & C2 - 22 µf, 15 v
C3 - 100 µf, 35 v
C4 - 510 pf, 500 v
C5 - 0.1 µf, 500 v
C6 - 3 µf, 500 v
C7 - 0.01 µf, 500 v
L1 - 15 µh
R1 - 2.74, 2 w
R2 - 3.32, 2 w
R3 - 511, 2 w

T1: N_P = 18 T #16 AWG
N_S = 290 T #25 AWG
N_F = 3 T #22 AWG
Core: Toroid, Magnetic Metals Inc. 51026-ID or equivalent.

NOTES:
1. All Resistance Values in ohms, 5% Tolerance.
2. All Resistor Wattage Ratings at 125°C Ambient.
3. Capacitor Voltage Ratings at 125°C Ambient.
4. Q1 and Q2 on Same Heat Sink, $\theta_{C\text{-}HS} + \theta_{HS\text{-}A} \leq 4$ C°/w each.

1.3.3 Texas Instruments 10 kHz dc-to-dc converter delivers 400V at up to 120W.

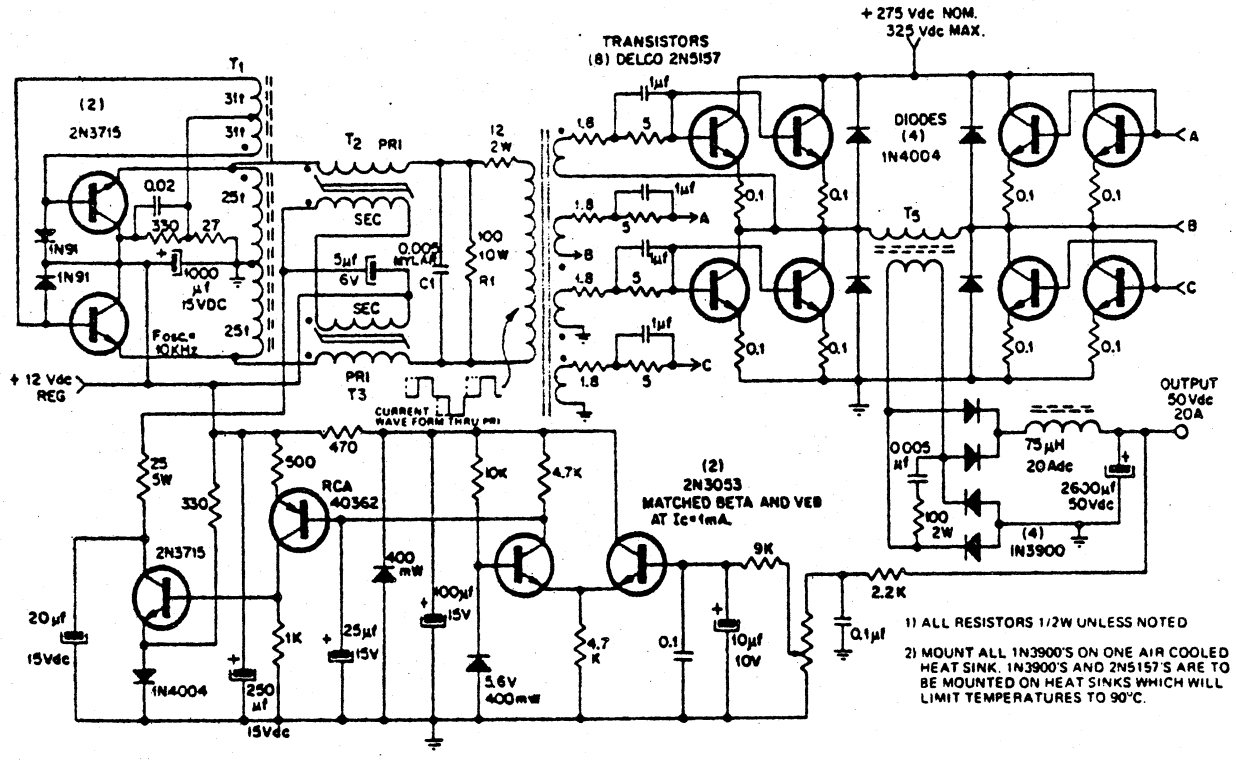

T1 - PRI: 50t tap @ 25t #22 AWG. SEC: 62t tap @ 31t #25 AWG. CORE: FERROXCUBE INC. 846T250-3E2A	T4 - PRI 75t #25 ALL SEC'S 12t #25 CORE MAGNETICS INC. 50076-1D	L1 - 70t of 5 Pcs. #16 in PARALLEL CORE: ARNOLD ENG. MOLY PERMALLOY A109156-2
T2, T3 - PRI: 150t #29 SEC: 150t #29 CORE: ARNOLD ENG. 4T551S-S500	T5 - PRI 7?t #16 SEC 18t of 6 Pcs. #16 in PARALLEL CORE USE 2 Pcs. FERROXCUBE 144T500-365	

1.3.11 Delco pulse-width-modulated power converter capable of 1 kW output at 87.5% efficiency. Input and output dc voltages are 275 and 50V, respectively. A voltage regulator is used to compensate for changes in load or input voltage. The switching frequency is 10 kHz. Tape-wound toroid cores are used with magnetic amplifier circuitry to create a controllable delay in the base-drive waveforms of the bridge output circuit. The converter occupies a volume of ¼ cubic foot (0.325m) and weighs less than 6 lb (2.72 kg).

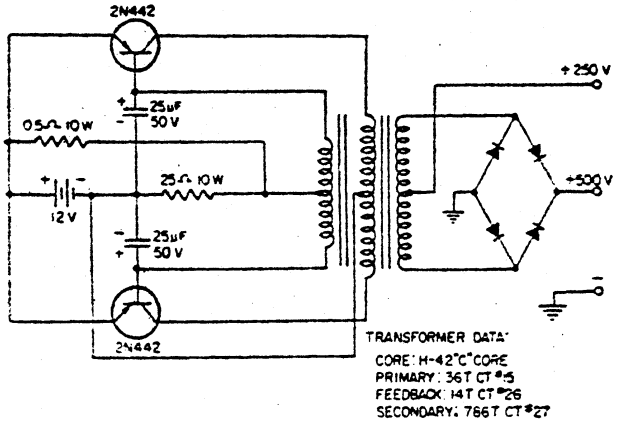

COMMON-EMITTER CONVERTER: 100W 800 Hz

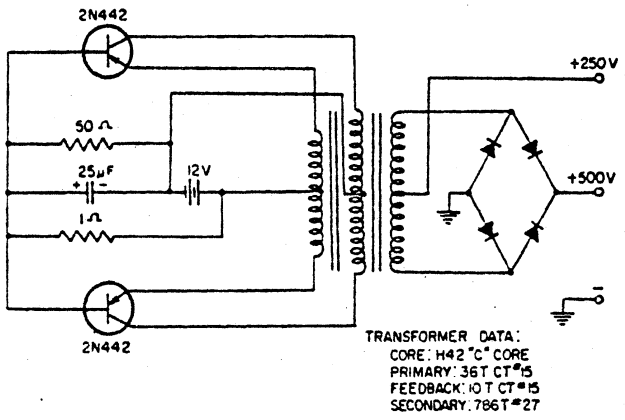

COMMON-BASE CONVERTER: 100W 800Hz

1.3.12 Delco dc-to-dc converters.

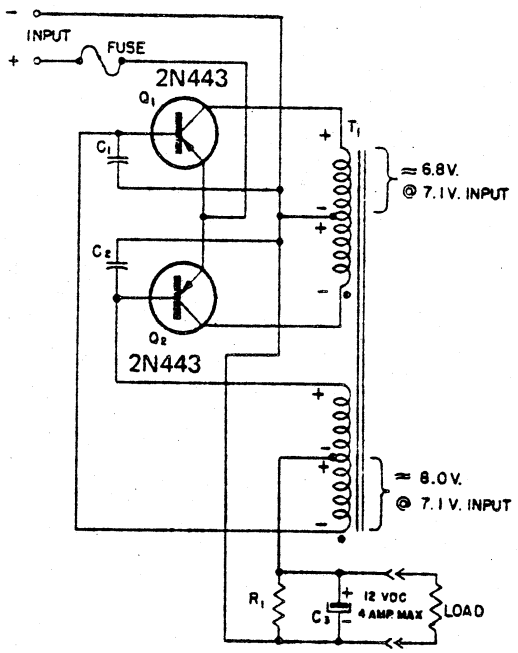

Q_1 Q_2 – Delco 2N443
C_1 C_2 – .5μF @ 100V Paper
C_3 – 1500 μF 15Vdc
R_1 – 470Ω 1watt Carbon
Fuse – 10 A Slo-Blo
T_1 – Primary
48 Turns #17
tap @ 24 t
Feedback
56 Turns # 17
tap @ 28 t
Core: H-3 Hypersil
Type "C" Core

NOTES:

Nominal frequency of oscillation = 300 Hz
Mount both transistors on one Delco 7281352 Heat Sink
Ambient temperature = −60°C to + 71°C

1.3.13 Delco rectifierless 6-to-12V dc-to-dc converter. Voltage multiplication is achieved by adding the feedback voltage to the supply voltage. Assume that Q1 is turning on. Voltages will be generated by the windings of the transformer. A negative voltage is being applied to the base of Q1. Since this is positive feedback, Q1 will continue to conduct until the transformer core saturates. With Q1 fully turned on, approximately 6.8V is applied across the upper half of the primary winding. This develops 8V in each half of the feedback winding. The voltage developed in the lower half of the feedback winding is of a polarity that adds algebraically to the supply voltage to develop 14V across the load resistor. The current path is from the lower end of the feedback winding through the emitter diode to the positive terminal of the input voltage source; thus the voltage in the feedback winding is added to the 6V source. Of the 16V developed across the feedback winding, 15V appears as reverse bias across the emitter diode of Q2. The 2V drop is the forward conducting voltage of the Q1 emitter. As the transformer core saturates, the magnetic field collapses and voltages of the opposite polarity will be generated in both windings. Thus Q1 will be cut off and Q2 will begin conducting. The emitter diodes may be considered as diodes rectifying in a full-wave circuit with the dc output being taken from the centertap of the feedback winding. The polarity across the load resistor does not change.

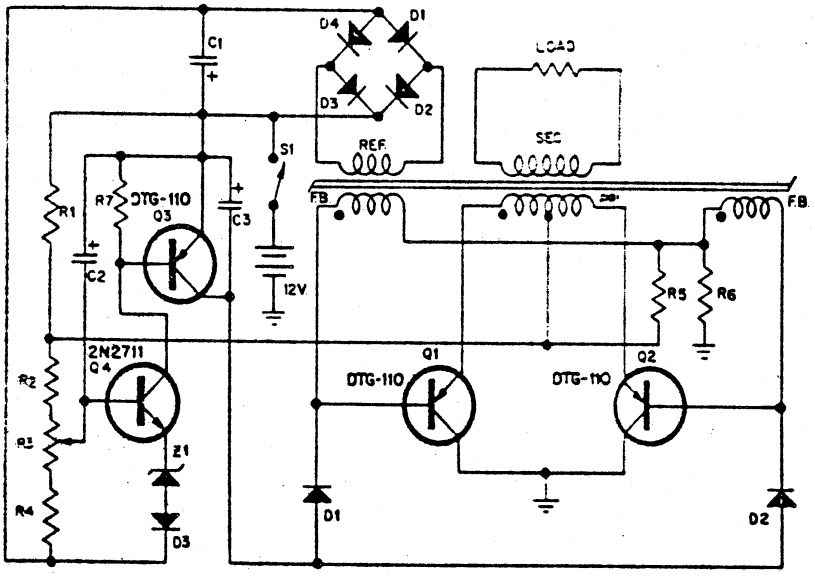

Q_1, Q_2, Q_3 – Delco DTG-110's
Q_4 – 2N2711
$D_1, D_2, D_3, D_4, D_5, D_6, D_7$ – Silicon, DRS-102
Z_1 – 1N3018 or Equiv., 8.2V
C_1, C_2 – 50μF, 25V
C_3 – 1000μF, 25V
R_1 – .25 Ω 2W
R_2, R_4 – 100 Ω 1W
R_3 – 400 Ω 2W
R_5 – 68 Ω
R_6 – 1.5K Ω
R_7 – 15 Ω
Toroid – Magnetics Inc.
51001-2A
Windings – Pri
60T #18 C.T.
Feedback
92T #30 C.T.
Reference
49T #29
Sec.
310 #24
Heat Sinks – For Q_1 & Q_2, Delco
7270725
For Q_3, Delco
7271357

1.4.8 In this 400 Hz dc-to-ac inverter using Delco DTG-110 transistors, both output voltage and frequency are regulated. Base drive to the output transistors is controlled by a series regulator that senses the output of an additional reference winding. This inverter is capable of providing 10W output and is intended to satisfy the requirements of a low-cost regulated ac power source for automotive applications. Output is 115V, 400 Hz; efficiency at full load (10W) is 72%.

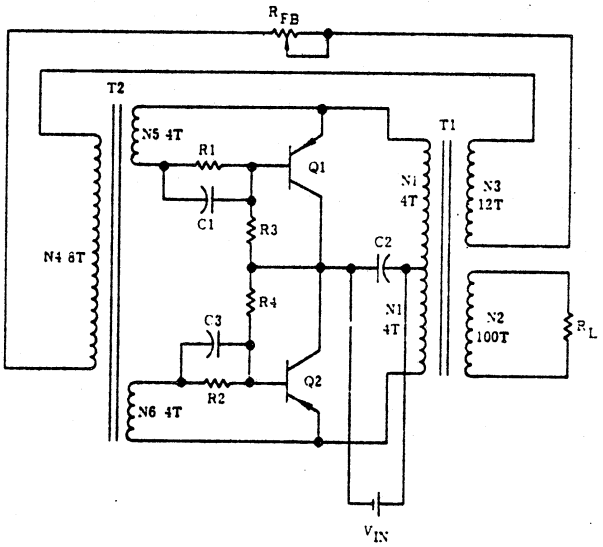

R_1	0.75Ω, 5 w
R_2	0.75Ω, 5 w
R_3	7.5Ω, 5 w
R_4	7.5Ω, 5 w
R_{FB}	1Ω, 5 w
C_1	20 μf, 6 v
C_2	10.000 μf, 6 v
C_3	20 μf, 6 v
T_1	Phoenix Transformer PX2127
T_2	Phoenix Transformer PX2128
Q_1, Q_2	2N2728
VIN	2V 50A

1.4.9 Motorola inverter circuit converts low voltages to high. The extremely low saturation voltage of the 2N2728 power transistor enables switching currents up to 50A efficiently. The saturation voltage of the transistor will be less than 0.1V at 50 amperes if the transistor is driven with a forced gain of 10. This is a resistance of 0.002 ohm, the equivalent of a 12 in. (30.48 cm) length of 12-gage wire. The frequency is set by adjusting the feedback voltage. For this application, the core was set to oscillate at 1 kHz.

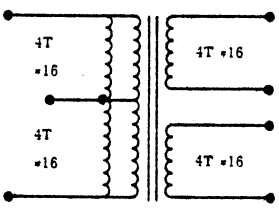

CORE: HI NICKEL STEEL LAMINATIONS.
ALLEGHENY LUDLUM STEEL COMPANY
1 4" x 1" STACK OF 1-DU
(PX-2126)

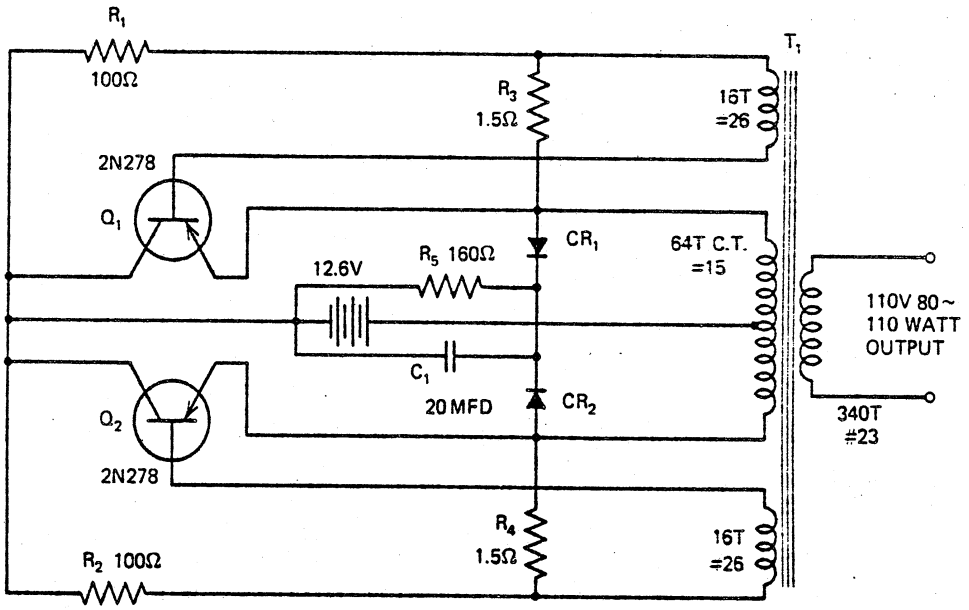

AMBIENT TEMPERATURE RANGE 71°C TO −55°C

Parts List

R1, R2	100 ohms, 5W wirewound
R3, R4	1.5 ohms, 5W wirewound
R5	150 ohms, 5W wirewound
CR1, 2	1N4004
C1	20 μF 50V dc electrolytic
Q1, Q2	2N278 Delco power transistor
T1 core	1 5/16 in. (3.34 cm) stack of 125 E.I. 0.014 in. (1.5 mm) silicon iron
Heatsink	Delco 7270725

1.4.10 Delco dc-to-ac inverter operates from car battery and delivers 110W at 117V, 60 Hz.

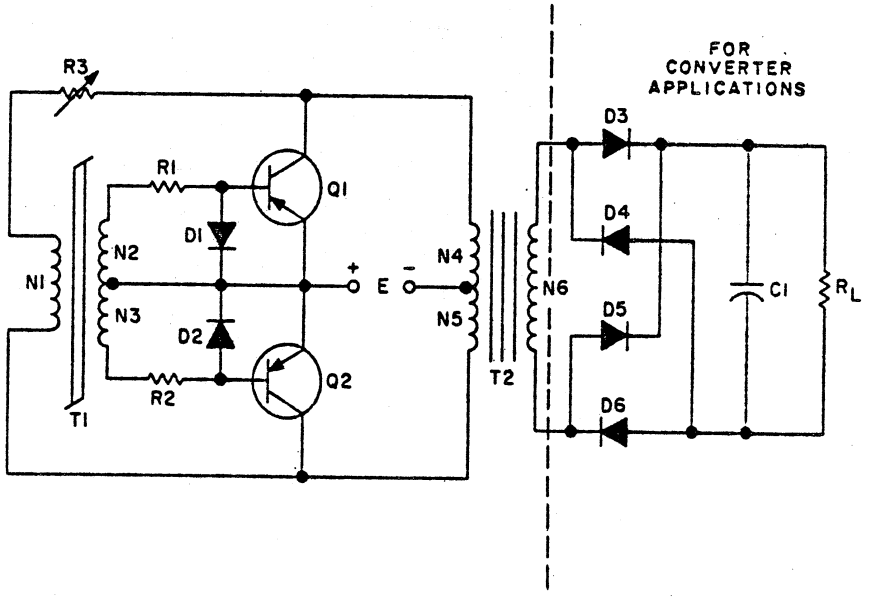

E	28V
P_o	50W
V_o	70V
f	18 kHz
Efficiency	85%
Transformers	Stackpole No. 55-420 Ceramag 24A
N1	24 turns
N2–N3	6 turns
N4–N5	20 turns
N5	50 turns
Q1–Q2	D43C5
D1–D2	1N914
D3–D6	A114B
R1–R2	33 ohms
R3—	0–500 ohms
R_L	100 ohms
C1	10 μF, 100V

1.4.11 GE two-transformer inverter for use at higher power levels. A more efficient, nonsaturating transformer (T2) can be used on the output, and the saturating base-drive transformer (T1) can be made much smaller, thus reducing the losses in the saturating core. The saturation current is now limited by resistor R3 and, because the voltage on input winding N1 decreases as the saturation current increases, the base drive falls off more rapidly so that switching is enhanced and power dissipation excursions are not as severe as in one-transformer inverters.

APPENDIX B

Data Handling Equipment Information

Data Recorders

Dattel Systems Inc.
1020 Turnpike Street
Canton, MA 02021
TX: 617/828-8000
Contact: Eugene L. Murphy

Bell & Howell - Datatape Division
Pasadena, California
Contact: David Hansen

Bell & Howell
6021 Lincolnia Road -Suite 100
Alexandria, VA 22312
TX: 703/790-8930

NASA/Goddard Space Flight Center
Spacecraft Technology Division
Mechanical Recording Techniques Section
TX: 301/344-7779
Contact: John M. Hayes
NASA/GSFC
Code 714.2
Greenbelt, MD 20771

Lockheed Electronics Co., Inc.
Industrial Technology Division - West
717 North Coney Avenue
Azuza, CA 91702
TX: 213/334-8211
Contact: Glen T. Green, Jr.

NAGRA Magnetic Recorders, Inc. - New York
Farrell Associates, Inc.
416 Hungerford Drive
Rockville, MD 20850
TX: 301/424-9460
Contact: Tom Raber

Sun Systems, Inc.
P.O. Box 182
Sun Valley, Idaho 83353
TX: 208/726-9336
Contact: Wendell Harden

Electro/General Corp.
14960 Minnetonka Industrial Rd.
Minnetonka, MN 55343
TX: 703/527-3262

MFE Corporation
Salem, NH
TX: 301/268-0196
Contact: Harry H. Barnes
Bartek Associates
613 East Bayview
Hillsmere
Annapolis, MD 2140

Memodyne Corporation
385 Elliott Street
Newton-Upper Falls, MA 02164
TX: 617/527-6600

Braemar Computer Devices, Inc.

CS-400 Digital Cassette System

Information received February 19, 1979 after telecom.

The Braemar CS-400 is the most suitable system of the Braemar line. However, the Braemar line is a good example of a micro-computer tape deck that is not very good for our purposes. It is a cassette system with Z tracks requiring the cassette to be flipped over. There are many disadvantages to this system and so it is not recommended for our use.

Lockheed Electronics

Mark V - Type 4200 Spacecraft Recorder

Information received February 21, 1979 after telecom.

The Lockheed Mark V-Type 4200 Recorder has been designed specifically for spacecraft use. Therefore, it has been built to withstand the environmental conditions that SCORE will encounter. This is just a recorder, it does not have the support electronics, i.e., you must use an A/D converter to supply the NRZ-L (Lockheed) signal for recording. Lockheed Electronics probably manufactures the equipment to do all the necessary coding.

The suitability of this recorder is very high; mainly due to the fact that it was designed for our needs. However, a buffer type system should be used to extend the duration of the recorder. As it stands, maximum time of continuous recording is 2.4 hours. Unfortunately, a major weak point of this recorder is cost: $15,000 without support electronics. Special electronics for Lockheed may be needed, added further to the cost.

NAGRA SNS

Information received March 19, 1979 after telecom.

This recorder has been designed purely for ground use. Preliminary checkout reveals that the NAGRA SNS could be adapted to fit our needs. This is only a recorder, no coding hardware is supplied. The inputs appear to be anlog/audio type so calibration may be necessary. The temperature and power specs are good, but no vibration specs are given. It is doubted that this recorder is built to withstand our conditions. The duration of the slow version is 2.5 hours per track. However, the tape must be flipped to use both tracks. Therefore, use of this recorder is not recommended unless extensive modifications are practical.

ELECTROGENERAL DATAMYTE 400

Histogram Recorder

Information received April 3, 1979 after letter .

The ElectroGeneral Datamyte 400 is a solid state histogram recorder. The Datamyte 400 will first process and then store the information. This device will input an analog signal, process it, and increment a counter. In this manner a histogram is formed. If no time base is needed in the data, this device is recommended as a possible alternative to tape recording. Because it is solid state, it can withstand the conditions of space. This is a single channel device so only one experiment can be recorded per device. A major advantage of this system is that it processes the information immediately and can later be read out directly to a terminal the ground. Further study on this device should be conducted as a possible alternative to free up the main recorder a little bit or even replace it totally.

DATEL LPS-16 SERIES

Micro-Power Cassette Data Logger

Information received April 4, 1979 after letter.

This is a total data storage system. Of all the information received thus far, the Datel LPS-16 is the most attractive. It is a total system of recorder, multiplexer and A/D converter capable of handling 16 different analog inputs. It can be computer controled via the "random mode" to record from any one of the 16 inputs or it can sequentially step through all 16. This might be exactly what we need in one small, complete package. The only foreseeable drawback of this system is that it cannot withstand very much vibration (1 g @ 0-50 cps), and that its capacity may be limited. Both of these problems may be overcome fairly easily. This system practically negates everything said in the Data Recording section of the SCORE report because it is a good cassette system and uses incremental recording rather than a buffer system. This system deserves much more investigation as a very good candidate.

LPS-16 SYSTEM SPECIFICATIONS

DATA ACQUISITION SECTION	
ANALOG INPUTS	
NUMBER OF ANALOG INPUTS	16 (8 differential low level LPS-16-12B5)
INPUT CHANNEL CONFIGURATION	Single ended
INPUT VOLTAGE RANGES	0V to −5VFS or ±5VFS, 0 to +5VFS
CHANNEL INPUT IMPEDANCE	100 MegOhms "ON" or "OFF" NOTE: When the 12VDC system power is turned off each channel has an input impedance of 10K Ohms
CHANNEL INPUT OVERLOAD	±10V (max.)
CHANNEL MODE OF OPERATION	Random or Sequential
CHANNEL INPUT ACQUISITION TIME	100 μsec — includes input settling time
SYSTEM PERFORMANCE:	
SYSTEM APERTURE TIME	50 nsec
SYSTEM ACCURACY	±0.025% of FS ±1/2LSB
SYSTEM LINEARITY	±1/2LSB
A/D RESOLUTION	12 Binary Bits
SYSTEM TEMPERATURE COEFFICIENT	±0.004%/°C
SYSTEM THROUGHPUT RATE	200 msec per 16 bit word (12 bit A/D plus 4 bit channel address)
INPUT CHANNEL SCAN RATE	Up to 5 per second
A/D DIGITAL OUTPUT CODING	Straight Binary — Unipolar Input Offset Binary or 2's complement — Bipolar Input
CASSETTE TAPE STORAGE METHOD	Two channel NRZI: Track #1 — Data, Track #2 — Data (complement)
CASSETTE TAPE FORMAT (2)	16 bit words (12 A/D bits plus 4 bits for channel address)
CASSETTE TAPE RECORD GAP	Two bit gap separates each 16 bit word
CASSETTE TAPE END-OF-FILE GAP (3)	Twelve bit file gap every 64th word, or per order. See guide.
SYSTEM CONTROL INPUTS (1)	
RANDOM ADDRESS INPUTS	Selects analog channel Four lines 8-4-2-1-negative true logic
RANDOM/SEQUENTIAL INPUT	Selects multiplexer mode One line — logic zero selects random mode
DEVICE SELECT INPUT	Controls all input command lines One line — negative true logic
CONVERT INPUT	Initiates A/D conversion One line — negative true logic
MULTIPLEXER RESET	Resets multiplexer to channel one One line — negative true logic
STROBE INPUT	Strobes all input lines and internally stores them One line — negative true logic
AUXILIARY SERIAL DATA IN	Permits cassette recording of EXT. serial data in 16 bit bytes — One line
DATA SELECT INPUT	Permits recording of either A/D output or EXT. serial digital data One line — Logic one selects A/D output
START TWO IN	Initiates recording of external serial data One line — Triggers on negative going transition
STATUS	Positive during a recording cycle One line — positive true logic
LOAD FORWARD	Advances cassette tape off leader to recording position One line — negation true logic
SYSTEM CONTROL OUTPUTS (1)	
FRAME SYNC OUTPUT	Identifies channel one One line — positive true logic
A/D BUSY OUTPUT	Identifies A/D conversion in process One line — positive true logic (during conv.)
WRITE CLOCK OUTPUT	When gated with file gap output, it provides shift signals for auxiliary data input One line — positive true logic
FILE GAP OUTPUT	When gated with write clock output, it provides shift signals for auxiliary data input One line — positive true logic
POWER ON RESET OUTPUT	Generates negative going pulse when system power is turned on One line — negative true logic

NOTES: (1) All input/output control signals are at standard C/MOS logic levels, Logic zero — 0V to +3V, Logic one — +9V to +12V
(2) Jumper connections can be made on the formatter card allowing selection of either 12 or 16 bit words. For example an 8 bit A/D converter with 16 analog channels would require only a 12 bit word length.
(3) Jumper connections can be made on the formatter card allowing for file gaps every 1, 2, 4, 8, 16, 32, or 64 words.

16 SYSTEM SPECIFICATIONS (continued)

RECORDER CHARACTERISTICS

RAGE MEDIA	Standard Phillips certified data cassette 300 foot length
RAGE METHOD	2 channel NRZI
MBER OF TRACKS	TWO: Data on track one Data complement on track two
PE FORMAT	16 bit words (12 A/D data bits and 4 channel address bits)
CORD GAP	Two step record gap for every 16 bit word
E GAP	Twelve bit file gap every 64th word, or per order. See guide.
PE STORAGE CAPACITY	120,000 sixteen bit words including gaps and load forward
ITE SPEED	90 steps per second 5 sixteen bit words per second (max.)
TA INPUT/OUTPUT	Serial NRZI or parallel 16-bit thru the A/D Converter connector
AY-BACK SPEED	See Datel's LPR-16 Reader
TOR	Single 1.5° angle stepper coupled to take-up reel by slip clutch mechanism
TOR STEP ANGLE	1.5°
GULAR ACCURACY	±8 min. of arc non-accumulative
PE MOTION CONTROL	Single capstan pinch roller drive Head engages mechanically during write time
PE TENSION	0.4 oz. inches
ROR RATE	1 bit in 10^7
PE OF CASSETTE LOADING	Front
CORDING HEAD	Dual channel single gap High quality digital type
ERATING MODE	Write only
YSICAL ENVIRONMENTAL SPECIFICATIONS	
UT POWER REQUIREMENTS	+ 12VDC ± 8% 80ma when recording (960 mw) 10μa during standby (120 μw) NOTE: Includes tape transport plus all electronics
ERATING TEMPERATURE RANGE	-10°C to +60°C
ORAGE TEMPERATURE RANGE	-35°C to +70°C
LATIVE HUMIDITY	10% to 95% w/o condensation
OCK & VIBRATION	1.0G @ 0-50 cps, all 3 axes
YSICAL SIZE W/ELECTRONICS (includes electronics)	4" high x 4 1/2" wide x 7 1/2" deep (6 1/2" deep behind panel)
ECTRONICS	Contained on four plug-in PC cards mounted on a removeable PC mother board
IGHT	2 lbs. includes recorder and electronics
MATING CONNECTORS	Cinch-part #251-22-30-160 — (I/O Command Signals), Datel 58-2075060 Elco-part #00-8218-24-722-005-(16 channel analog, Datel 58-2077000 inputs, located on top rear of mux/S&H card)

TES:
1) The LPS-16 data logger is shipped completely assembled and ready to operate. It is only necessary to connect the analog input signals, control signals, and 12 VDC power source plus inserting a cassette to begin recording.
2) An extremely important factor in the reliability of the LPS-16 data logging system is the cassette itself. Only a properly certified tape cassette should be used. The mechanical tolerances of the cassette cartridge and tape tension are also significant factors in the reliability of operation of the LPS-16 system. The preffered tape cassette is Datel Systems Type 12123-1

ERING INFORMATION

16-12B- ___ ___ ___

SCALE ANALOG INPUT
V to -5V
5V, inverted analog
to +5V
5V, conventional
50mV, range may be anged by selecting resistor

A/D OUTPUT FORMAT
A = STRAIGHT BINARY, UNIPOLAR INPUT
B = OFFSET BINARY, BIPOLAR INPUT
C = 2's COMPLEMENT, BIPOLAR INPUT

FILE LENGTH
00 = NONE
01 = 1 WORD
02 = 2 WORDS
03 = 3 WORDS
04 = 4 WORDS
08 = 8 WORDS
16 = 16 WORDS
32 = 32 WORDS
64 = 64 WORDS
99 = EXTERNALLY CONTROLLED FILE LENGTH

XAMPLE:
-12B 4 B 32
4 = ±5V Conventional
B = Offset Binary
32 = 32 Words

MODEL	PRICE (1-9)
LPS-16-12B	$1295
Low Level LPS-16-12B5	$1450

Connectors are included with each unit.

Spare Connectors: Digital I/O, Datel 58-2075060, (1-9) $ 8.00
Analog In, Datel 58-207 7000, (1-9) $ 6.00

TAPE CASSETTE MODEL 12123-1 $10.50
PRERECORDED CASSETTE MODEL 37-6077-1 $37.50

GSA Contracted: Datel's products are available both direct and through the General Services Administration (GSA). If you are connected with a military or federal agency or receive federal funds, you may be entitled to purchase Datel's data loggers and other products through GSA to expedite requisitioning and order processing. Datel's data loggers are covered under FSC Group 66-56, Part II, Section K, Contract GS-00S-29002

APPENDIX C

Possible Sources for Timers and Sequencers

Possible Sources for Timers and Sequencers:

Cyclomatic Industries, Inc.
7520 Convoy Court
San Diego, CA 92111
Contact: Lloyd Nissley
TX: 714/292-7441

American Microsystems, Inc.
3800 Homestead Road
Santa Clara, CA 95051
TX: 408/246-0330

Encoder Products Company
1601 Dover Road
Sandpoint, Idaho 83864
Contact: Ray Pelland
TX: 208/263-2173

Texas Instruments, Inc.
Control Products Division
Mail Station 10-10
Attleboro, MA 02703
TX: 617/ 222-2800 ext. 6411

Xanady Controls
45 Fadem Road
Springfield, N. J. 07081
TX: 201/467-8100

Chronometrics, Inc.
2614 Silverdale Drive
Wheaton, MD 20906
Contact: Homer Guerra
TX: 301/ 933-3000

Note:

The above companies have been contacted for any general information. Whatever information is sent will be available in the 482 Library.

APPENDIX D

Transformation of Conductive Heat Transfer Equation to Cylindrical Walls

APPENDIX D

Transformation of Conductive Heat Transfer Equation to Cylindrical Walls

Basic Equation:

$$\dot{Q} = - kA \frac{dT}{dx} \qquad \text{(D-1)}$$

Replacing x by the radius r_1 and using the relation between the area A and the radius at any distance from the center yields

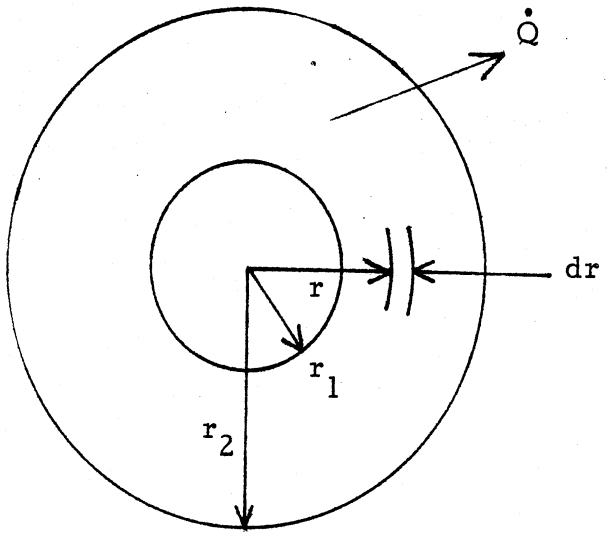

$$A = 2\pi r L \qquad \text{(D-2)}$$

Substituting (Eq. D-1) into (D-2) yields,

$$\dot{Q} = 2\pi r L k \frac{dT}{dr} \qquad \text{(D-3)}$$

Changing variables and integrating yields the desired result,

$$\int_{r_1}^{r_2} \dot{Q} \frac{dr}{r} = \int_{T_1}^{T_2} - 2\pi \, Lk dT$$

$$\dot{Q} = \frac{2\pi \, Lk(T_1 - T_2)}{\ln(r_2/r_1)}$$

APPENDIX E

Discussion of Radiation Shape Factor

APPENDIX E

Discussion of Radiation Shape Factor

To determine the geometric factor involved in radiant heat transfer, black bodies will be used. Consider two black surfaces A_1 and A_2. To obtain the general expression for the energy exchange between these two surfaces when they are maintained at different temperatures results in a problem of determining the amount of energy which leaves one surface and reaches the other. To solve this problem, the radiation shape factors are defined:

F_{1-2} = fraction of energy leaving surface 1 which reaches surface 2

F_{2-1} = fraction of energy leaving surface 2 which reaches surface 1

Now, the energy leaving surface 1 and arriving at surface 2 is $E_{b1}A_1F_{12}$, while the energy leaving surface 2 and arriving at surface 1 is $E_{b2}A_2F_{21}$, where the subscript b denotes black body. Since we are dealing with black surfaces, all of the incident radiation will be absorbed, by the definition of a black body. The net energy exchange between the two surfaces is

$$E_{b1}A_1F_{12} - E_{b2}A_2F_{21} = Q_{1-2} \qquad \text{(E-1)}$$

Now, consider the case where both surfaces are at the same temperature. If two surfaces are at the same temperature, there can be no heat

exchange between them ($Q_{1-2} = 0$), and their energies are the same, since E(T). Therefore, $E_{b1} = E_{b2}$ and Eq. (E-1) simplifies to

$$A_1 F_{12} = A_2 F_{21} \tag{E-2}$$

Eq. (E-2) is commonly referred to as the reciprocity theorem. The net heat exchange becomes

$$Q_{1-2} = A_1 F_{12}(E_{b1} - E_{b2}) = A_2 F_{21}(E_{b1} - E_{b2}) \tag{E-3}$$

The only problem that remains is the determination of F_{12} (or F_{21}). These solutions are generally complex; therefore, they have been represented graphically for three different geometries in Figures E-1, E-2, and E-3.

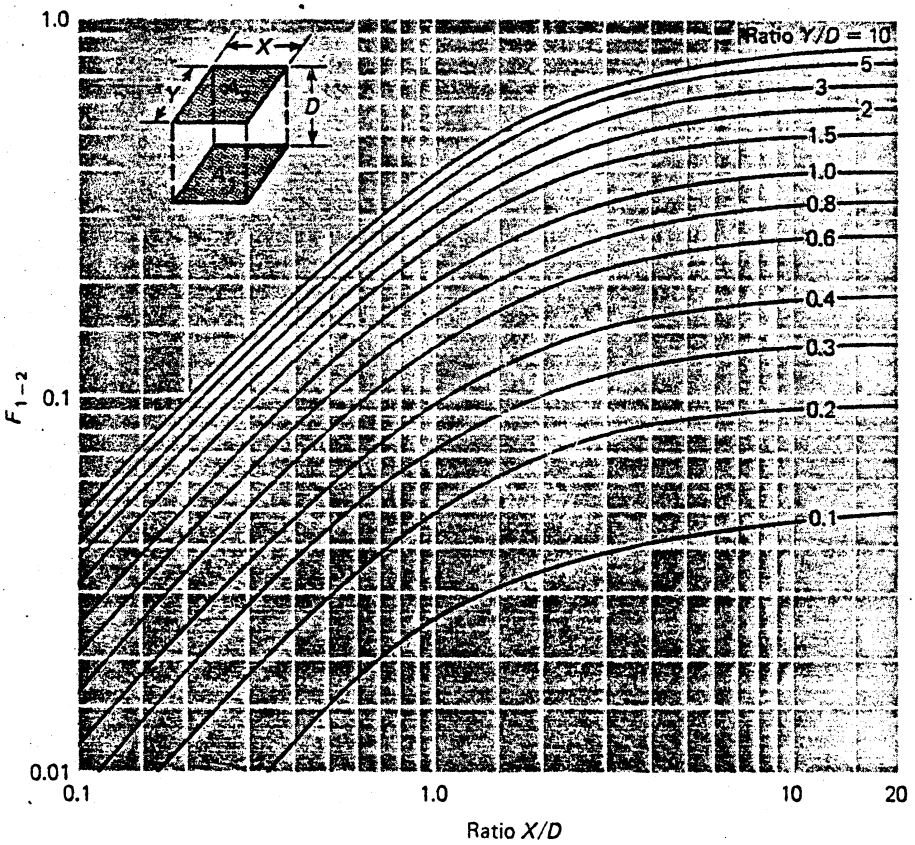

Figure E-1. Radiation Shape Factor for Radiation Between Parallel Rectangles. [Ref. 1]

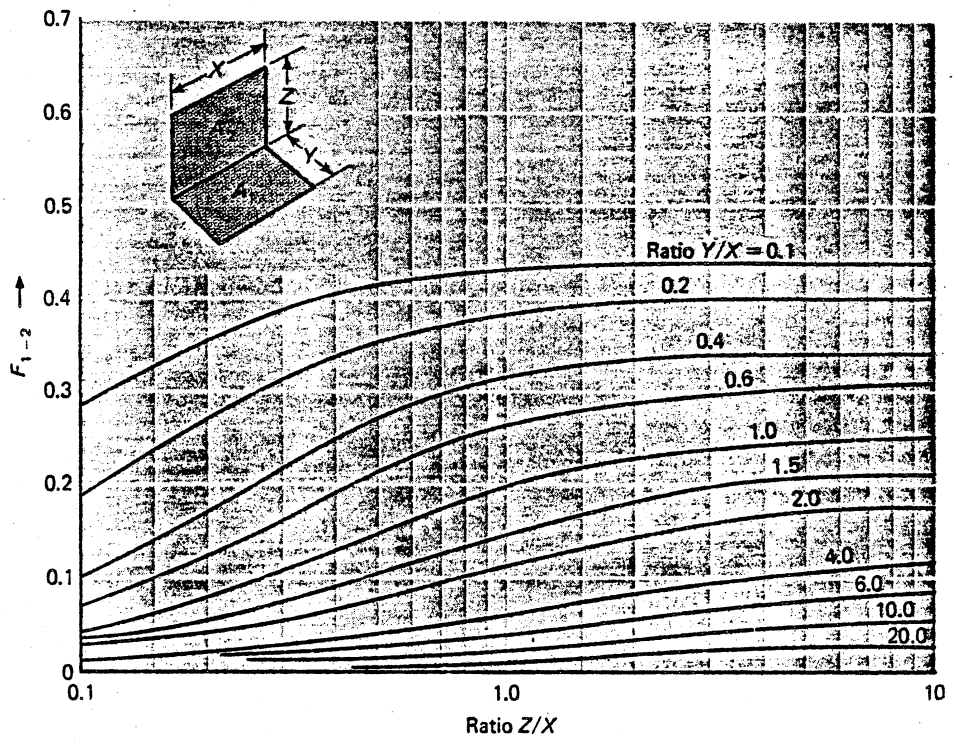

Figure E-2. Radiation Shape Factor for Radiation Between Perpendicular Rectangles With a Common Edge. [Ref. 1] .

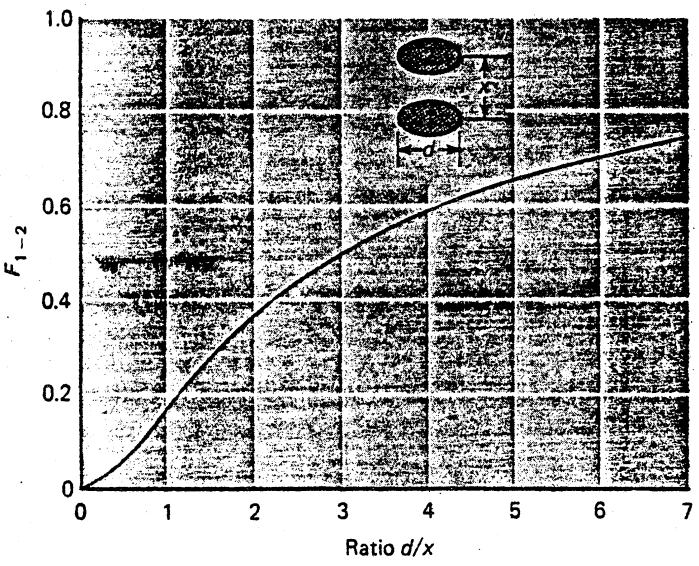

Figure E-3. Radiation Shape Factor for Radiation Between Parallel Disks. [Ref. 1]

APPENDIX F

Companies Offering Technical Assistance

APPENDIX F

Addresses of companies offering technical assistance to SCORE.

International Technical Associates (InTA)
1327 Northgate Square
Reston, Virginia 22090
TX: 203/437-5888

American Science and Engineering, Inc.
955 Massachusetts Avenue
Cambridge, Massachusetts 02139
TX: 617/868-1600 Telex: 921-458

Rockwell International
Space Division
12214 Lakewood Boulevard
Downey, California 90241
TX: 213/922-3344

Wyle Laboratories
Eastern Operations
7800 Governors Drive West
Huntsville, Alabama 35807
TX: 205/837-4411

APPENDIX G

Companies Offering GAS Insurance

APPENDIX G

Addresses of companies offering GAS insurance:

Nausch, Hogan, & Murray, Inc.
127 John Street
New York, New York 10038
TX: 212/269-7330 Telex: 125-387

Marsh & McLennan, Inc.
1221 Avenue of the Americas
New York, New York 10020
TX: 212/997-7840